INVESTIGATION OF TOOLTIP TEMPERATURE AND SURFACE ROUGHNESS IN TURNING OF AISI 1045 STEEL WITH COCONUT OIL-BASED HYBRID NANOFLUID UNDER MQL TECHNOLOGY

Viraj Niroshan Abeweera

(198400A)

Degree of Master of Engineering

Department of Mechanical Engineering

University of Moratuwa
Sri Lanka

November 2022

INVESTIGATION OF TOOLTIP TEMPERATURE AND SURFACE ROUGHNESS IN TURNING OF AISI 1045 STEEL WITH COCONUT OIL-BASED HYBRID NANOFLUID UNDER MQL TECHNOLOGY

Viraj Niroshan Abeweera

(198400A)

Dissertation submitted in partial fulfilment of the requirements for the Master of Engineering in Manufacturing Systems Engineering

Department of Mechanical Engineering

University of Moratuwa
Sri Lanka

November 2022

Declaration

I declare that this is my work, and this thesis does not incorporate without acknowledgement any material previously submitted for a Degree or Diploma in any other University or institute of higher learning, and to the best of my knowledge and belief, it does not contain any material previously published or written by another person except where the acknowledgement is made in the text.

Also, I hereby grant the University of Moratuwa the non-exclusive right to reproduce and distribute my thesis, in whole or in part, in print, electronic or other mediums. I retain the right to use this content in whole or part in future works (such as articles or books).

Signature: Date:

The above candidate has carried out research for the master's thesis under my supervision.

Name of the supervisors: Dr. G.I.P. Perera

Dr. H.K.G. Punchihewa

Mr. R.K.P.S. Ranaweera

Signature of the supervisor: Date:

Name of the supervisor: Dr. G.I.P. Perera 18.11.2022

Signature of the supervisor: Date: 18/11/2022

Name of the supervisor: Dr. H.K.G. Punchihewa

Signature of the co-supervisor: Date:

Name of the co-supervisor: Mr. R.K.P.S. Ranaweera

Dedication

To the most courageous individuals who guided me to great accomplishments: my beloved mother, *Nandanie Sumanarathna* and my wife, *Bimba Veenavi Yoshinika*

Acknowledgement

As a graduate student in the Faculty of Engineering at the University of Moratuwa, I had to complete a research project in partial fulfilment of the Manufacturing Systems Engineering Master of Engineering degree requirements. I chose " Investigation of tooltip temperature and surface roughness in turning of AISI 1045 steel with novel coconut oil-based hybrid nanofluid under MQL technology" as my topic. I am incredibly grateful to the University of Moratuwa for providing this opportunity. I would like to thank Dr G.I.P. Perera, Dr. H.K.G. Punchihewa, and Mr. R.K.P.S. Ranaweera for their guidance, constant supervision, and provision of project-related information and for their assistance in completing this research project. Their cooperation and encouragement motivated me to finish this project. In addition, I appreciate Mrs. M. Hennayake (QA manager @ CSCL) and Mr. M.M.L.C. Malmessa (DGM of technical @ CSCL) for their insightful comments and for giving extra support to complete my research. I would also like to express my sincere appreciation and gratitude to the University of Ruhuna for providing me with information, time, and engineering workshop facilities for the research. My gratitude and appreciation also goes to my project development colleagues and those who have voluntarily assisted me with their skills.

Abstract

Over the past few years, positive changes have occurred in the manufacturing industry and many other fields as a direct result of current breakthroughs in nanotechnology. The integration of nano-sized solid lubricants into aerosols, suspensions, and emulsions can lead to an enhancement of the end product's tribological and thermal properties. This is because of the constituent materials' unique chemical and physical properties. Therefore, this makes it possible for lubricants or coolants to perform their functions to attain a high level of productivity in machining processes.

This study aimed to investigate the effect on average surface roughness and tooltip temperature in turning AISI 1045 steel with novel coconut oil-based hybrid nanofluid under MQL technology. Al_2O_3 and TiO_2 were chosen as the two nanoparticles to use in the experiments after conducting a survey of the relevant research in the field. In order to reach this aim, Taguchi's L16 orthogonal array, which is comprised of four factors, was utilized. Concentrations of Al_2O_3, TiO_2, cutting speed, and air pressure are the four factors considered in this study. In this experimental design, the responses considered were average surface roughness and the temperature of the tooltip. Using the Minitab 17 software, the model fitting and optimization were carried out. The values that recorded as being optimal were,

- 0.75 wt. % of Al_2O_3,
- 0.00 wt. % of TiO_2,
- 2.5 bar of air pressure,
- 96 m/ min of cutting speed

As a direct consequence, it is clear that the developed MWFs show significantly higher performance than the other two techniques, dry cutting and coconut oil-based MQL cooling. The percentages show a 23.92 % and 37.97 % reduction in tooltip temperature compared to dry cutting conditions for MQL+ CC and Nano+ MQL+CC conditions, respectively. Also, the average surface roughness was reduced by 33.87 % and 94.85 % compared to dry cutting conditions for MQL+ CC and Nano+ MQL+CC conditions, respectively. For future work, we can use thermophysical and tribological factors rather than cost as a determining factor for better results.

Keywords: Minimum quantity lubrication/ nanoparticle/ machining/ surface roughness/ tooltip temperature

Table of contents

List of Figures

Page

List of Tables

Page

List of abbreviations

Abbreviation	Description
AISI	American Iron and Steel Institute
Al_2O_3	Aluminium oxide
ANOVA	Analysis of variance
CC	Coconut Oil
CSCL	Ceylon Steel Corporation Limited
DOE	Design of Experiments
FOE, UOR	Faculty of Engineering, University of Ruhuna
FNG	Functionalized Nano Graphite
MCF	Metal Cutting Fluid
MOO	Multi-objective optimization
MQL	Minimum Quantity Lubrication
MWF	Metal Working Fluid
NBA	Nano Boric Acid
NDM	Near Dry Machining
NG	Nano Graphite
OA	Orthogonal Array
PGPR	Polyglycerol polyricinoleate
Ra	Average Surface Roughness
T_{tip}	Tool tip temperature
TiO_2	Titanium dioxide
VB	Flank wear

List of Appendices

1 CHAPTER: INTRODUCTION

In recent decades, the majority of manufacturing industries have increased production rates in response to increased demand for machined products, which is critical to achieving this goal [1], [2]. Machining is the most adaptable mechanized strategy, as it entails removing excess material in the form of tiny chips or flakes to achieve the desired size, shape, and surface finish [3]. Lubricating and cooling are the two most important aspects of machining, and the majority of researchers uncovered a wealth of data on various lubricating and cooling systems that improve the efficiency of machining processes [4].

The friction between the tooltip and the workpiece interface generates significant heat in the machining zone, and this produced heat has various adverse thermal effects [5]. During machining processes, cutting fluids are utilized to reduce friction between the tooltip and the workpiece by delivering appropriate lubrication and cooling; also, the chips are removed from the machining zone by washing, and to decrease unfavourable thermal effects, cutting edges are employed [6]. However, when excessive amounts of cut fluids are used, it pollutes the environment and harms the workers' health [7]. As a result, dry machining could be an option for minimizing the use of cutting fluids.

Low cutting speeds are appropriate for dry machining and are favoured for easily machinable materials; however, high cutting speeds and depths of cut are not advised for dry operation because tool edge built-up affects the workpiece's dimensional accuracy and workpiece reduces tool life [8]. For such cases, dry machining technology is regularly converted into flood cooling technology. Nevertheless, metal-cutting fluids are used extensively, which is a major contributor to environmental pollution and human health concerns [9]. Therefore, Minimum Quantity Lubrication (MQL) can be utilized to limit the consumption of cutting fluids and the negative consequences of dry machining.

Green cutting, particularly MQL, likewise called near-dry machining (NDM), was established in the twenty-first century as a trade-off between the benefits and drawbacks of dry cutting and machining with plenty of soluble oil, as environmental consciousness increased laws and regulations; also, it is a process in which a little amount of any metalworking fluid is sprayed into the cutting zone under high pressure to improve penetration and chip contact [10]. MQL machining performance was studied by Reddy et al., who compared it to dry machining [11]. They concluded that surface roughness, cutting forces, tool wear, and machining temperature were significantly reduced compared to dry machining. Padmini et al. studied the performance of the machining of MQL and revealed that it produced lower tool wear and cutting forces than in dry conditions [12]. Khan et al. studied MQL's machining performance and compared it to flood cooling, finding that MQL reduced machining temperature by 10% while decreasing tool wear and surface roughness [13]. Based on the facts mentioned above, it is evident that MQL technology is superior to dry cutting and flood cooling to achieve the present demand. MQL is a superior option to flood cooling for low- to medium-speed machining and high-speed machining; evidence for the usage of MQL is unclear, and it has been discovered that coolant has trouble reaching the cutting region during high-speed machining, making the cooling useless, according to the majority of researchers [14]–[16].

A number of researchers have been able to perform machining operations when working with macro and micro-sized solid particles and synthetic or vegetable oils; thermal conductivity and lubricity were superior in this mixed-cutting fluid [17]. Since micro-sized particles could clog and make the machine unstable, their use has been limited [18]. Owing to its unique and enhanced properties, nanoparticle-assisted manufacturing has revolutionized manufacturing over the past decade [19]. Both functionalized and unfunctionalized nanoparticles are used in manufacturing, and nanoparticles' evolution, synthesis, properties, applications, and health and environmental implications are all covered in recent publications [20]. Nanoparticles differ from their microscale counterparts in that they are smaller and have a larger surface area, and potential heat transfer fluids are cutting fluids that comprise nanometer-sized metallic and nonmetallic particles (≤100 nm) [21]. An international team of scientists found that the base fluid's thermal conductivity could be remarkably improved when the inclusion of various nanoparticles of metallic materials, such as metal oxides, metal carbides, carbon materials, and metal nitrides [22]–[24]. It concluded that adding nanoparticles into MQL-based metal cutting fluids (MCFs) has a higher performance than micro-size particles.

It is estimated that mineral oils supply 85 percent of the market demand for MCFs for machining and that mineral oils meet most of the requirements, but they have significant environmental consequences due to non-biodegradability, toxicity, and improper disposal [25]. As a result, the use of biodegradable and environmentally friendly MCFs has increased. The biodegradability of cutting fluids is the most critical factor in determining their environmental compatibility, as it refers to microorganism-mediated degradation [26]. The superior biodegradability of vegetable oils over mineral oils is illustrated graphically in Figure 1-1.

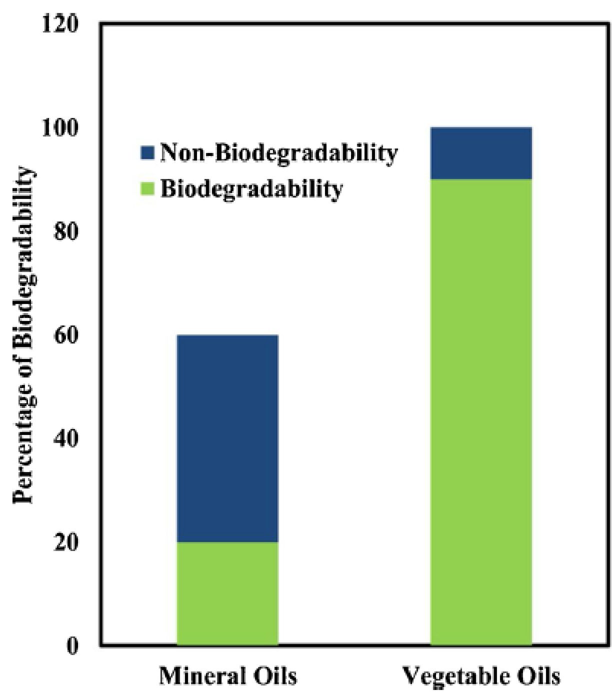

Figure 1-1: The superior biodegradability of vegetable oils over mineral oils [25]

Using bio-based oils as MWFs remains low on the list of priorities. Figure 1-2 demonstrates that green solutions are gaining popularity as a means of achieving more sustainable operations and cleaner production. It clearly shows the number of publications has increased significantly over the last decade. Consumption has also risen and is expected to keep rising. Figure 1-3 indicates that bio-based MCFs could have the potential to grow in the U.S. market [25], [27]–[30].

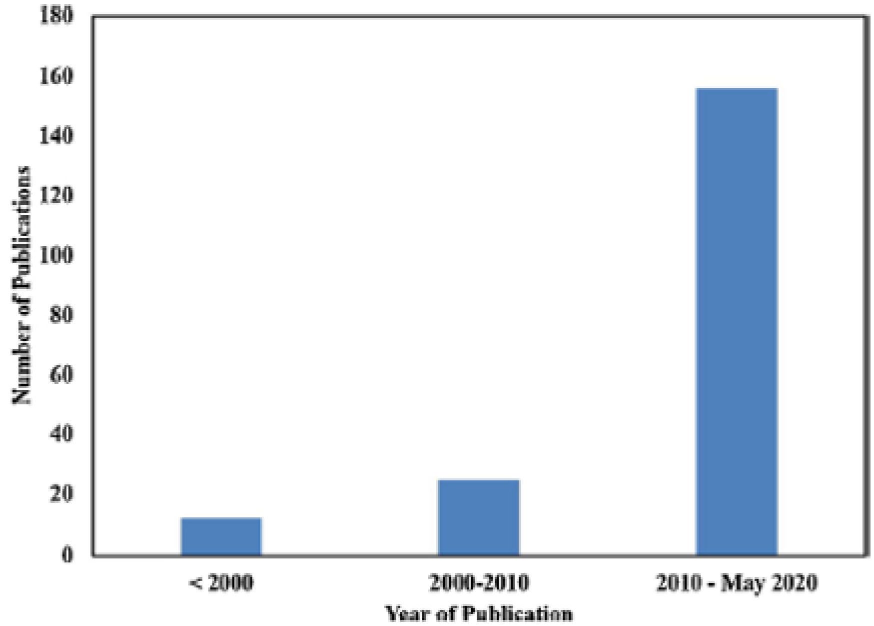

Figure 1-2: Popularity of green solution [25]

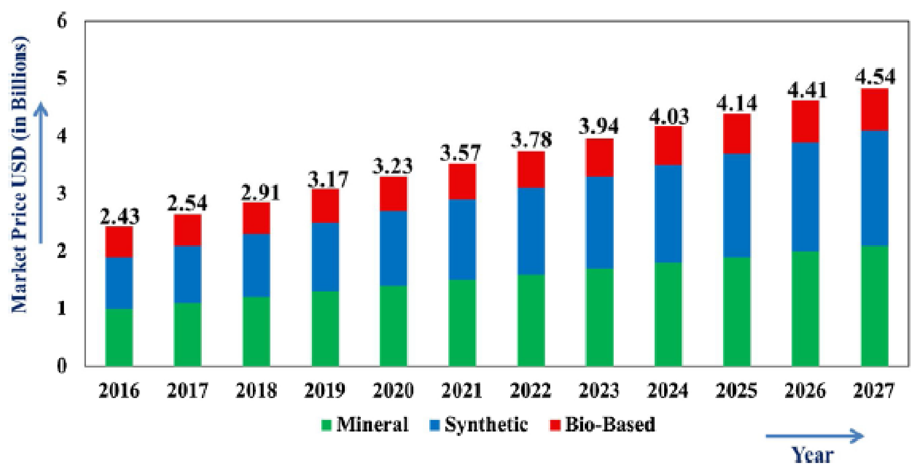

Figure 1-3: Market share of MCFs in the United States in Billions [25]

In 2014, the Faculty of Engineering (FOE), University of Ruhuna (UOR), started investigating coconut oil as an MWF. In 2017, they developed a novel coconut oil and tested it against mineral oil-based MWFs, demonstrating that it outperformed the available conventional MWFs [31]–[34]. They investigated the novel coconut oil with MQL technology in 2019 [35], [36]. As described in the preceding paragraphs, adding nanoparticles to pure base fluid improves its performance. Figure 1-4 depicts the future direction of cutting fluids containing nanoparticles, as determined by H. Babar et al. [37]. FOE, UOR has created a novel coconut oil formulation and tested it under MQL conditions; the next step is to improve its thermophysical and tribological capabilities by including nanoparticles. By undertaking this research, the author intends to fill this gap.

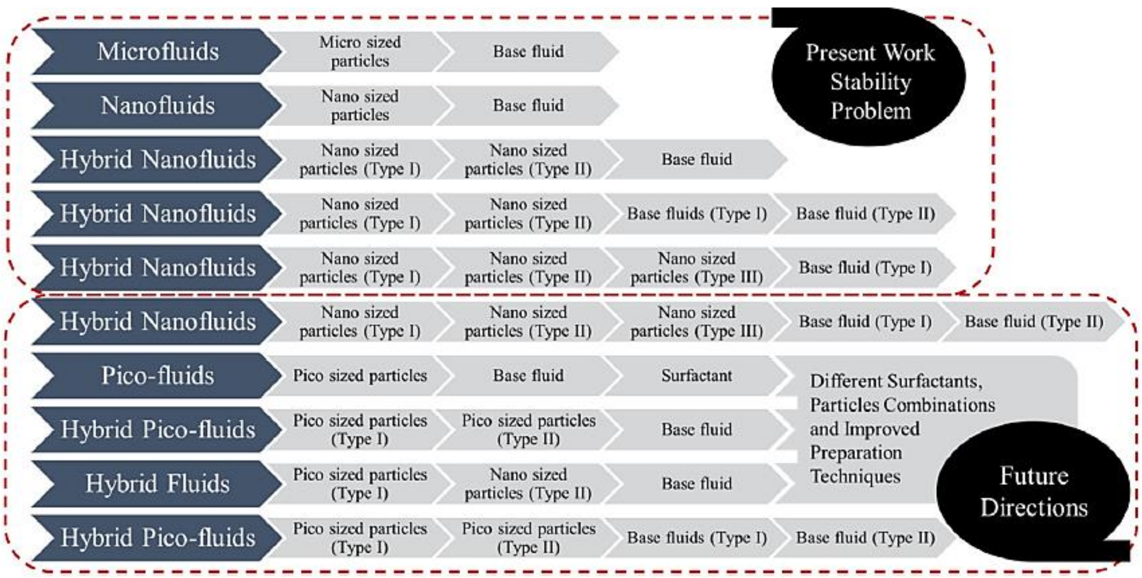

Figure 1-4: Present and future direction of nanofluids [37]

Based on the above introduction, cooling, lubricating, and removing chips from the cutting zone are the basic requirements of metalworking fluid, and the MWFS has become a more researchable field over time.

1.1 Aim

Investigate the effect of hybrid nanoparticles based on coconut oil metalworking fluid on tooltip temperature and surface roughness when turning AISI 1045 steel using MQL technology.

1.2 Objectives

Determine the effect of nanoparticles on vegetable oil base metal working fluid in the context of minimum quantity lubrication technology.

Determine the most significant parameters for minimum tooltip temperature and surface roughness with coconut oil-based MWFs using MQL technology.

Fitting a mathematical model to represent the tool temperature and surface roughness with MWFs based on coconut oil with nanoparticles using MQL technology.

Make recommendations for optimal variable settings for effective machining.

1.3 Methodology

Based on the problem definition, the literature review is conducted to rectify the significant variables and nanoparticles. Again, based on the literature survey, the process factors and screening of those factors were undertaken to determine the significant ones. To fulfil the first two objectives, choosing an appropriate experimental design and conducting the necessary tests are necessary.

Based on the chosen DOE, results must be analyzed. Then predict, the model and the model's fitness is evaluated. Finally, the actual and anticipated variations are compared. Once the objective has been attained, optimization must be performed. A confirmation test was done to compare the proposed model to actual behaviour. Figure 1-5 is a flowchart summarising the methodology described in this section.

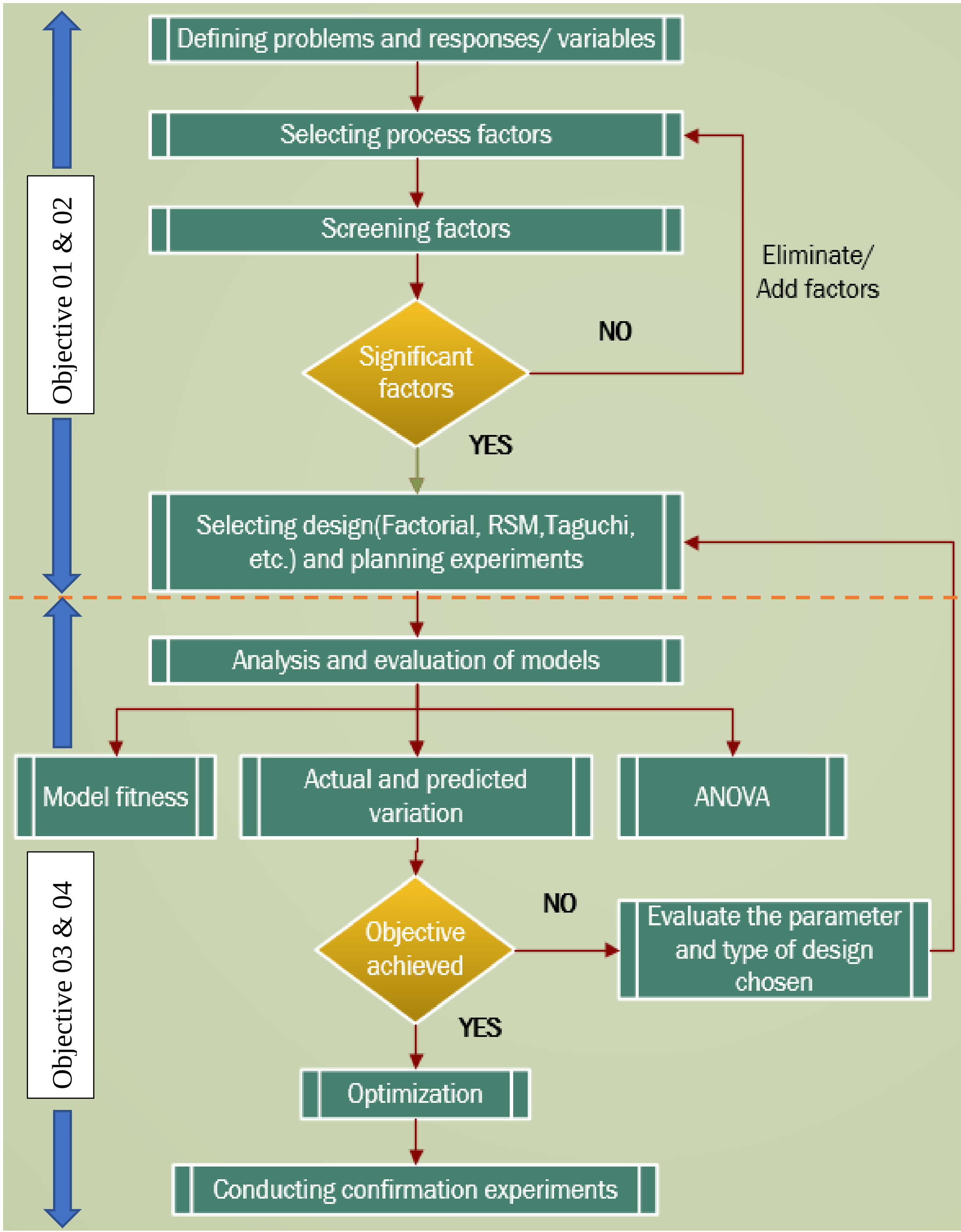

Figure 1-5: Research methodology

1.4 Thesis Overview

This dissertation is divided into five Chapters. The author has discussed the research's background in the first section of this study. The second section goes over the literature review. The third section discusses the methods that were used. In chapter four, the outcomes of the experiments and their analysis are explained. It further includes findings and analysis. The fifth chapter summarizes the findings and future research recommendations.

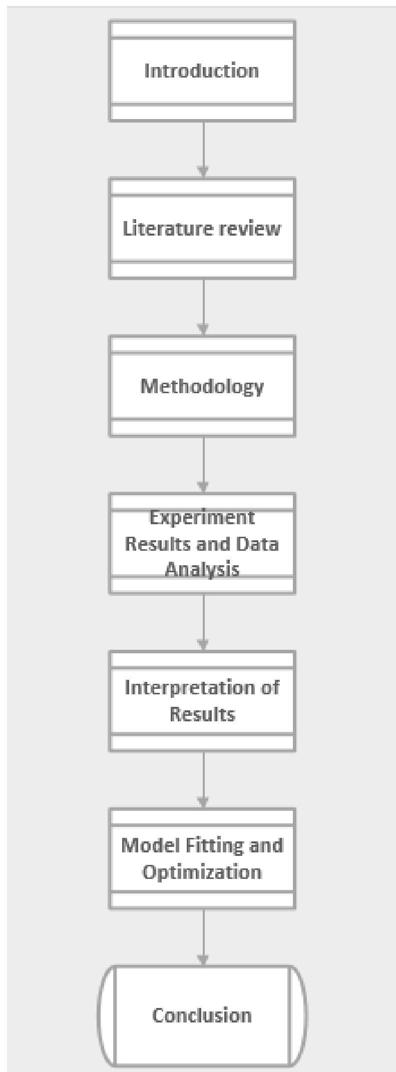

Figure 1-6: Thesis flow

2 CHAPTER: LITERATURE REVIEW

This chapter provides a comprehensive account of the development of cutting fluids and cooling and lubricating techniques. In addition, the author has carried out another review in which turning, milling, and drilling operations were taken into consideration in order to investigate the effect of nanoparticle behaviour with vegetable oil to select nanoparticles for the experiments in order to investigate suitable nanoparticles for the investigation. After that, the author researches the factors that influence surface roughness and the tool's temperature.

2.1 Evolution of Cooling/ Lubricating and MWF

2.1.1 Cooling and Lubricating

Regarding the cutting criteria, cutting speed is one of the most important aspects influencing performance. The generated heat between the workpiece-tool and tool-chip increases as the cutting speed is increased due to friction, and this needs to be reduced. Simultaneously, producers strive for high production rate, dimensional precision, surface finish, high quality, cost reduction, and low environmental effects. To overcome those issues, a considerable quantity of cutting fluid is pushed to spray onto the cutting zone to cool and lubricate the tool–chip and tool–work interface. As a result, produced friction and temperature are decreased. This process produced little tool wear, a good surface, and low cutting forces during machining. Even with all these advantages, cutting fluids have disadvantages, including transportation challenges, disposal issues, the fluid's toxicity, and environmental pollution, including water pollution, soil pollution, and air pollution. As a result of these factors, machining operations face a new challenge. As depicted in Figure 2-1, Sharma et al. summarized various cooling strategies for lowering the generated cutting zone temperature in 2009 [38]. These included flood cooling, MQL/NDM, high-pressure coolants, solid lubricants, and compressed air/gas coolants, among others. The evolution of cooling techniques in machining is briefly explained in the below paragraphs.

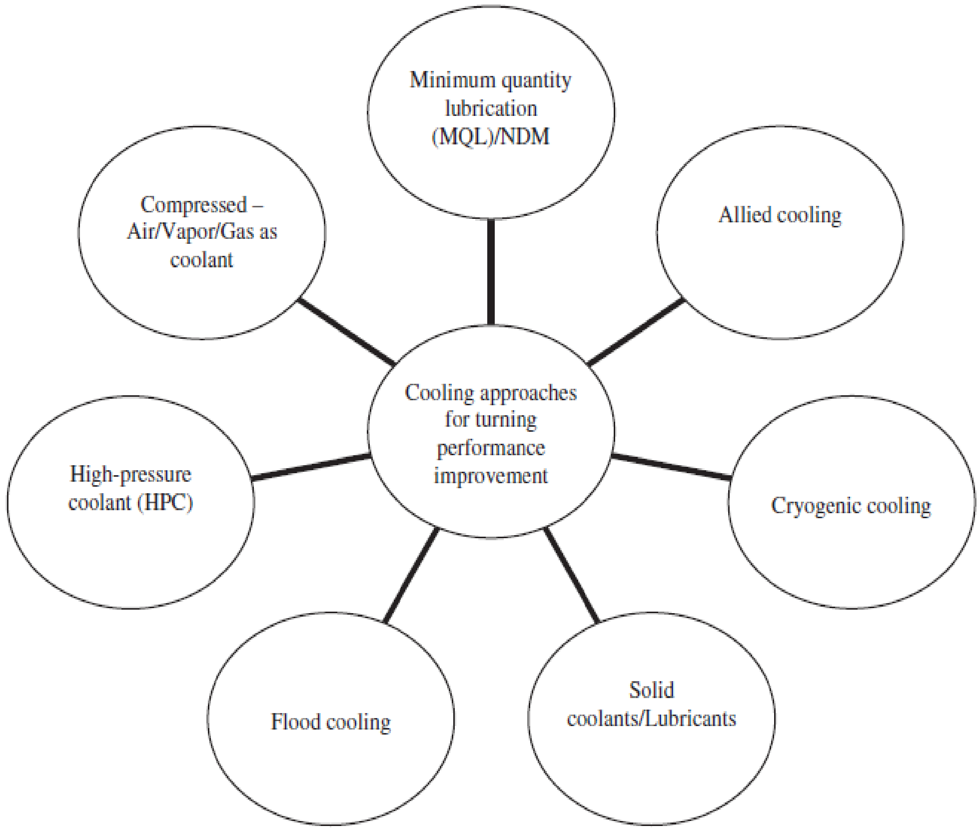

Figure 2-1: Techniques for the reduction in heat generation during turning [38]

i. Dry Machining

Dry machining, in which no cutting fluids are employed, is characterized by modest cutting speeds and easily machined materials. This method eliminates problems associated with cutting fluid, such as contamination, disposal, and harmful components, but ultimately the finished product may not have a good surface finish or accurate dimensions. This occurred due to increased heat generation during the machining process; increased heat increases the likelihood of the built-up layer forming. Because of its unstable nature, this built-up layer breaks and removes a portion of the tool material, resulting in tool wear. The broken segments deteriorate the surface finish when stuck to the machined surface. Thus, dry machining without lubrication or cooling enhancement is not recommended [39]. To address these issues, technology advances into the wet machining process.

ii. Wet Machining

Wet machining is classified into several types, some of which are described below with basic characteristics.

a) Conventional Flood Cooling

Flooding is the most common method in the machining industry to achieve cooling and lubrication functions, and it is typically used with coolant-type cutting fluids. This approach produces a continuous liquid supply onto the tool-workpieces, a too-chip interface for machining operations. For single-tooth to multiple-tooth cutters, the usual flow rates range from 10 l/min to 225 l/min. Tool flooding from the chip side is the most typical way of flooding. Flooding cutting fluid is more effective in cooling the clearance face, especially when the pressure is above 300 kPa [40]. There are, however, drawbacks to using cutting fluids, including the following.

- Elimination of waste-cutting fluid
- The price of the cutting fluid
- The distribution of cutting fluid throughout the machine.
- Harmful residuals
- The discarding of soggy chips
- Less visibility

b) Minimum Quantity Lubrication (MQL)

When looking at a general viewpoint of the machine industry, Flood coolant use in machine shops demands considerable maintenance to monitor coolant conditions and fix up leaks that constitute a health and safety risk in the workshop. However, as mentioned above, the negative impacts on higher temperatures, tool life, and poor achievement make it not applicable to most situations. Therefore, MQL has the potential to aid in extending tool life and improving machining performance in surface finish, cutting forces, and process capabilities, even when users have a defined dry-cutting process [41]. With MQL technology, the cutting zone only receives a trickle of a highly efficient coolant crushed in a compressed gas stream, as opposed to the standard coolant flow of 120,000-720,000 ml/h (2-12 l/min) [42].

c) Nano-Lubrication

According to the findings of certain researchers, MQL performs significantly better during low-speed and medium-speed machining processes, but it is completely ineffective during high-speed machining. That is because, at high-speed operation, the coolant cannot reach the cutting region [43]. Then, researchers became interested in combining synthetic and vegetable oils with macro and micro-sized solid particles. This mixture provided superior thermal conductivity and lubricity at high-speed machining compared to the pure MQL system. Even though micro-sized particles (<100nm) had improved cooling characteristics, their usage in MQL machining was limited due to clogging and stability issues [18]. Nanofluids typically have additives such as carbon nanoparticles, non-metallic nanoparticles, metal nanoparticles, and nano-droplets. Hussain H et al. classified nanoparticles, as shown in Figure 2-2 [44].

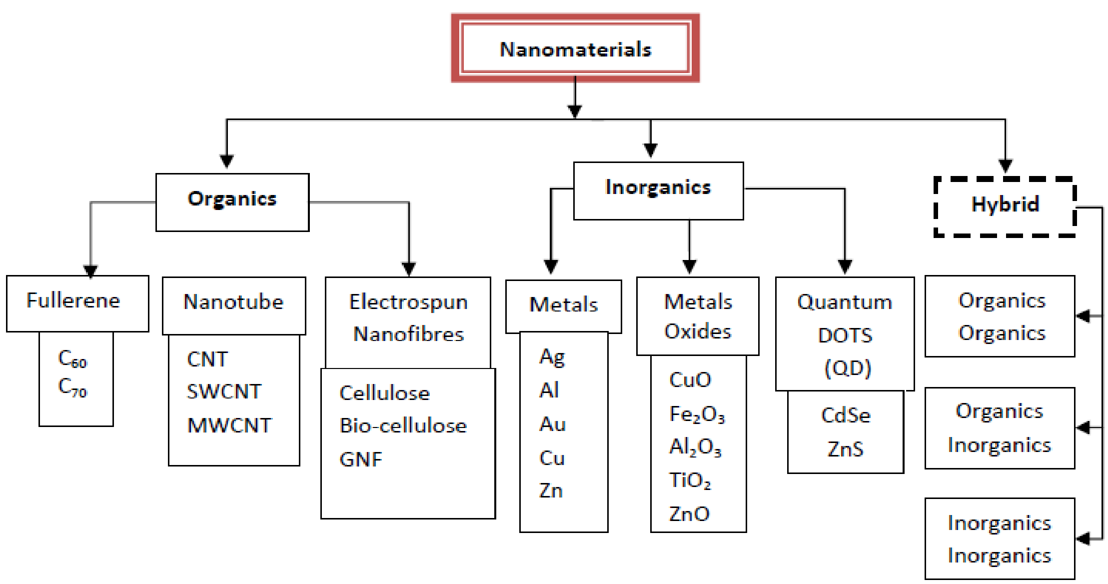

Figure 2-2: Classification of nanomaterials [44]

2.1.2 Metal Working Fluid

In the manufacturing business, cutting fluids are the standard solution for dealing with heat created during machining. As shown in Figure 2-3, Baradie categorized cutting fluids in 1996, along with the development of nanodroplet cutting fluids (NDCFs)[10].

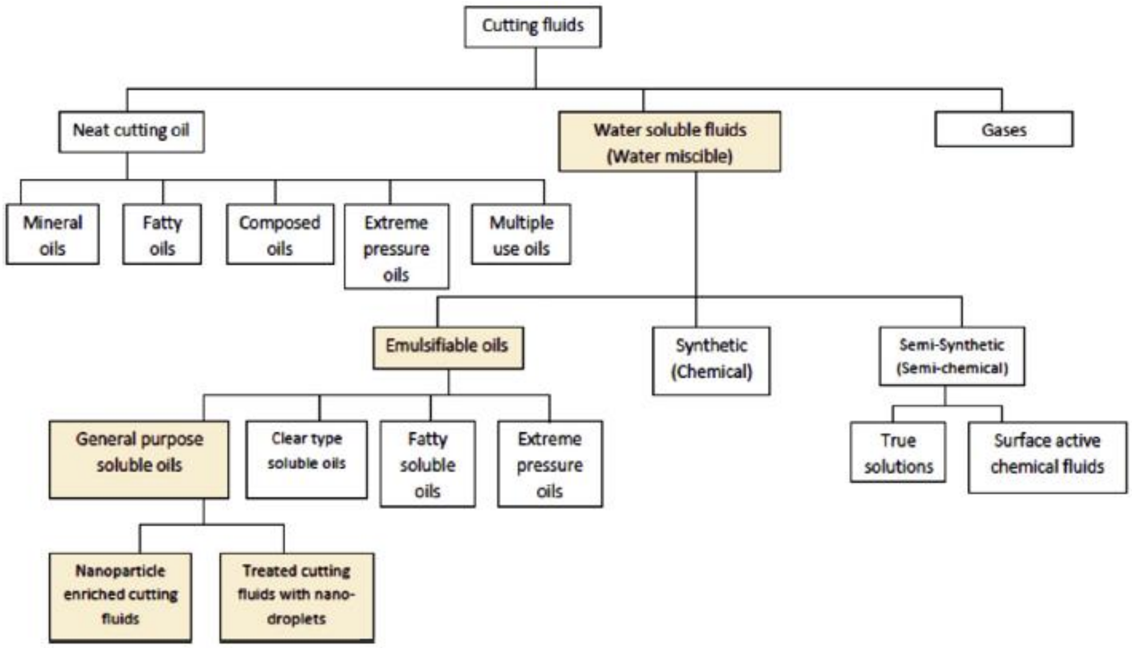

Figure 2-3: Cutting fluid classification [10]

2.2 Machining with Vegetable Oil-Based Nanofluids

Vegetable oil containing nanoparticles improves the cooling capabilities of MWFs, according to a significant number of researchers. This new cutting fluid can be used in various machining techniques, and this section illustrates how they affect key machining performance metrics.

2.2.1 Turning

Lubricants were made by dissolving nano boric acid particles in SAE-40 and coconut oils. [45]. In this experiment, cutting temperatures increased with increasing speed regardless of nano-lubricant but were lower with coconut oil than with SAE-40 oil, according to P.V. Krishna et al. Further, in all lubricating conditions, cutting temperatures increased as the feed rate increased. Also, it is observed that lubricants based on coconut oil have a higher heat transfer coefficient than lubricants based on SAE-40 oil, and suspensions of coconut oil are consistently superior to those of SAE-40 oil. The superior lubricating properties of coconut oil are due to the fundamental composition of vegetable oil molecules and the oil's chemical structure.

Surface roughness, tool wear, cutting force, and temperature were all reduced in Inconel 600 alloy MQL machining with 6 vol. % Al_2O_3 particle nanofluids, as reported by V. Vasu et al. [11]. Also, the experimental results indicate that the feed rate is the most influential factor on surface roughness, whereas the depth of cut is the most significant factor on temperature.

M.M.S. Prasad et al. found that the percentage of nano graphite in the fluids increases, and it appears that fluid properties and machining responses, such as tool-workpiece temperatures, surface roughness, and tool wear, improve [46]. At this time, the best combination appears to be 0.3% nano graphite particle inclusions at a flow rate of 15 ml/min.

A reduction in cutting forces of 8.8% and a reduction in workpiece surface roughness of 7.5% were observed in 2014 for cutting fluids containing nanoparticles recorded by L. Prabu et al. it was noticed that the addition of silver nanoparticles to the cutting fluid significantly decreased tool tip temperature, cutting force, and workpiece surface roughness [47].

For the responses of tool life, cutting forces, and temperature, $nMoS_2$ nanoparticles in the base fluid are more effective than $mMoS_2$ nanoparticles, according to R. Padmini et al., who studied H_3BO_3 and MoS_2 nanoparticle-based machining [48]. Also, they did another research (2015) focusing on three separate base fluids. These are Canola oil (CAN), Sesame oil (SS), and Coconut oil (CC). It has been shown that 0.5 percent CC + $nMoS_2$ has the best machining performance of all the lubricant conditions. CC + $nMoS_2$ at 0.5 percent nanoparticle inclusions reduces cutting forces, temperatures, tool wear, and surface roughness by about 37%, 21%, 44%, and 39% compared to dry machining, respectively [12].

A.K. Sharma et al. evaluated that, using a mist of nano-cutting fluid in machining, In comparison to dry, conventional mist, and wet machining, the average surface roughness of the workpiece is reduced by 47.8%, 29.1%, and 25.5%, respectively [49]. In addition, it was discovered that increasing the concentration of nanoparticles improved the thermal conductivity, viscosity, and density of nanofluids while decreasing the specific heat. Also, TiO_2 nanoparticles were used in another study by the same authors, and the results show that tool wear was reduced by up to 58.1% when using dry machining and by 35.85% when using conventional mist machining [50]. Additionally, it decreased cutting force by 62.7%, 33.9% (dry mist), and 35.7% (wet mist) compared to dry machining.

Nanofluid MQL performed better than other nanofluids because of its excellent heat-carrying capability, according to M. K. Gupta et al. [51]. Chetan et al. found that the average surface roughness was reduced by 47.8%, 29.1%, and 25.5% when nano-cutting fluid was used during turning compared to dry machining, standard mist, and wet machining, respectively [52].

Andhare et al. discovered in 2017 that MWCNT-based nanofluids had been reported to reduce tool wear by 49% and 30% compared to machining without any fluid and with mineral oil-based fluids [53]. Further, compared to conventional cutting fluid, using nanofluid reduced cutting force by 5% to 8% while improving surface finish by 9% to 22%.

B.C.Behera et al. recorded that the wetting behaviour of nanofluids led to decreased chip curling radius, tool wear, and coefficients of friction [54]. In 2018, M. Ukamanal et al. found that 0.03% concentrated nanofluid was found that the tool temperature and the chip temperature were found to be minimum [55]. R.K. Behera et al. investigated that MQL machining with nanofluid outperforms traditional dry machining and MQL machining with vegetable oils in terms of cutting performance [56]. K.Venkatesan et al. investigated that ribbon chips are seen in different sizes, and the curl diameter increases by increasing the nanoparticle concentration [57].

M. Sarkaya et al. executed hBN nanoparticle-based turning for Ni-based Inconel 625 and discovered that the best surface quality was obtained under cooling conditions with nano-MQL containing 0.5vol% hBN. In terms of cooling/lubricating conditions, the cutting fluid containing 1% hBN exhibited the lowest temperature [58]. Pure MQL, nano-MQL (0.5vol %), and nano-MQL (1vol %) showed temperature improvements of 12.45%, 16.91 %, and 30.25%, respectively, compared to dry cutting.

It was discovered in 2019 that nanofluid with 0.25% alumina nanoparticles performed best at 100 ml/min and a feed rate of 0.14 mm/rev when tested by K.Venkatesan and colleagues using coconut oil as the base fluid [59]. C.V. Yıldırım et al. observed that when nano-additives were compared, 0.5 vol% hBN produced better results than Al_2O_3 because hBN has a higher heat coefficient than Al_2O_3 [60]. When compared to dry machining, the utilization of MQL and liquid nitrogen resulted in a temperature improvement of 26.8% and 45.6%, respectively, in the tool-chip contact temperature. Furthermore, the recovery temperature increased by 58.3% when mixing liquid nitrogen and nanofluids. Additionally, the level of improvement in surface roughness increased when the 0.5vol% hBN+LN2 technique was utilized. Surface quality was 44.5% higher with the 0.5vol% hBN+LN2 technique than with dry machining.

A.K. Sahoo et al. compared the machinability of Al_2O_3 and TiO_2 nanoparticles at 0.005 wt.%, 0.01 wt.%, and 0.05 wt.% [61]. Compared to nano Al_2O_3, nano TiO_2 cutting fluid has a better result due to its superior lubricity and wetting properties. It could also be due to Al_2O_3's larger particle size when compared to TiO_2.

In 2019 M. Khajehzadeh et al. observed that TiO_2 nanofluid reduces VB_{max} by an average of 35.9% when compared to dry cutting, according to the results of this study, and increases the concentration of nanoparticles from 0.5% to 3%, and the VB_{max} decreases from 30.1 to 41.3% [62]. S.S. Rahman et al. evaluated an excellent surface finish achieved by using a canola nanofluid containing 0.5% Al_2O_3, and canola nanofluid enriched with

0.5 volume percent Al_2O_3 produced a superior nanofluid. MoS_2 has been discovered helpful in temperature reduction and r_c enhancement [63]. H. Hegab et al. studied Ti-6Al-4V with nano-particle-based near-dry machining (MQL) and found the best performance when the cutting speed of investigated three types of nanoparticles (Al_2O_3, CuO, and Fe_2O_3) and found that CuO nanofluid demonstrated the best performance, followed by Fe_2O_3 nanofluids and Al_2O_3 nanofluids in that order [64].

Q. Song et al. evaluated that, MoS_2 and graphite-based nanofluids both performed well at high cutting speeds; however, graphite-based nanofluids outperform the other two nanofluids in terms of cooling and lubrication properties, and Inconel-800 alloy's machinable qualities are vastly enhanced by a small amount of graphite in vegetable oil [65].

2.2.2 Milling

P.Y. Kwonet el. revealed that vegetable oil with xGnP added to it increased wettability on the cutting surface and decreased surface friction; however, xGnP with a bigger diameter did not form a stable suspension in vegetable oil, leading to the segregation of graphene and oil [66]. A concentration of 0.1wt% xGnP with a 1 μm diameter demonstrated excellent cutting performance with no segregation issues.

In 2016 M.S. Najiha et al. investigated that milling with a nanofluid based on titanium dioxide and water; results in less chipping, a faster cooling rate, and a lubricating effect [67]. According to the findings of M.M. Rahman et al., only 0.5% of nano-particles experience built-up edges as a consequence of inadequate lubrication [68]. Nano-particles with a fraction of 4.5% nanoparticles did not give the anticipated level of lubrication either. That is because the nano-particle pumping is done at constant pressure and has a higher density. Regarding the potential for tool damage, nanoparticle percentage fractions of 2.5% appear more feasible. When the cutting speed was increased, it was observed that the edge remained intact, in contrast to the edge breakage that occurred when the cutting speed was lower.

In MQL milling, Alper Uysala et al. found that the lubricating effect of $nMoS_2$ particles in the cutting fluid reduced tool wear and surface roughness [69]. T. Kıvak et al. found that A significant improvement in tool life was achieved through nanofluids, as tool wear was reduced significantly compared to the dry and base oil states [70]. B. Sen et al. investigated that Adding 1% silica-deposited nanofluid resulted in an increase in tool life, a reduction in chip curvature, and a simultaneous minimization of roughness and milling force [71].

2.2.3 Drilling

S.W. Lee et al. found that increasing the amount of ND added to paraffin oil to 1 vol% was more effective than increasing it to 2 vol% [39]. In order to achieve good performance in reducing the drilling torque and thrust force when machining with vegetable oil, it was necessary to use two-volume percent of ND. Lubrication with compressed air results in a greater increase in the number of drilled holes than does the use of nanofluid.

Micro-drilling with a 2 wt% nanodiamonds/MQL mixture decreases burr formation, consumed power, and torque compared to dry and increases tool life, as demonstrated by W.T. Huang et al. [72]. Nanoparticle deposition on the surface and physical film formation, which may reduce friction and wear, are the anti-wear mechanisms suggested by T. Singh et al. that MQL-based vegetable oil nanofluid shows excellent performance in friction and wear reduction [73].

Findings from nanofluid research by J. Zhang et al. show that nanofluid density significantly impacts torque and power consumption. The minimum torque and thrust forces are achieved at the nanofluid concentrations of 1.4 vol% and 4 vol%, respectively [74].

Work-piece surface roughness and drilling temperature were found to be significantly reduced when TiO_2 nanoparticles were dissolved in soluble oil during drilling, as discovered by S. Z. Heris et al. Adding nanoparticles to the base fluid and then increasing the concentration improves the convective heat transfer coefficient even further [75] and

2017 they conducted another experiment and concluded that improved heat transfer rate and reduced operating temperature were found to be achieved by using a soluble oil-based TiO_2 nanofluid in the drilling procedure, with the concentration of TiO_2 being an important factor. The thermal and lubricating properties of soluble oil-based TiO_2 nanofluid make it a viable alternative [76].

Thermal conductivity and good heat transfer coefficients resulted in better cooling and eliminated microchipping, resulting in less tool wear, according to a study by S. Muthuvel et al. (2018). Tool wear was reduced by 73% and 62% on conventional coolant and oil conditions. Compared to traditional technology, 71% less surface roughness and 53% less flank wear has been found to be achieved [77].

Iron nanoparticles in Jatropha oil were studied by B. Sopko et al. in 2018. Improved lubrication and cooling can be achieved by adding nanoparticles to Jatropha oil. After drilling to a depth of 10 millimetres, the temperature of all samples gradually increased, peaked, and then gradually decreased. Only the main cutting edges and dead center of HSS drill bits for all fluid models show signs of wear [78]. P.J. Liew et al. observed that using the nanofluid resulted in lower cutting temperatures and surface roughness than using the base fluid [79]. S.W. Lee et al. investigated that, when using the nanofluid, there was a significant reduction in friction in the drilling region. Additionally, there was a reduction in thrust forces, drilling torques, and tool wear [80].

According to the review, adding nano additives to a base fluid can improve the lubricant's heat transfer, anti-abrasion, and anti-friction properties. The temperature within the cutting zones is reduced due to improved heat transfer characteristics, which reduces cutting tool temperatures and wear mechanisms.

Nanofluids' MQL parameters and wetting characteristics, tribological and thermophysical properties influence process performance, according to S. Chinchanikar et al. When a specific type of nanoparticle or a combination of nanoparticles is added to the nanofluids, the MQL's working performance has been observed to vary significantly [43].

Based on the above literature, it is clear that adding nanoparticles into vegetable-based MWFs improves the performance of the base fluid, such as increasing surface finish, dimensional accuracy of the workpiece, low tool wear, etc. Table 2-1 shows the summarised details for a section of the nanoparticles.

Table 2-1: Literature to select nanoparticles

No	Reference	Operation	Nanoparticle	Base fluid	Particle size	Workpiece
1	S.W. Lee et al. [81]	Drilling	Nano Diamond	Paraffin oil and Vegetable oil	30 nm	Aluminum 6061
2	W.T. Huang et al. [82]	Drilling	Nano Diamond	Vegetable oil	-	7075-T6 aluminum alloy
3	T. Singh et al. [73]	Drilling	Al_2O_3	Refined soybean oil	20 nm	Aluminum 6063
4	J. Zhang et al. [74]	Drilling	Nano Diamond	Vegetable oil	-	-
5	S.Z. Heris et al. [83]	Drilling	TiO_2	Soluble oil	20 nm	-
6	S.Z. Heris et al. [76]	Drilling	TiO_2	Soluble oil	20 nm	-
7	P.Y. Kwonet el. [84]	Milling	xGnP	Vegetable oil	10 nm	-
8	M.Amrita et al. [85]	Turning	NG, NBA, $nMoS_2$	Water-based soluble oil	80nm,100nm, 100 nm	AISI 1040
9	R. Padmini et al. [48]	Turning	H_3BO_3, MoS_2	Coconut (CC), Sesame (SS)	-	AISI 1040
10	R. Padmini et al. [86]	Turning	$nMoS_2$	Coconut (CC), Sesame (SS) Canola (CAN) oils	-	AISI 1040
11	M.K. Gupta et al. [87]	Turning	Al_2O_3, MoS_2, Graphite	Vegetable oil	40 nm	Titanium (grade-2) alloy
12	B. Sen et al. [71]	Milling	SiO_2	Palm oil	5 nm	INCONEL® alloy 690
13	A. Uysala et al. [69]	Milling	MoS_2	Vegetable oil	-	AISI 420

No	Reference	Operation	Nanoparticle	Base fluid	Particle size	Workpiece
14	A.K. Sharma et al. [88]	Turning	SiO_2	Vegetable oil-water emulsion	-	AISI 1045
15	Chetan et al. [89]	Turning	Al_2O_3, Ag	Water + sunflower oil	-	Nimonic90alloy
16	A.K. Sharma et al. [49]	Turning	Al_2O_3	Vegetable oil-water emulsion	-	AISI 1045
17	A.K. Sharma et al. [50]	Turning	TiO_2	Vegetable oil-water emulsion	-	AISI 1040
18	P.V. Krishna et al.[45]	Turning	H_3BO_3	SAE-40 and Coconut oil	50 nm	AISI 1040
19	M. Sarıkaya et al. [58]	Turning	hNB	Vegetable-based oil	-	Ni-based Inconel 625
20	K. Venkatesan et al. [59]	Turning	Al_2O_3	Coconut oil	-	Incoloy 800H
21	C.V. Yıldırım [90]	Turning	Al_2O_3, hBN	Vegetable oil	70 nm, 70 nm	Inconel 625
22	M.M.S. Prasad et al. [46]	Turning	Nano-graphite	Water soluble oil	80 nm	AISI 1040
23	K.Venkatesan et al. [91]	Turning	Al_2O_3	Coconut oil	40 nm	Inconel X-750
24	T. Kıvak et al. [70]	Milling	Hbn, MoS_2 & graphite	Vegetable oil	80 nm, 80 nm, 80 nm	Inconel X-750 superalloy
25	S.W. Lee et al. [92]	Drilling	Diamond	Vegetable oil	-	Titanium Alloy (Ti-6Al-4V)
26	S. Muthuvel et al. [77]	Drilling	Copper	Coconut oil	70 nm	AISI 4140

No	Reference	Operation	Nanoparticle	Base fluid	Particle size	Workpiece
27	B. Sopko et al. [78]	Drilling	Iron	Jatropha oil	25 nm	CSN 11 523
28	S.W. Lee et al. [80]	Drilling	Nano Diamond	Vegetable oil	35 nm,80 nm	Titanium Alloy(Ti-6Al-4V)
29	S.S. Rahman et al. [93]	Turning	TiO_2, Al_2O_3, MoS_2	Canola, Extra virgin olive oil	100 nm, 135 nm, 135 nm	Titanium Alloy(Ti-6Al-4V)
30	H. Hegab et al. [94]	Turning	Al_2O_3	Rapeseed oil	22 nm	Titanium Alloy(Ti-6Al-4V)
31	Q. Song et al. [95]	Turning	Al_2O_3, MoS_2 & graphite	Sunflower oil	Average 40 nm	Inconel-800 Alloy
32	S.R. Das et al. [64]	Turning	Al_2O_3, CuO, Fe_2O_3	Rice bran oil	Average 50 nm	AISI 4340
33	V. Vasu et al. [96]	Turning	Al_2O_3	Vegetable oil	-	Inconel 625 alloy
34	R.K. Behera et al. [56]	Turning	Al_2O_3	Vegetable oil	-	Inconel 600
35	H. Hegab et al. [97]	Turning	MWCNT	Vegetable oil	13 to 20 nm	Ti-6Al-4V
36	S. Datta et al. [98]	Turning	MWCNT	Rice bran oil	10 to 15 nm	Ti–6Al–4V Superalloy
37	S. Datta et al. [99]	Turning	MWCNT	Coconut oil	10 to 15 nm	Inconel 718
38	M.S. Kumar et al. [100]	Turning	MWCNT	Coconut oil	12 nm	stainless steel 420 grade
39	H. Hegab et al. [101]	Turning	MWCNT, Al_2O_3	Vegetable oil	13 to 20 nm, 20nm	
40	Chetan et al. [52]	Turning	Al_2O_3, Ag	Sunflower	40 nm, 10 nm	Nimonic 90

No	Reference	Operation	Nanoparticle	Base fluid	Particle size	Workpiece
41	Q. Song et al. [95]	Turning	Al_2O_3, MoS_2 & graphite	Sunflower oil	40 nm	Inconel-800 Alloy
42	Mayurkumar A. et al. [102]	Turning	$nMoS_2$	Pure palm oil	70 to100 nm	Inconel 718
43	R. Padmini et al. [103]	Turning	$nMoS_2$	Pure coconut oil, sesame oil, canola oil	-	AISI 1040
44	J. Wang et al. [104]	Grinding	MoS_2, Al_2O_3	Pure palm oil,	Average 50 nm	Inconel 718, ductile cast iron, and AISI 1045 steel
45	T.T. Long [105]	Turning	Al_2O_3 + MoS_2	Soybean oil	45 nm,30 nm	AISI 304
46	K.R. Watto et al. [106]	Turning	Al_2O_3 + GnP	Vegetable oil	-	AISI 304
47	Jamil et al. [107]	Turning	Al_2O_3 + CNT	Vegetable oil	30 nm,10 to 30 nm	Ti-6Al-4V
48	M.S. Kumar et al. [108]	Turning	Al_2O_3 + CuO	Coconut oil	-	En24 Steel
49	Gogulothu et al. [109]	Turning	MWCNT + MoS_2	Sesame oil	30 nm,30 nm	AISI 1040

2.3 Nanoparticles with Base Fluid

As per the above review, several lubricants are used as base oils for metalworking fluids in manufacturing industries. Common base oils include water, distilled water, mineral oil, synthetic oil, and vegetable oil, among others. Some pure or unrefined base oils are chemically unbalanced and have a limited shelf life, causing corrosion. The addition of additives then enhances the base oil. Additives vary based on the chosen base oil. Additives are chemical ingredients that enhance base oil performance by reducing their unfavourable qualities. Others are anti-wear, anti-corrosion, and anti-oxidant. Adding additives to base oils makes them more stable and user-friendly.

As mentioned in literature reviews, the size and shape of nanoparticles and their concentration in base fluids are the most critical factors affecting machining performance. Additionally, the machining process is influenced by nanofluid application methods and the process parameters such as spraying distance, nozzle orientation angle, air pressure, and cutting fluid flow rate, including flood, mist, and MQL [110]. The literature demonstrates that nanoparticle-mixed MWFs improve surface quality by increasing nanoparticle fractions during machining. However, improved lubrication can be achieved by rolling, sliding, and filming nanoparticles [111]. With nanoparticle-enriched cutting fluid, dimensional accuracy is improved, and furthermore, reduced tool wear, power consumption, machining zone temperatures, cutting forces, and friction in cutting zones, machining with nanofluids enhances efficiency [112]. According to the literature review, the performance of the process of nanofluid NDM is influenced by the tribological (wear and coefficient of friction) and thermophysical (thermal conductivity and viscosity) properties of the nanofluids used. The graphical representation of different mechanisms involved with nano lubricant is shown in Figure 2-4 [113]. In addition, the characteristics of nanoparticles differed depending on their concentration, type, shape, and size, as well as the base fluid's thermal conductivity used to synthesize the particles. NDM performance was discovered to be affected by the wetting properties (angle of contact) of a nanofluid droplet that changes with the quantity of nanoparticles in various lubricating media. However, only a few studies have established a link with MQL machining operations.

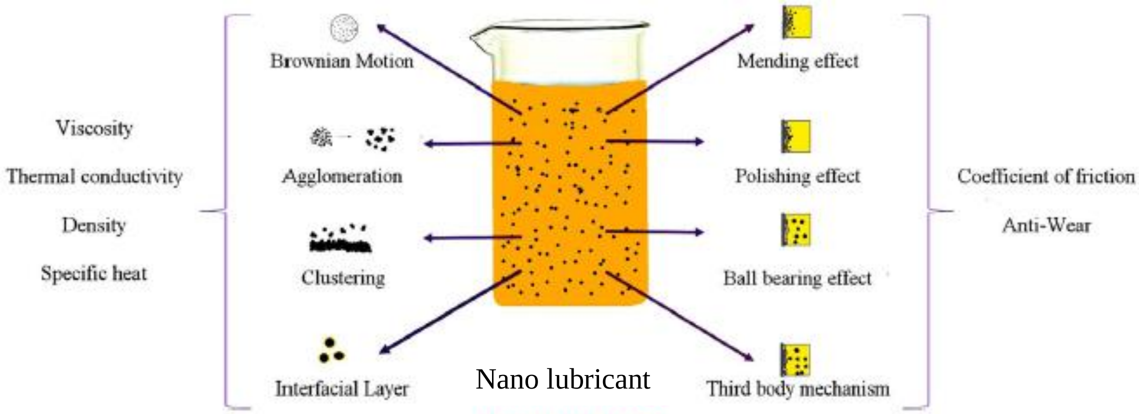

Figure 2-4: Graphical representation of different mechanisms involved with nano - lubricant [113]

Based on the literature, the most frequently used nanoparticles are listed below, as cited by S. Chinchanikar et al. [43], A M Zetty Akhtar et al. [114], and K. Venkatesh et al. [115].

- Multi-walled carbon Nanotubes (MWCNT)
- Zirconium dioxide (ZrO_2)
- Aluminum oxide (Al_2O_3)
- Nano boric acid (NBA)
- Hexagonal boron nitride (hBN)
- Titanium dioxide (TiO_2)
- Molybdenum disulfide (MoS_2)
- Copper oxide (CuO)
- Graphite Nanoplatelets (GnP)
- Nanodiamond (ND)
- Silicon dioxide (SiO_2)

And further, S. Chinchanikar et al. concluded that the most frequently used hybrid nanoparticles are,

- Al_2O_3 + GnP
- CuO + TiO_2
- Fe_3O_4 + SiC
- SiO_2 + Diamond
- ZrO_2 + CNT
- Al_2O_3 + CNT
- SiO_2 + GnP

According to R.K. Singh et al. [116], H. Muhammad Ali et al. [37], M.S. Kumar et al. [117], and A.R. Ibna Ali [118], the thermal conductivity of nanoparticles is shown in Table 2-2.

Table 2-2: Thermal conductivity of materials

Nanoparticles	**Thermal conductivity (W/ (m.K))**
Diamond	2300
MWCNT	2000–3000
SiC	490
Ag	429
Cu	398
Au	315
Al	247
Si	148
MgO	54.9
Al_2O_3	40
CuO	19.6
ZnO	100
TiO_2	20

2.4 Effects of Machining Parameters on Responses

In recent years, several investigations have been conducted to ascertain the optimum machining settings that will result in the lowest possible surface roughness and tool temperature [119]–[121]. As a result of this research, these factors have been divided into six major portions, which are depicted in Figure 2-5.

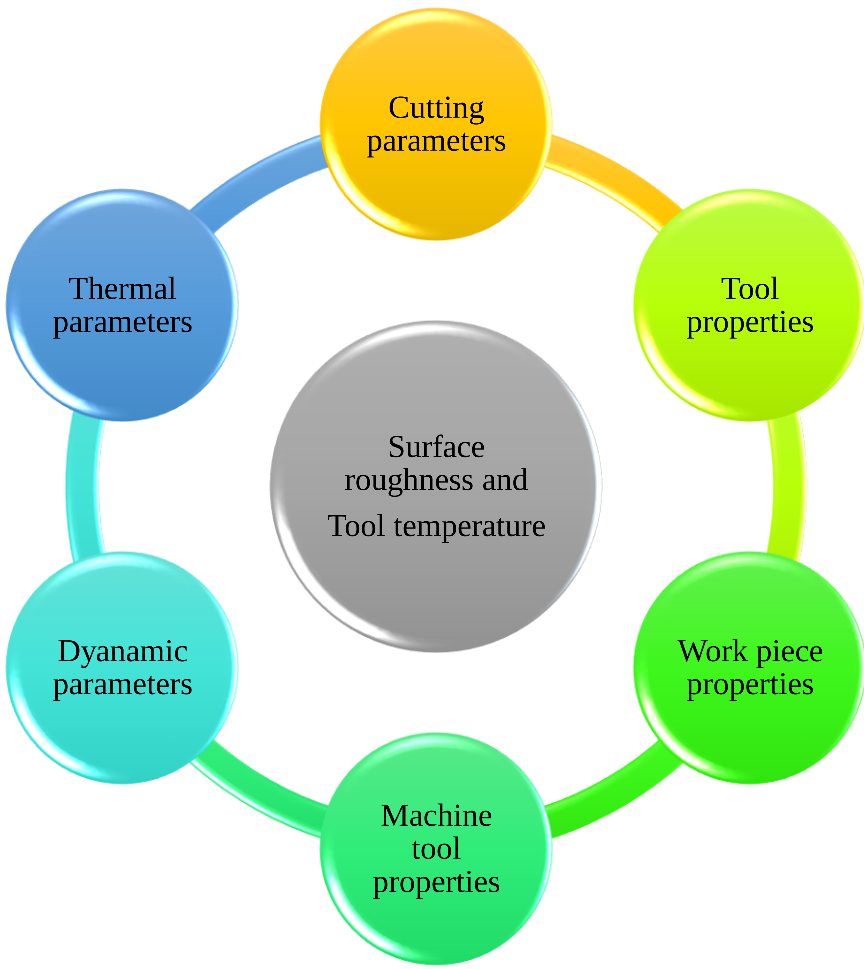

Figure 2-5: Factors affecting surface roughness and tool temperature

2.4.1 Cutting Parameters

According to S. Debnath et al. experiment, feed rate contributed 34.3% to work-piece surface roughness[122]. Further cutting fluid flow rate also contributed significantly (33.1%). Surface roughness was not affected by cutting speed or depth, and depth of cut

(35.8%) and cutting speed (43.1%) dominated tool wear. The greatest amount of tool wear was caused by cutting fluid (13.7%), while the feed rate contributed the least. The best conditions for surface roughness and tool wear were achieved with a low feed rate, a medium depth of cut, a high cutting speed, and low-flowing, high-velocity cutting fluid flow.

In 2011 V. Vasu et al. experimented by using Al_2O_3 nanoparticles with Inconel 600 and noticed that feed rate is the most influential element on surface roughness, whereas the depth of cut is the most significant factor on temperature [123]. Also, they noted that the feed rate and depth of cut are the main parameters that influence the cutting force and tool wear.

Akhil C. H. et al. studied the behaviour of the three cutting parameters (cutting speed, feed rate, and depth of cut) in relation to the tool temperature and determined that the tool temperature is affected most by the depth of cut, then by cutting speed and feed rate [124].

By analyzing the cutting forces and vibrations that happened throughout the turning process, Risbood et al. were able to create an accurate estimate of the surface roughness and dimensional deviation [119], [125]. The inputs for this process consisted of selecting the cutting speed, feed rate, and depth of cut, and the workpiece was steel bars. The depth of cut, feed rate, and cutting speed was discovered to have a substantially more significant effect on surface roughness than the steel bar's length and diameter. The chip removal action is enhanced when the feed rate is decreased, producing a surface of superior quality. However, when the feed rate was increased, there was a decline in surface quality.

The researchers Brezocnik and colleagues noticed in 2004 that the feed rate is the most important component determining surface roughness [126]. According to the findings of Mohd Zain et al., the best surface roughness could be accomplished by cutting at high speed with a radial rake angle while maintaining a low feed rate [127].

According to the literature summarized under "various machining operations (turning, drilling, and milling)" and "cutting parameters," the influencing factors of tool temperature and surface roughness are spindle speed, feed rate, feed direction, depth of cut, and the width of the cut relative to the diameter of the cutter. In addition, while other all the conditions and parameters are constant, the feed rate is the most influential element for surface roughness, while the depth of cut and cutting speed are the most influential factors for tool temperature.

3 CHAPTER: METHODOLOGY

The first section of this chapter is described the nanofluid preparation, including base fluid and nanoparticle selection strategies. Followed by the selection of machines and equipment with parameters based on the responses is explained. Then the experimental design selection is concluded, and finally, the setup arrangement is presented. Also, before the experiment, the prepared novel coconut oil was conducted for its thermophysical properties.

3.1 Base Fluid Preparation

Novel coconut oil developed by FOE, UOR, was used as the base fluid in this experiment (85 % water + 15 % oil). Eventually, samples of this base fluid were compared to mineral oil-based soluble oil for biodegradability, pH value, and viscosity. As a result of these tests, it was established that the produced metalworking fluid has better environmental compatibility with the mineral oil-based soluble oils already on the market [128], [129]. Based on the formulated weight percentage, two surfactants (PGPR and Tween 80) are created, and the base fluid is prepared using the identical processes described in the

Figure 3-1: Base fluid preparation; [a]- Preparing of PGPR and TWEEN 80 mixture; [b]- Adding coconut oil into the pre- prepared mixture and stirring; [c]- Adding water into pre- prepared mixture

literature, followed by white coconut oil, water, and a magnetic stirrer to create a good dispersion and stable base fluid preparation of based fluid shown in Figure 3-1.

3.2 Nanoparticle Selection for Experiment

Nanoparticles significantly alter and enhance the properties of the metalworking fluid. Several studies have examined various "machining applications" using different nanoparticles and vegetable oil-based metalworking fluids, and the following study is based on those applications.

The author has reviewed forty-nine literature papers (Table 2-2) that used MQL-based vegetable oil nano lubricants as MCFs. This literature study on vegetable oil-based nanoparticles attempts to identify two nanoparticles for the experiments. According to the review, there were no comparable parameter/s to measure the nanoparticles' performance. Because of this, the author decided to select the most popular nanoparticles from the specified literature study by employing the frequency of popularity as the first strategy.

The top five nanoparticles were selected based on the above strategy, and the next step was to reduce it up to two. The selected five nanoparticles are shown below in Table 3-1 with their percentage contribution.

Due to the limited available cost, the author decided to select the cost factor as the second criterion for nanoparticle selection. The cost comparison is shown in Table 3-2, and based on that; the author selected Al_2O_3 and TiO_2 as the two nanoparticles to conduct the experiments [130].

Table 3-1: Selected five nanoparticles

Nanoparticle	Percentage contribution
Al_2O_3	18
Nanodiamond	10
MoS_2	8
MWCNT	8
TiO_2	6

Table 3-2: Price comparison of selected nanoparticles [130]

Nanoparticle	Price
MoS_2	US $ 20.0-40.0 /kilogram
TiO_2	US $ 2.15-3.524 /kilogram
Al_2O_3	US $ 8.0-20.0 /kilogram
ND	US $ 800.0-835.0 /kilogram
MWCNT	US $ 99.0-160.0 /kilogram

3.3 Nanofluid Preparation

The formation of nanofluids involves spreading nanoparticles across a base fluid. In order for nanofluid applications to be successful, adequate dispersion is essential. As a consequence of this, surfactants are sometimes added to nanofluids in an effort to improve their stability. The stability of nanofluids may also be improved through surface modification of dispersed particles and high forces applied to clusters of scattered nanoparticles. Nanofluids are prepared using two fundamental techniques (Figure 3-2): single-step and double-step methods [131].

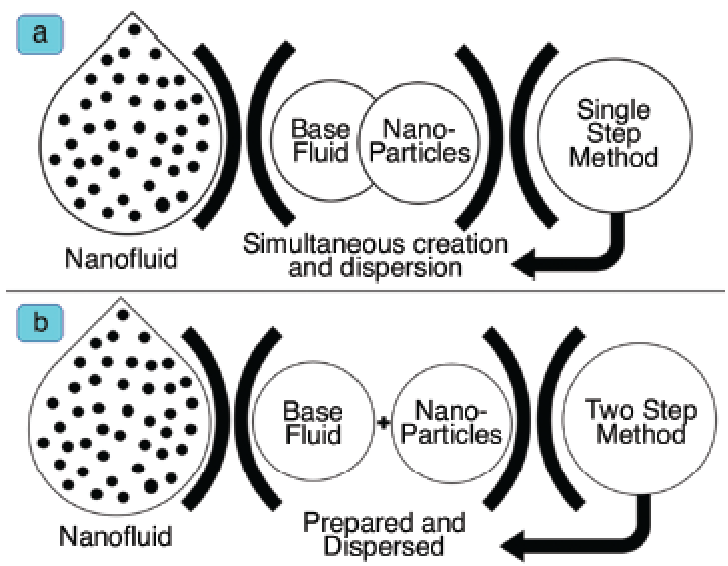

Figure 3-2: Preparation methods (a) One-step method (b) Two-step method [131]

The single-step method allows for simultaneous synthesis of nanoparticles and dispersion in base fluid; on the other hand, all procedures are completed in a single step.

Nevertheless, residual reactants are still present in the nanofluids, and the price is quite significant; these are the major disadvantages of the one-step method. As a result, the author decided to create the nanofluid in a two-step method. It is the least expensive way to produce hybrid nanofluids. There is no interdependence between the steps involved in preparing the nanoparticles and distributing them throughout the base fluid. Nanofluids can be created in bulk using this method, however, despite the prepared sample's stability duration being significantly shorter than that of the single-step technique. Cohesive and Van der Waals interactions between particles further complicate the issue of particle stability. Several more approaches can be utilized to overcome this problem besides the addition of surfactants, pH modification, magnetic stirring, ultrasonication, and high-pressure homogenization [4],[132]–[134]

The nanofluids were prepared with Al_2O_3 and TiO_2 nanoparticles imported from MKnano (a division of MK Impex Corp.), Ontario, Canada. The Al_2O_3 and TiO_2 Certificate of Analysis table is shown in Table 3-3. Each nanofluid type was synthesized at four different concentrations: 0 wt%, 0.25 wt%, 0.5 wt%, and 0.75 wt%, and the steps are shown in Figure 3-5. The nanoparticle concentrations to disperse in the base fluid were determined and weighted using a digital micro weighing scale (Figure 3-3 [a]). All concentrations were obtained by mixing the base fluid and nanoparticles for two hours on a magnetic stirrer (Figure 3-3 [b]) and then sonicating digitally for another three hours in a sonicator (Figure 3-3 [c]). The lengthy sonication process was necessary to ensure that the nanoparticles were evenly dispersed throughout the base fluid. The prepared sixteen samples are shown in Figure 3-4.

Table 3-3: Al_2O_3 and TiO_2 particle content

Certificate of Analysis			
Aluminum oxide (alpha ~ 90 %)		**Titanium Dioxide (anatase)**	
APS: 40 nm, Purity: ≥ 99.5%		**APS: 50 nm, Purity: ≥ 98%**	
Components	**Contents(ppm)**	**Components**	**Contents(ppm)**
Ca	1.6	Al	≤ 20
Co	0.8	Ca	≤ 75
Fe	0.2	Mg	≤ 65
Na	<300	Nb	≤ 119
Si	3.5	S	≤ 165
		Si	≤ 102

[a] [b] [c]

Figure 3-3: Nanofluid preparation steps

Figure 3-4: Prepared samples

3.4 Machine and Equipment

This subsection describes the machine, workpiece, and tool that have been used for the experiments.

3.4.1 Workpiece

AISI 1045 is medium-strength alloy steel widely used to manufacture guide rolls, guide rods, light gears, worms, sockets, ratchets, crankshafts, spindles, pins, bolts, axles, studs and connecting rods [135]. The tested object measured 55 mm in diameter and 305 mm in length (Figure 3-4). The work material's chemical composition was determined using a Spectrometer (model: MAXx LMM05, made in Germany). The tested chemical composition is listed in Table 3-4, and the mechanical properties provided of the supplier are listed in Table 3-5.

Figure 3-5: Work piece (AISI 1045)

Table 3-4: Chemical composition of AISI 1045

Element	C	Si	Mn	P	S	Cr	Mo	Ni	Al	Co	Cu
Composition (%)	0.469	0.223	0.614	0.001	0.001	0.010	0.176	0.017	0.018	0.007	0.028

Table 3-5: Mechanical properties of AISI 1045

Mechanical Properties	Metric
Hardness, Vickers (Converted from Brinell hardness)	170
Tensile Strength (yield)	310 MPa
Tensile Strength (Ultimate)	565 MPa
Modulus of Elasticity	200 GPa
Elongation at Break (in 50 mm)	16.00%
Reduction of Area	40.00%

3.4.2 Machine and Tool

The CM (model 6241X1000) lathe machine was used to turn AISI 1045 steel using the NDM technique, and the lathe machine is shown in Figure 3-6. The coated carbide inserts (Mitsubishi CNMG 120408- MS VP15TF; Figure-3-7) were selected as the cutting insert based on the workpiece material's chemical composition, speed range provided by the supplier, and it was fastened mechanically to a rigid tool holder. (MCLNR- 2020K12).

Figure 3-6: Model 6241X1000 lathe machine

Figure 3-7: Mitsubishi CNMG 120408- MS VP15TF tool tip

The MQL system involves a flow and air controller unit, a compressor (with a pressure gauge), a spray nozzle, and an air dryer. S.A.S Amiril et al. proved that when closer the nozzle to the tool, the greater the cutting force and the increase in the tool life [136], and A. Yassin et al. investigated that when nozzle angle 20^0 provided the optimum flank wear [137]. Based on the literature, the author arranged the MCFs discharge nozzle distance of 40 mm (as much as close to the tool with safety distance) at a 20^{o} angle from the rake surface of the cutting tool insert. Consequently, the nano-cutting fluid mist effectively enters the cutting zone. The mixing chamber and tool arrangement are shown in Figure 3-8.

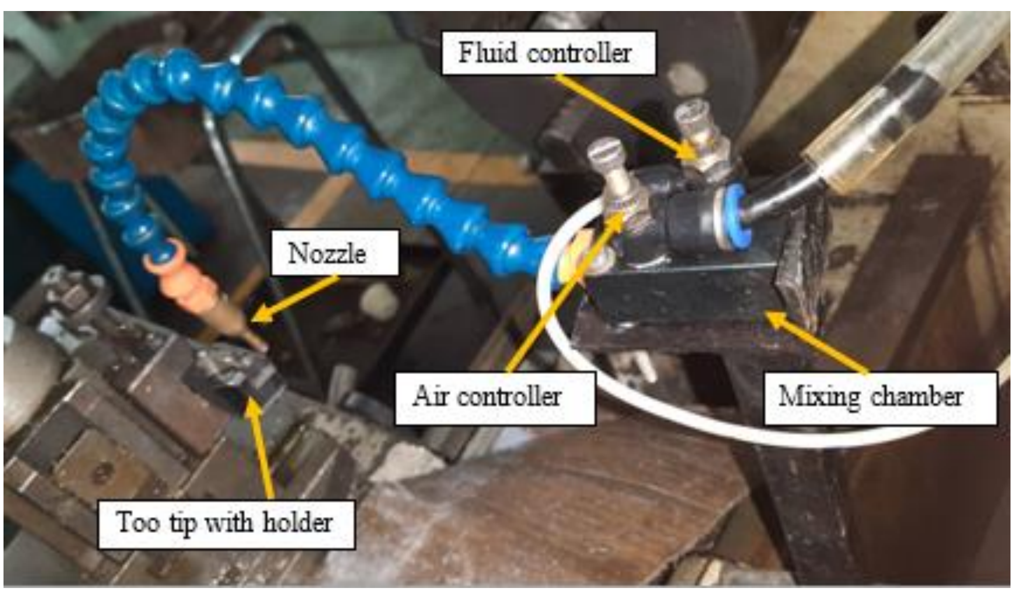

Figure 3-8: MWFs and tool arrangement

3.5 Experimental Design

Design of experiments (DOE) explores and specifies all feasible experimental settings, taking into account a number of variables. The key benefit of the Taguchi approach is that it requires fewer experiments to discover the relevant component in less time. The experimental array L16 (4^4) orthogonal array (OA) was designed to measure tooltip temperature and average surface roughness using the Taguchi approach. The standard OA includes sixteen experiments for this experiment, each with four control factors and four experimental state levels. The control variables were nanoparticle concentrations (Al_2O_3 and TiO_2), air pressure, and cutting speed, whereas the response variables included tooltip temperature and surface roughness.

Here, the author has selected both nanoparticles separately as a controlling factor in order to ascertain the actual influence of each nanoparticle's behaviour on the tool tip temperature and surface roughness and has considered each nanoparticle concertation range of 0 to 0.75 wt%. The zero level was chosen to capture the only MQL condition behaviour with machining, and based on the literature review higher level was limited to 0.75 wt% concentration on each nanoparticle. That is because increasing the particle concertation into the based fluid tends to cluster and not show performance; however, a few studies have done more than 1 wt%, and the majority have done below the 1 wt% of nanoparticle concentration. Furthermore, there is no explicit statement regarding the combination weight percentage in a base fluid. The third control factor, "Air pressure," is a major concern when adding nanoparticles to the base fluid. When mixing nanoparticles with base fluid, it tends to pressure drop in the flow, so there is a need to maintain the flow as much as possible to avoid that issue; so that the author has selected the third factor as air pressure considering the most efficient pressure levels of based on the literature review [43],[73],[138]–[144].

When it comes to cutting operation, the best possible circumstances include a limited amount of cutting time, a substantial amount of tool life, and a high degree of cutting precision. It is required to select cutting conditions and tools in accordance with the work material's hardness, shape, and capabilities of the machine in order to achieve these conditions. Feed, depth of cut, and cutting speed should all be considered control elements when carrying out a turning operation. In the same way, cutting speed directly affects heat generation; consequently, tool life and feed rate directly affect surface roughness. Changing the depth of the cut has little impact on the tool's life. In addition, when cutting a workpiece's hardened layer, small depths of cut result in friction.

Consequently, the durability of the tool is diminished [145]–[150]. The author has selected cutting speed as the fourth experimental variable while keeping optimal feed (0.25 mm/rev) and depth of cut (0.5 mm) parameters, based on the (Figure 3-9 for optimum depth of cut; Figure 3-10 for optimum feed) work-piece material and cutting tool properties provided by manufacture [151]. The speed range is selected based on the manufacturer's specifications.

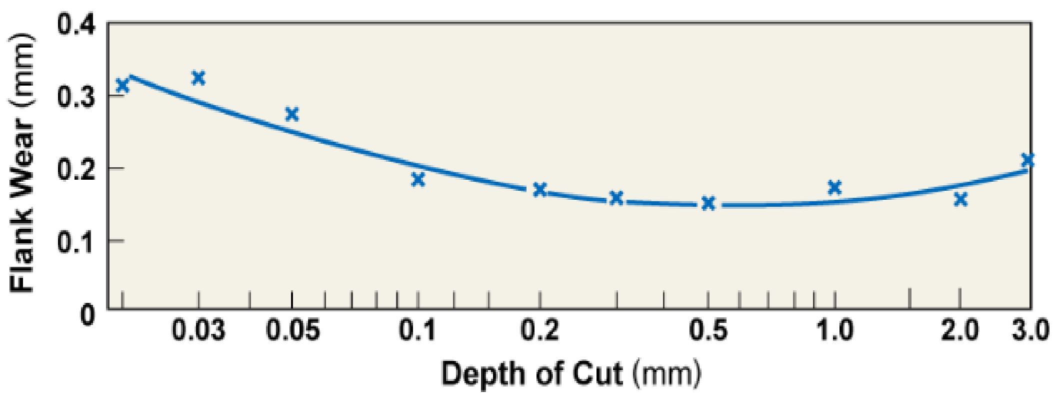

Figure 3-9: Depth of cut and Flank wear behaviour in medium carbon turning [151]

According to the research conducted, there are numerous ways to set up an experimental MQL system. According to the research that has been conducted, the optimal conceptual design for this investigation was determined by means of a morphological analysis. This analysis was conducted based on the subsystems discovered in the aforementioned literature for various experimental setups. While constructing the modified final design, ambient air was subjected to approximately 7.5 bar of pressure generated by a compressor

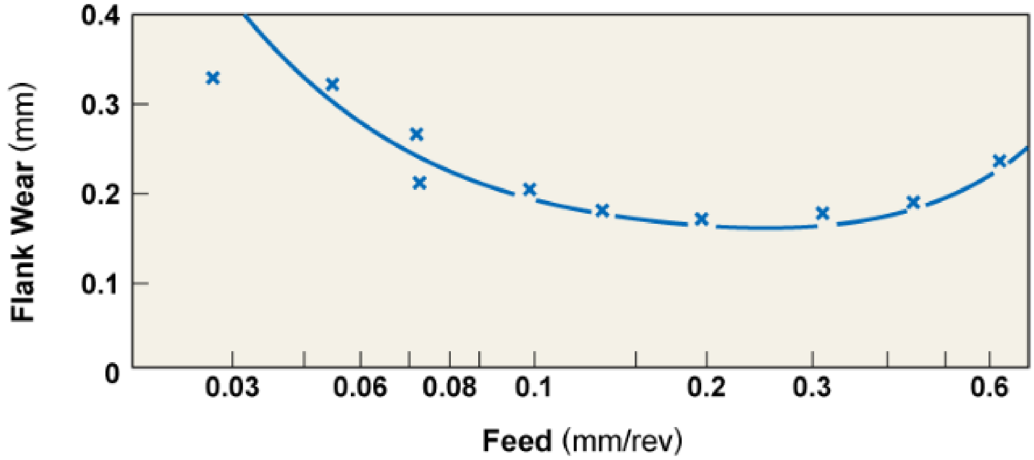

Figure 3-10: Feed and Flank wear relationship in medium carbon turning [151]

within the MQL experimental setup. The compressed air was then introduced into the mixing chamber, and that chamber consisted of air and fluid controllers. The airflow regulator at the mixing unity was entirely opened, and the compressor controlled the airflow. The flow rate was kept constant throughout the studies by regulating the MCFs controller in the mixing chamber. The mixing chamber's suction action aided in the flow of MWF. Compressed air and MWFs were blended in the mixing chamber. The nozzle delivered the air and MWFs mixture into the cutting zone. In this experiment, the flow rate was maintained at 60 ml/h in order to determine the MQL condition [129], [152], [153].

The experimental settings for each control factor and orthogonal array are detailed in Tables 3- 6 and 3-7, respectively. All experiments were conducted in triplicate, and the mean of the results was considered. In addition, all tests were conducted arbitrarily to eliminate any other unseen variables that could have influenced the cutting temperature and average surface roughness.

Table 3-6: Machining parameters and their levels

Control Factors	Symbols	Units	Level 01	Level 02	Level 03	Level 04
Al_2O_3	W_1	wt. %	0.00	0.25	0.50	0.75
TiO_2	W_2	wt. %	0.00	0.25	0.50	0.75
Air Pressure	P	bar	2.00	3.00	4.00	5.00
Cutting Speed	V	m/ min	88	101	133	155

Table 3-7: Standard L_{16} (4^4) Orthogonal Array

Control factors and experiment levels				
Exp. No	**W_1**	**W_2**	**P**	**V**
1	1	1	1	1
2	1	2	2	2
3	1	3	3	3
4	1	4	4	4
5	2	1	2	3
6	2	2	1	4
7	2	3	4	1
8	2	4	3	2
9	3	1	3	4
10	3	2	4	3
11	3	3	1	2
12	3	4	2	1
13	4	1	4	2
14	4	2	3	1
15	4	3	2	4
16	4	4	1	3

A testo 871- thermal imager measures the average tool tip temperature (T_{tip}). All the measurements are conducted at the same distance and under room temperature conditions. The INNOVATEST TR-200 performs measurements of the average surface roughness (R_a) of the workpiece following each turning operation while maintaining the same machining conditions. This instrument has been calibrated and validated against the test samples that have been provided to guarantee that the inaccuracy in the displayed value is

±10 percent. This procedure was repeated three times at various reference points along the cylindrical surface of the workpiece, and the average value was then computed. The INNOVATEST TR-200 is a contact-type measuring device with a probe that may travel on the surface of the workpiece. The probe's diamond tip has a radius of 5 μm. The device has a measuring range of 160 μm, a measuring speed of 0.135 millimetres per second, a probe returning speed of 1 millimetre per second, a cut-off length of 0.08 millimetres, and a measuring force of 4 mN. The whole configuration arrangement is illustrated in Figure 3-11.

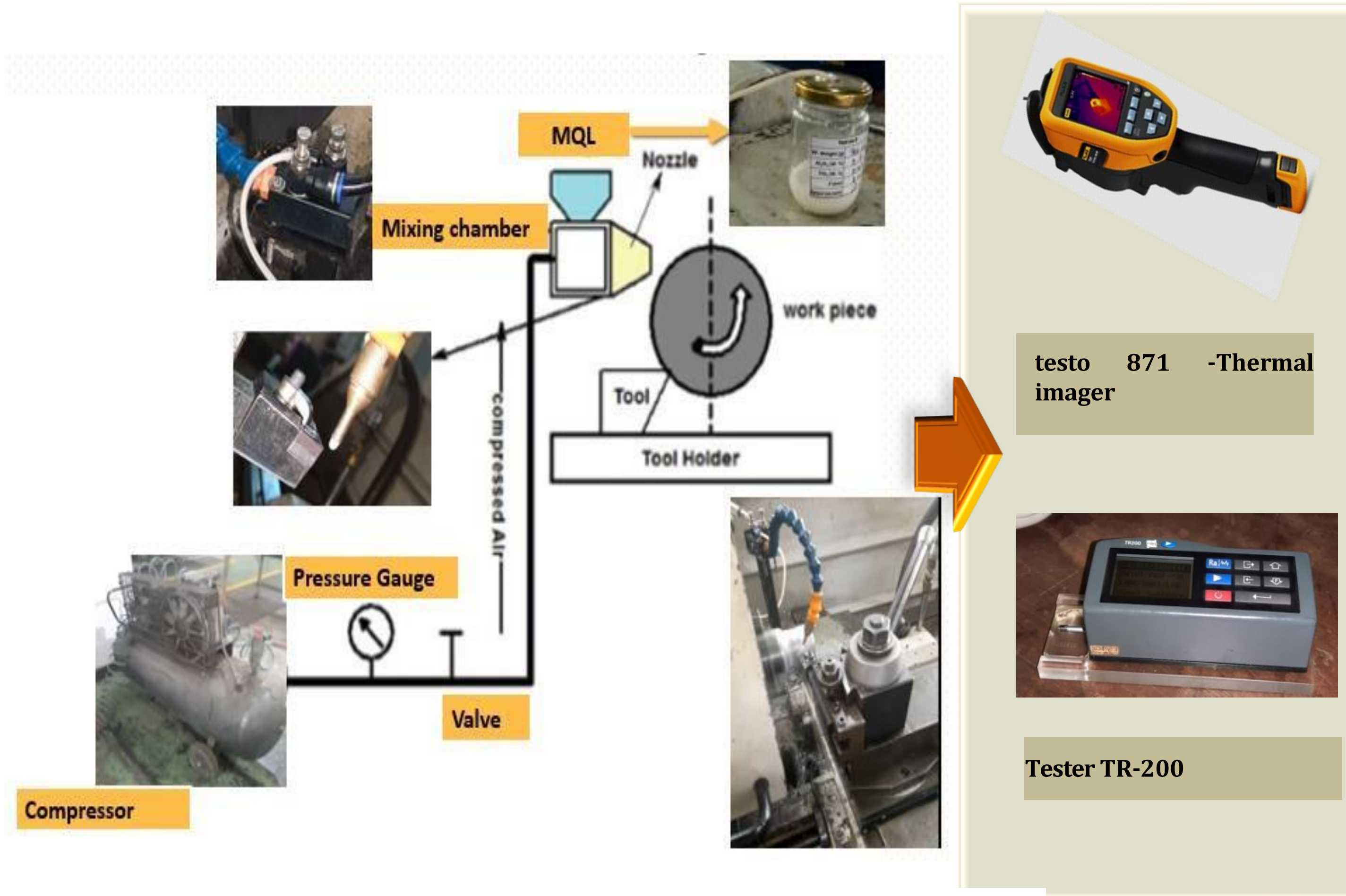

Figure 3-11: Setup arrangement

4 CHAPTER: RESULTS AND DISCUSSION

4.1 Experimental Results

In accordance with the experimental design, turning operations were performed on AISI 1045 by altering MQL and machining parameters, including Al_2O_3 nano weight percent, TiO_2 nano weight percent, air pressure, and cutting speed. This was done in order to evaluate the machining performance of nanofluids based on Al_2O_3 and TiO_2 in terms of the temperature of the tooltip and the average surface roughness. Tables 4-1, 4-2, and 4-3 display the temperature measurement, average surface roughness, and the OA tables for each factor and response.

Table 4-1: Observed temperature results from the thermal infrared camera

Ex. No	Test 01	Test 02	Test 03	Average Temp. (^{0}C)
1	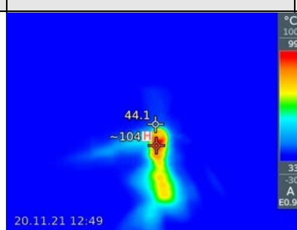	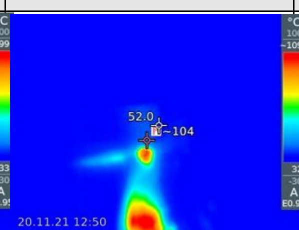	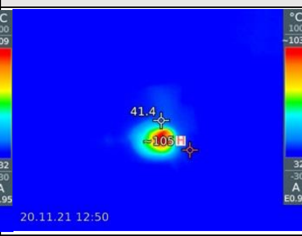	104
2	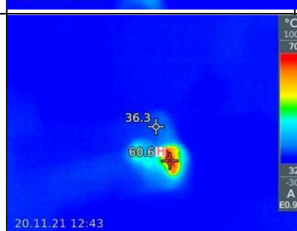	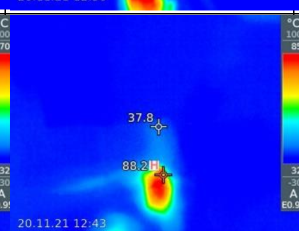	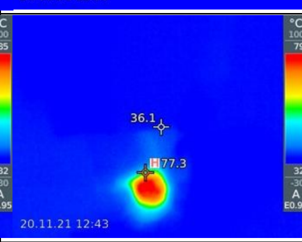	75
3	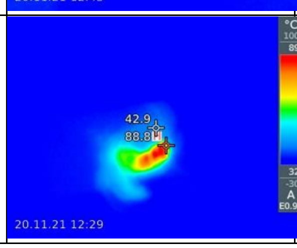	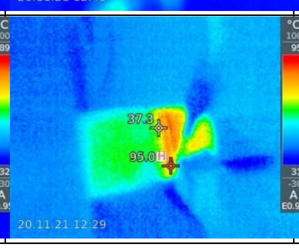	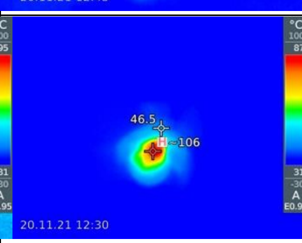	97

Ex. No	Test 01	Test 02	Test 03	Average Temp. (^0C)
4	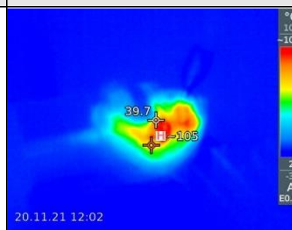	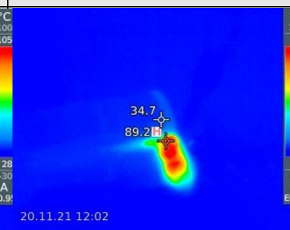	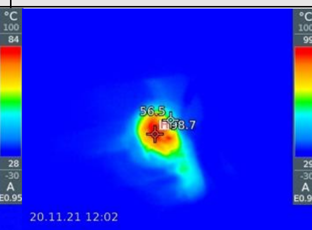	98
5	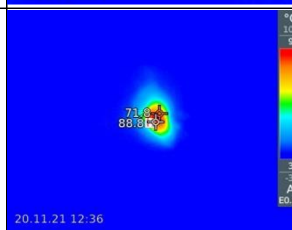	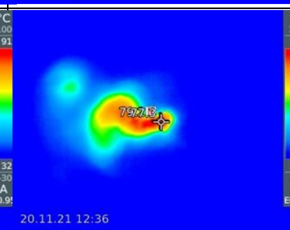	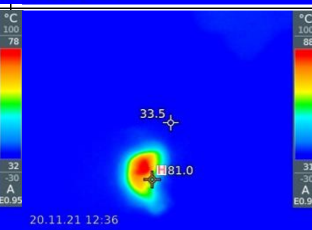	82
6	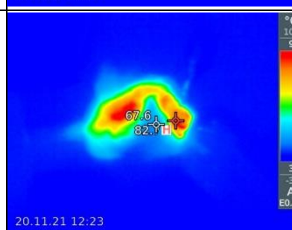	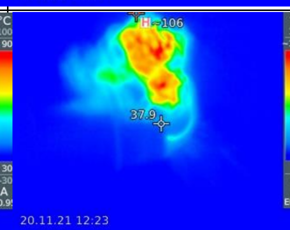	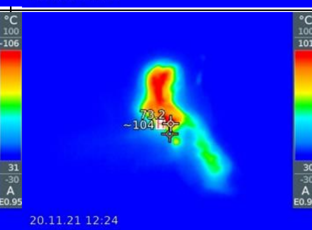	98
7		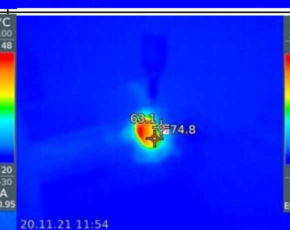	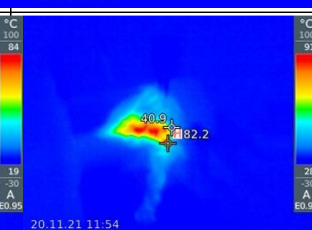	72
8	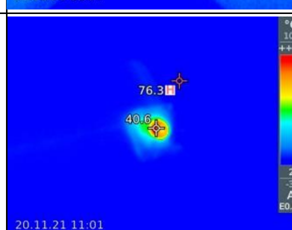	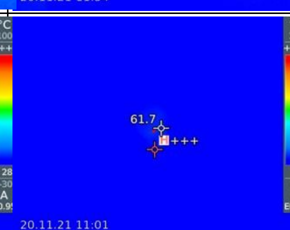	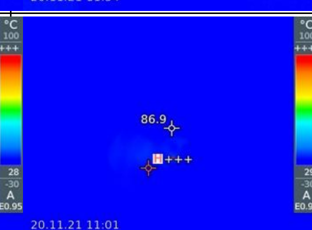	75
9		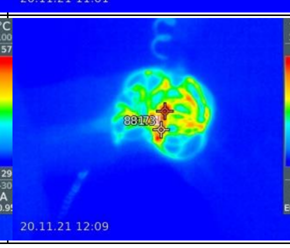	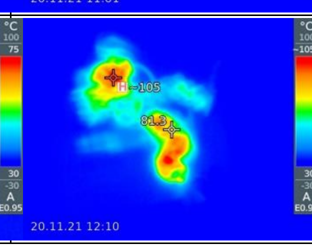	76

Ex. No	Test 01	Test 02	Test 03	Average Temp. (^0C)
10	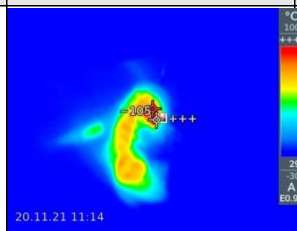	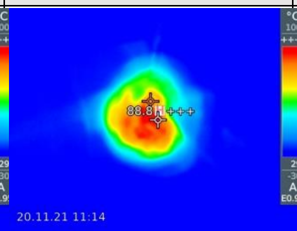	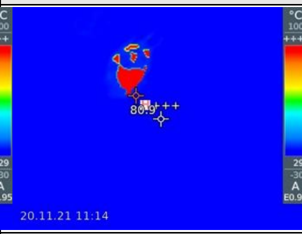	92
11	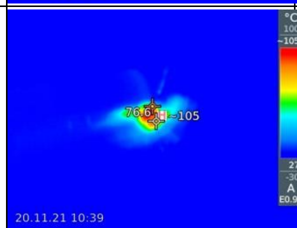	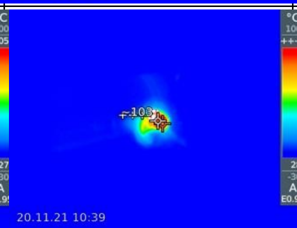	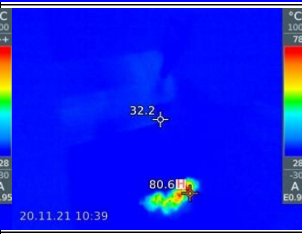	96
12	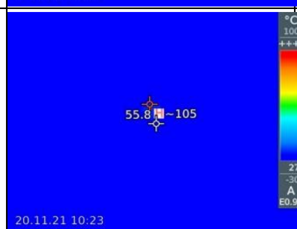			87
13		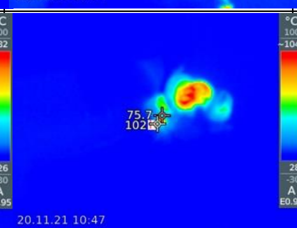	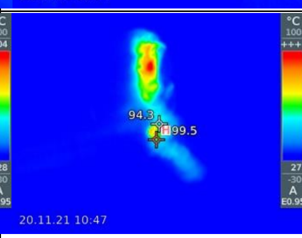	86
14	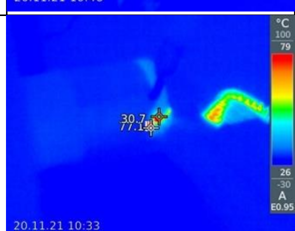	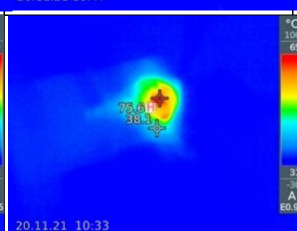	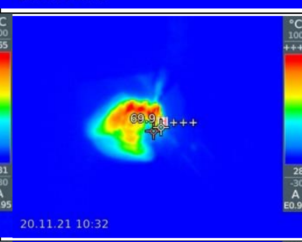	74
15		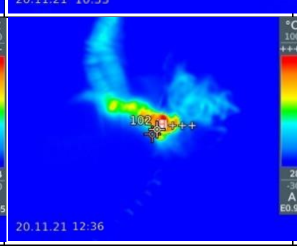	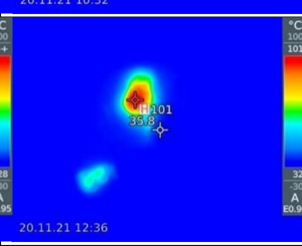	96

Ex. No	Test 01	Test 02	Test 03	Average Temp. (^0C)
16	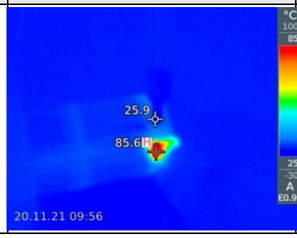	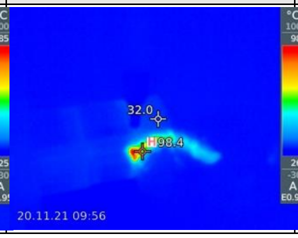	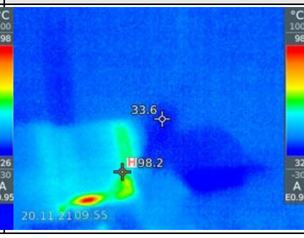	94

Table 4-2: Observed R_a results from TR200 surface roughness

Sample No	Test 01	Test 02	Test 03	Average Surface roughness
1	0.641	0.612	0.607	0.620
2	0.531	0.511	0.530	0.524
3	0.591	0.576	0.573	0.580
4	0.575	0.572	0.566	0.571
5	0.376	0.391	0.373	0.380
6	0.364	0.366	0.350	0.360
7	0.301	0.267	0.242	0.270
8	0.271	0.293	0.276	0.280
9	0.349	0.345	0.329	0.341
10	0.301	0.306	0.293	0.300
11	0.249	0.264	0.267	0.260
12	0.233	0.241	0.216	0.230
13	0.355	0.381	0.344	0.360
14	0.104	0.101	0.095	0.100
15	0.341	0.323	0.299	0.321
16	0.337	0.301	0.292	0.310

Table 4-3: L16 Orthogonal Array for responses and variables values

Exp.No	W_1 (wt%)	W_2 (wt%)	P (bar)	V (m/ min)	T (^0C)	Ra (μm)
1	0	0	2	88	104	0.620
2	0	0.25	3	101	75	0.524
3	0	0.5	4	133	97	0.580
4	0	0.75	5	155	98	0.571
5	0.25	0	3	133	82	0.380
6	0.25	0.25	2	155	98	0.360
7	0.25	0.5	5	88	72	0.270
8	0.25	0.75	4	101	75	0.280
9	0.5	0	4	155	76	0.341
10	0.5	0.25	5	133	92	0.300
11	0.5	0.5	2	101	96	0.260
12	0.5	0.75	3	88	87	0.230
13	0.75	0	5	101	86	0.360
14	0.75	0.25	4	88	74	0.100
15	0.75	0.5	3	155	96	0.321
16	0.75	0.75	2	133	94	0.310

After collecting raw data, the next step was to convert it into useful information for user decision-making. Because ANOVA is a technique that may be used to identify how each variable interacts with the others, it has been utilized here to evaluate the raw data. Utilizing the analysis's percentage distributions, the influence of each control factor on the quality criterion was estimated.

4.2 Data Analysis- ANOVA

A statistical ANOVA establishes the significance of process characteristics that influence performance metrics. This section covers ANOVA for a variety of desirable performance indicators.

In this work, ANOVA was utilized to assess the influence of air pressure, cutting speed, and nanoparticle concentrations on the average surface roughness and tooltip temperature. The mathematical models of the controls and their interactions were developed using multiple regression analysis. ANOVA is a technique that can be performed to determine how each variable factor interacts with the others [154]. The influence of each control element on the quality criterion was calculated using the percentage distributions in the analysis. A 95% confidence level was established for the experimental plan that was carried out.

4.2.1 Sum of Squares

As a statistical dispersion indicator, squared deviations from the mean are calculated. It is determined by adding the squares of the outlying values relative to the mean. When determining the overall sum of squares, we take into account both the factor sum of squares and any random or erroneous squares that may have been introduced. Below explains the notation for the calculation with the sample data set.

An equation for total variation (SS_T) is given by,

$$SS_T = SS_{W1} + SS_{W2} + SS_P + SS_V + SS_e$$

$$SS_T = \sum_{i=1}^{n} y_i^2 - \frac{T^2}{n}$$

Where variation owing to factor Al_2O_3 is denoted by SS_{W1}

$$SS_{W1} = \sum_{i=1}^{n} \frac{W1_i^2}{n_{w1i}} - \frac{T^2}{n}$$

Where variation owing to factor TiO_2 is denoted by SS_{W2}

$$SS_{W2} = \sum_{i=1}^{n} \frac{W2_i^2}{n_{w2i}} - \frac{T^2}{n}$$

Where variation owing to factor air pressure is denoted by SS_P

$$SS_P = \sum_{i=1}^{n} \frac{P_i^2}{n_{Pi}} - \frac{T^2}{n}$$

Where variation owing to factor cutting speed is denoted by SS_V

$$SS_{\mathrm{V}} = \sum_{i=1}^{n} \frac{V_i^2}{n_{Vi}} - \frac{T^2}{n}$$

Hence,

$$SS_e = -(\mathrm{SS_{W1}} + \mathrm{SS_{W2}} + \mathrm{SS_P} + \mathrm{SS_V}) + \mathrm{SS}_T$$

Where variation owing to factor error (SSe)

Also, W_1-Al_2O_3 wt%, W_2-TiO_2, P-Air Pressure, V-Cutting Speed, e-Error, T - Summation of response, n - Number of observations

Based on the above first stage data calculation Table 4-4; below is the ANOVA sample data calculation for tool temperature

$$SS_T = \sum_{i=1}^{n} y_i^2 - \frac{T^2}{n}$$

$$SS_T = 104^2 + 75^2 + 97^2 + 98^2 + 82^2 + 98^2 + 72^2 + 75^2 + 76^2 + 92^2 + 96^2 + 87^2 + 86^2 + 74^2 + 96^2 + 94^2 - \frac{1402^2}{16}$$

$SS_T = \underline{\underline{1653.49}}$

$$SS_{\mathrm{W1}} = \sum_{i=1}^{n} \frac{W1_i^2}{n_{w1i}} - \frac{T^2}{n}$$

$$SS_{W1} = \frac{(104 + 75 + 97 + 98)^2}{4} + \frac{(82 + 98 + 72 + 75)^2}{4} + \frac{(76 + 92 + 96 + 87)^2}{4} + \frac{(86 + 74 + 96 + 94)^2}{4} - \frac{1402^2}{16}$$

$SS_{W1} = \underline{\underline{274.72}}$

Based on the above first stage data calculation Table 4-5; below is the ANOVA sample data calculation for surface roughness,

$$SS_T = \sum_{i=1}^{n} y_i^2 - \frac{T^2}{n}$$

$$SS_T = 0.620^2 + 0.524^2 + 0.580^2 + 0.571^2 + 0.380^2 + 0.360^2 + 0.270^2 + 0.280^2 + 0.341^2 + 0.300^2 + 0.260^2 + 0.230^2 + 0.360^2 + 0.100^2 + 0.321^2 + 0.310^2 - \frac{5.807^2}{16}$$

$SS_T = \underline{\underline{0.31}}$

$$SS_{W1} = \sum_{i=1}^{n} \frac{W1_i^2}{n_{w1i}} - \frac{T^2}{n}$$

$$SS_{W1} = \frac{(0.620 + 0.524 + 0.580 + 0.571)^2}{4} + \frac{(0.380 + 0.360 + 0.270 + 0.280)^2}{4} + \frac{(0.341 + 0.300 + 0.260 + 0.230)^2}{4} + \frac{(0.360 + 0.100 + 0.321 + 0.310)^2}{4} - \frac{5.807^2}{16}$$

$SS_{W1} = \underline{\underline{0.24}}$

Likewise, we can find the rest of the parameter values by following the same procedure.

Table 4-4: First stage data calculation for tool temperature

	Control factors & experiment levels				Control factors & experiment levels				Temperature	Level 01				Level 02				Level 03				Level 04			
Exp. No	W_1	W_2	P	V	W_1	W_2	P	V	(°C)	W_1	W_2	P	V	W_1	W_2	P	V	W_1	W_2	P	V	W_1	W_2	P	V
1	1	1	1	1	0.00	0.00	2	88	104	104	104	104	104	0	0	0	0	0	0	0	0	0	0	0	0
2	1	2	2	2	0.00	0.25	3	101	75	75	0	0	0	0	75	75	75	0	0	0	0	0	0	0	0
3	1	3	3	3	0.00	0.50	4	133	97	97	0	0	0	0	0	0	0	0	97	97	97	0	0	0	0
4	1	4	4	4	0.00	0.75	5	155	98	98	0	0	0	0	0	0	0	0	0	0	0	0	98	98	98
5	2	1	2	3	0.25	0.00	3	133	82	0	82	0	0	82	0	82	0	0	0	0	82	0	0	0	0
6	2	2	1	4	0.25	0.25	2	155	98	0	0	98	0	98	98	0	0	0	0	0	0	0	0	0	98
7	2	3	4	1	0.25	0.50	5	88	72	0	0	0	72	72	0	0	0	0	72	0	0	0	0	72	0
8	2	4	3	2	0.25	0.75	4	101	75	0	0	0	0	75	0	0	75	0	0	75	0	0	75	0	0
9	3	1	3	4	0.50	0.00	4	155	76	0	76	0	0	0	0	0	0	76	0	76	0	0	0	0	76
10	3	2	4	3	0.50	0.25	5	133	92	0	0	0	0	0	92	0	0	92	0	0	92	0	0	92	0
11	3	3	1	2	0.50	0.50	2	101	96	0	0	96	0	0	0	0	96	96	96	0	0	0	0	0	0
12	3	4	2	1	0.50	0.75	3	88	87	0	0	0	87	0	0	87	0	87	0	0	0	0	87	0	0
13	4	1	4	2	0.75	0.00	5	101	86	0	86	0	0	0	0	0	86	0	0	0	0	86	0	86	0
14	4	2	3	1	0.75	0.25	4	88	74	0	0	0	74	0	74	0	0	0	0	74	0	74	0	0	0
15	4	3	2	4	0.75	0.50	3	155	96	0	0	0	0	0	0	96	0	0	96	0	0	96	0	0	96
16	4	4	1	3	0.75	0.75	2	133	94	0	0	94	0	0	0	0	0	0	0	0	94	94	94	0	0

Table 4-5: First stage data calculation for surface roughness

	Control factors & experiment levels				Control factors & experiment levels				Ra (µm)	Level 01				Level 02				Level 03				Level 04			
Exp. No	W_1	W_2	P	V	W_1	W_2	P	V		W_1	W_2	P	V	W_1	W_2	P	V	W_1	W_2	P	V	W_1	W_2	P	V
1	1	1	1	1	0.00	0.00	2	88	0.620	0.62	0.62	0.62	0.62	0.00	0.00	0.00	0.00	0.00	0.00	0.00	0.00	0.00	0.00	0.00	0.00
2	1	2	2	2	0.00	0.25	3	101	0.524	0.52	0.00	0.00	0.00	0.00	0.52	0.52	0.52	0.00	0.00	0.00	0.00	0.00	0.00	0.00	0.00
3	1	3	3	3	0.00	0.50	4	133	0.580	0.58	0.00	0.00	0.00	0.00	0.00	0.00	0.00	0.00	0.58	0.58	0.58	0.00	0.00	0.00	0.00
4	1	4	4	4	0.00	0.75	5	155	0.571	0.57	0.00	0.00	0.00	0.00	0.00	0.00	0.00	0.00	0.00	0.00	0.00	0.00	0.57	0.57	0.57
5	2	1	2	3	0.25	0.00	3	133	0.380	0.00	0.38	0.00	0.00	0.38	0.00	0.38	0.00	0.00	0.00	0.00	0.38	0.00	0.00	0.00	0.00
6	2	2	1	4	0.25	0.25	2	155	0.360	0.00	0.00	0.36	0.00	0.36	0.36	0.00	0.00	0.00	0.00	0.00	0.00	0.00	0.00	0.00	0.36
7	2	3	4	1	0.25	0.50	5	88	0.270	0.00	0.00	0.00	0.27	0.27	0.00	0.00	0.00	0.00	0.27	0.00	0.00	0.00	0.00	0.27	0.00
8	2	4	3	2	0.25	0.75	4	101	0.280	0.00	0.00	0.00	0.00	0.28	0.00	0.00	0.28	0.00	0.00	0.28	0.00	0.00	0.28	0.00	0.00
9	3	1	3	4	0.50	0.00	4	155	0.341	0.00	0.34	0.00	0.00	0.00	0.00	0.00	0.00	0.34	0.00	0.34	0.00	0.00	0.00	0.00	0.34
10	3	2	4	3	0.50	0.25	5	133	0.300	0.00	0.00	0.00	0.00	0.00	0.30	0.00	0.00	0.30	0.00	0.00	0.30	0.00	0.00	0.30	0.00
11	3	3	1	2	0.50	0.50	2	101	0.260	0.00	0.00	0.26	0.00	0.00	0.00	0.00	0.26	0.26	0.26	0.00	0.00	0.00	0.00	0.00	0.00
12	3	4	2	1	0.50	0.75	3	88	0.230	0.00	0.00	0.00	0.23	0.00	0.00	0.23	0.00	0.23	0.00	0.00	0.00	0.00	0.23	0.00	0.00
13	4	1	4	2	0.75	0.00	5	101	0.360	0.00	0.36	0.00	0.00	0.00	0.00	0.00	0.36	0.00	0.00	0.00	0.00	0.36	0.00	0.36	0.00
14	4	2	3	1	0.75	0.25	4	88	0.100	0.00	0.00	0.00	0.10	0.00	0.10	0.00	0.00	0.00	0.00	0.10	0.00	0.10	0.00	0.00	0.00
15	4	3	2	4	0.75	0.50	3	155	0.321	0.00	0.00	0.00	0.00	0.00	0.00	0.32	0.00	0.00	0.32	0.00	0.00	0.32	0.00	0.00	0.32
16	4	4	1	3	0.75	0.75	2	133	0.310	0.00	0.00	0.31	0.00	0.00	0.00	0.00	0.00	0.00	0.00	0.00	0.31	0.31	0.31	0.00	0.00

4.2.2 Mean Squares

The variance of a population can be measured using mean squares. The value of this variable can be calculated by dividing the total number of squares by the total number of degrees of freedom.

$$Mean\ Squire = \frac{Sum\ of\ Squares}{DOF}$$

$$Mean\ Square\ Al_2O_3 = \frac{274.715}{3}$$

$Mean\ Square\ Al_2O_3 = \underline{\underline{91.57}}$

Likewise, we can find the rest of the parameter values by following the same procedure.

4.2.3 Main Effect Plot

The main effect plot is another type of data representation to understand each factor's behaviour; also, this is not showing the interaction of parameters

On the main effect plots, there is a line that connects the mean response of each level factor to one another. When the horizontal line is present, there is no primary effect. It's feasible that even a small deviation from the horizontal will have a major effect on the reaction when the line isn't perfectly straight. The greater the slope of the line, the more significant the primary effects [155].

We consider the corresponding response value against the control factors to calculate these values. The calculation for the mean values of the W_1 control factor is shown below.

Based on the OA table, the upper-level response values are 104, 75, 97, and 98 ^{0}C. To take the upper mean value, we divide those four by four.

$$Ttip_{upper\ level} = \frac{104 + 75 + 97 + 98}{4}$$

$Ttip_{upper\ level} = \underline{\underline{93.50}}$

$$Ttip_{mid\ level1} = \frac{82 + 98 + 72 + 75}{4}$$

$Ttip_{mid\ level1} = \underline{\underline{81.75}}$

$$Ttip_{mid\ level2} = \frac{76 + 92 + 96 + 87}{4}$$

$Ttip_{umid\ level2} = \underline{\underline{87.75}}$

$$Ttip_{lower\ level} = \frac{86 + 74 + 96 + 94}{4}$$

$Ttip_{lower\ level} = \underline{\underline{87.50}}$

In the same manner, we are able to compute the mean values for the other control factors. The outcomes of the derivation will be discussed and explained in the following chapter.

4.3 Interpretation of Results

4.3.1 Tooltip Temperature

The outcomes of ANOVA for tooltip temperatures are shown in Table 4-6. From this analysis, it is clear that the pressure is the most significant parameter (40.29%), and it is followed by the concentration of Al_2O_3 (16.61%), cutting speed (14.74%), and concentration of TiO_2 (3.97%) respectively, and the effect is graphically shown in factor plot diagram in Figure 4-1.

Table 4-6: Derived ANOVA for T_{tip}

Factor	DF	Seq SS	Adj SS	Adj MS	F	P	Impact (%)
W_1	3	274.70	274.70	91.57	0.68	0.620	16.61
W_2	3	65.61	65.61	21.87	0.16	0.915	3.97
P	3	666.21	666.21	222.07	1.65	0.345	40.29
V	3	243.78	243.78	81.26	0.60	0.655	14.74
Residual Error	3	403.15	403.15	134.38			24.38
Total	15	1653.44					

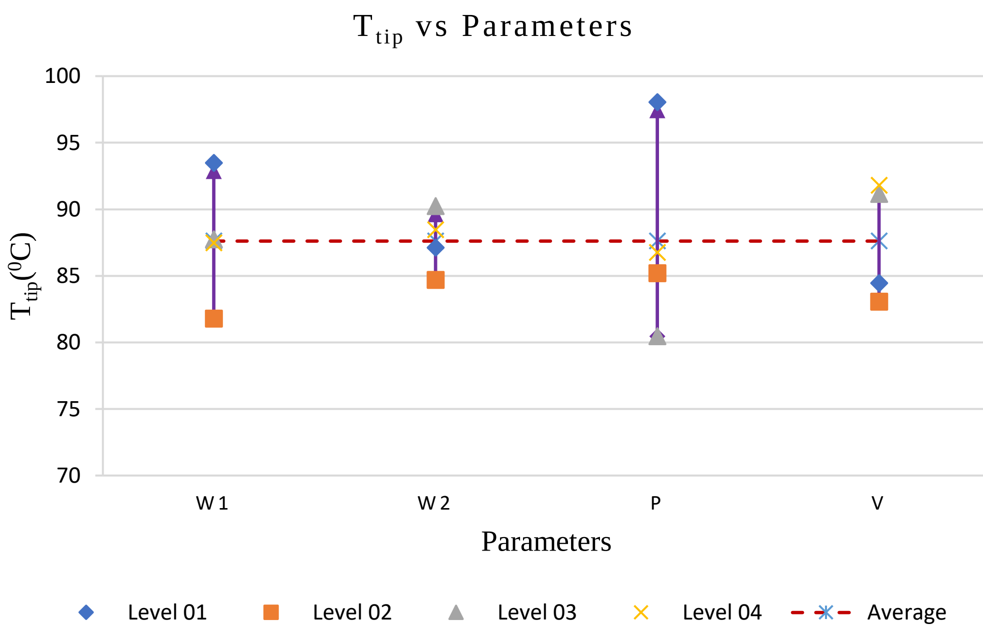

Figure 4-1: Factor plot tooltip temperature for AISI 1045

4.3.2 Average Surface Roughness

Table 4-7 represents the results of an analysis of variance performed on the average surface roughness. From the analysis, it is clear that the concentration of Al_2O_3 is the most influencing parameter (79.62%) and is followed by the concentration of TiO_2 (7.75%), cutting speed (7.25%), and air pressure (2.86%), respectively, and the effect is graphically shown in factor plot diagram in Figure 4-2.

Table 4-7: Derived ANOVA for R_a

Factor	DF	Seq SS	Adj SS	Adj MS	F	P	Impact (%)
W_1	3	0.242564	0.242564	0.080855	31.53	0.009	79.62
W_2	3	0.023597	0.023597	0.007866	3.07	0.191	7.75
P	3	0.008704	0.008704	0.002901	1.13	0.461	2.86
V	3	0.022103	0.022103	0.007368	2.87	0.205	7.25
Residual Error	3	0.007694	0.007694	0.002565			2.53
Total	15	0.304661					

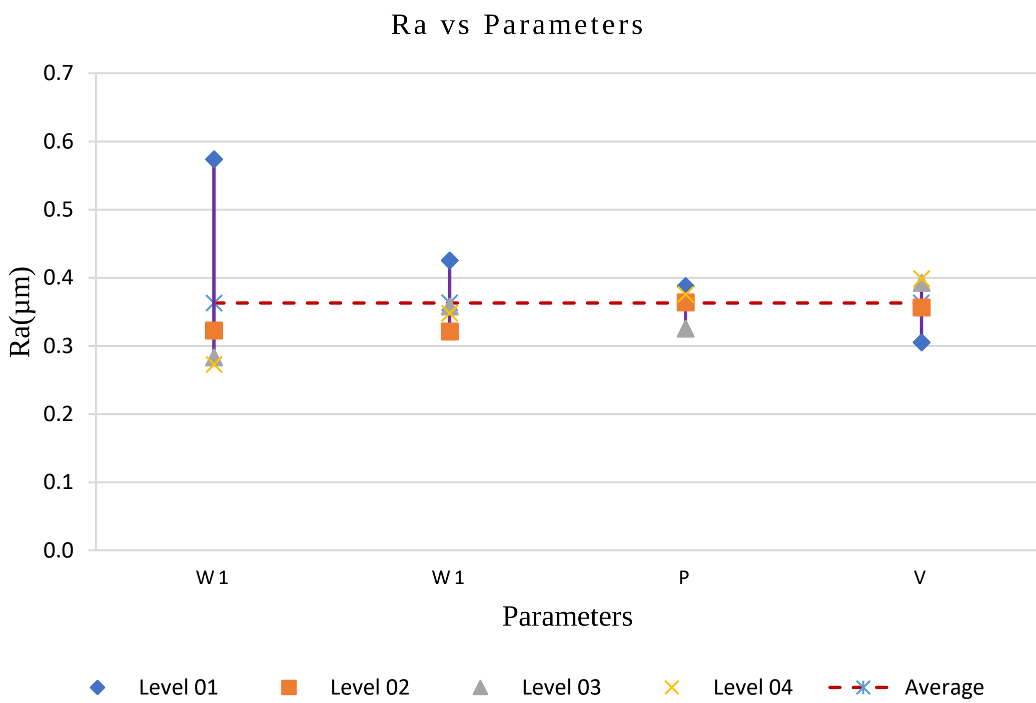

Figure 4-2: Factor plot surface roughness for AISI 1045

4.3.3 Plots of Main Effects for Responses

Result Table for T_{tip}

The response table for the tooltip temperature was calculated and shown in Table 4-8, and the plotted graph is shown in Figure 4-3.

Table 4-8: Derived response table for means of T_{tip}

Level	W1	W2	P	V
1	93.48	87.1	98.04	84.45
2	**81.77**	**84.68**	85.19	**83.04**
3	87.73	90.22	**80.46**	91.15
4	87.46	88.44	86.75	91.80
Delta	11.72	5.55	17.58	8.76
Rank	2	4	1	3

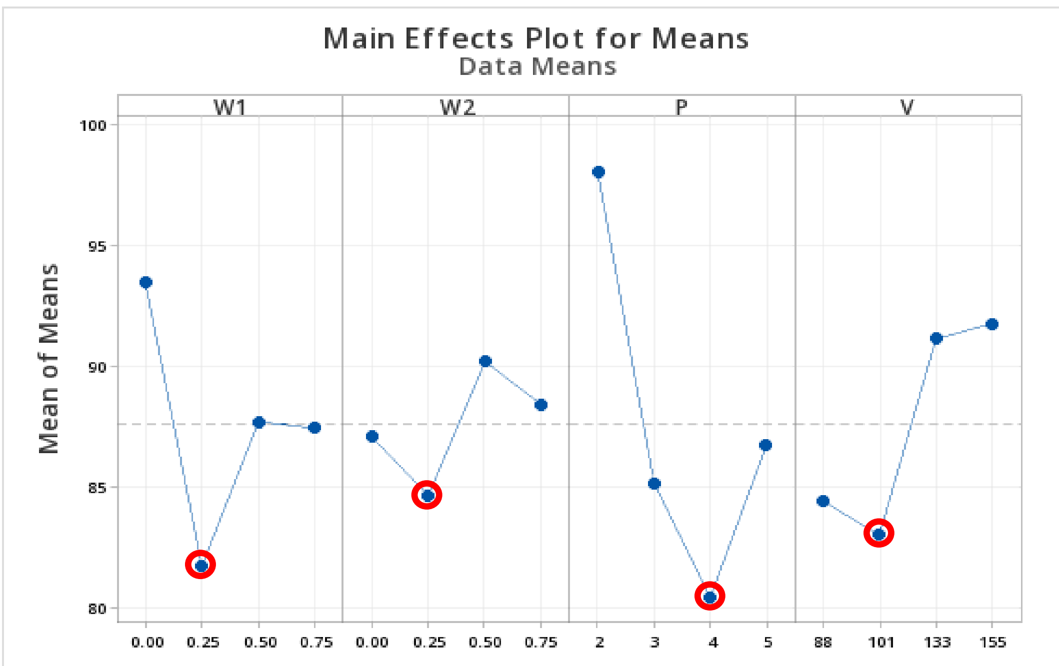

Figure 4-3: Main effects plot for the mean of T_{tip}

The Al_2O_3 concentration that produced the best tool tip temperature was level 2 (0.25 wt %, mean = 81.77), the TiO_2 concentration was level 2 (0.25 wt %, mean = 84.68), the air pressure was level 3 (4 bar, mean = 80.46) and the cutting speed was level 2 (101 m/min, mean = 83.04). In other words, according to the OA table, the combination of the 2,2,3,2 yielded the best value for tool tip temperature on the surface of the object

Result Table for R_a

Table 4-9 displays the calculated response table for the average surface roughness, and the plotted graph is shown in Figure 4-4.

Table 4-9: Derived response table for means of R_a

Level	W1	W2	P	V
1	0.574	0.425	0.388	**0.305**
2	0.323	**0.321**	0.364	0.356
3	0.283	0.358	**0.325**	0.392
4	**0.273**	0.348	0.375	0.398
Delta	0.301	0.104	0.062	0.093
Rank	1	2	4	3

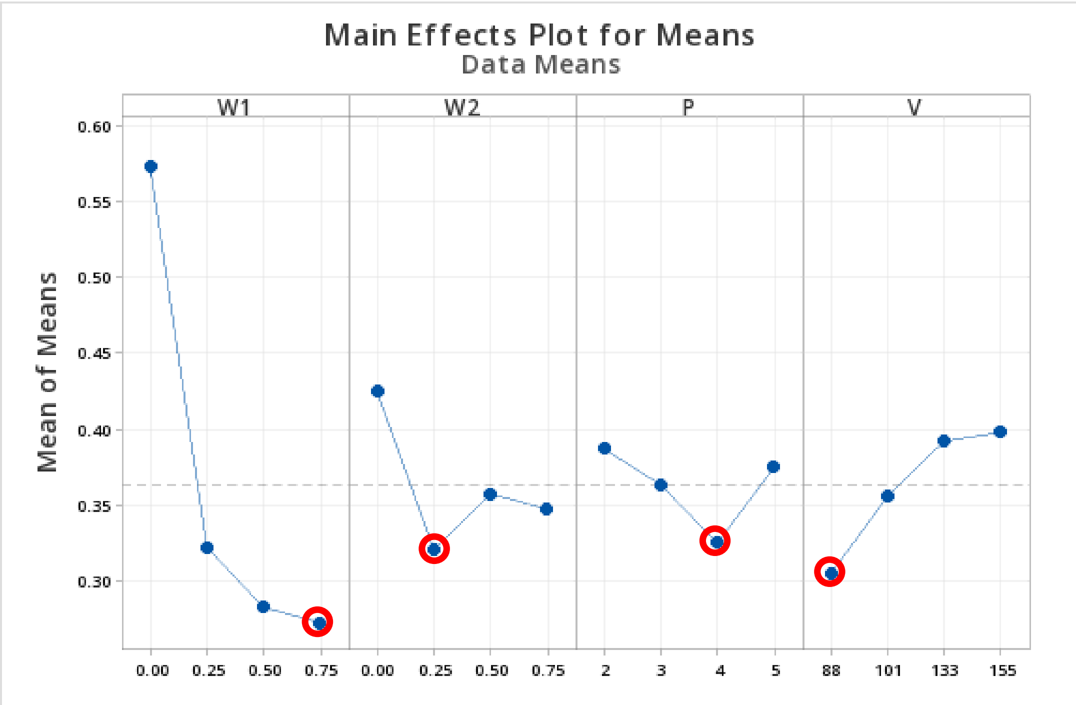

Figure 4-4: Main effects plot for the mean of R_a

The Al_2O_3 concentration that produced the best tool tip temperature was level 4 (0.75 wt %, mean = 0.273), the TiO_2 concentration was level 2 (0.25 wt %, mean = 0.321), the air pressure was level 3 (4 bar, mean = 0.325) and the cutting speed was level 1 (88 m/min, mean = 0.305). In other words, according to the OA table, the combination of 4,2,3,1 yielded the best value for tool tip temperature on the surface of the object.

4.4 Model Fitting and Optimization

4.4.1 Model Fitting

Mathematical and statistical techniques are combined in regression analysis, which is used to construct empirical models. Experiments and regression analysis can aid in the construction of a model of the response to a variety of different input elements. Equation 1 represents the conventional mathematical models (response function). Where Y represents the response of the machining operation, *K* stands for the response function, X_1, X_2, X_3, and X_4 are independent variables of the machining operation, and *C* stands for the error. Typically, the general polynomial response equation of second order is employed. It also demonstrates that this model effectively explains the link between the independent variables and outcomes [156].

$$Y = K\,(X_1, X_2, X_3, X_4) \pm C, \qquad (1)$$

Equation 2 can be used to fit the second-order model's response surface[157], which has been used to elucidate the connection between response and machining parameters as follows. *Y* is the response variable, and 'W_1', 'W_2', 'P', and 'V' are control factors. $\beta_1, \beta_2, \beta_3, .. \beta_n$ are coefficients of regression.

$$Y = \beta_0 + \beta_1 W_1 + \beta_2 W_2 + \beta_3 P + \beta_4 V + \beta_5 W_1 W_2 + \beta_6 W_1 P + \beta_7 W_1 V + \beta_8 W_2 P + \beta_9 W_2 V + \beta_{10} PV + \beta_{11}(W_1^2) + \beta_{12}(W_2^2) + \beta_{13}(P^2) + \beta_{14}(V^2) \qquad (2)$$

Where; Al_2O_3 (wt %), TiO_2 (wt %), Air pressure, and Cutting speed are W_1, W_2, P, and V, respectively.

To obtain predictive quantitative relationships, the reactions of the machine and factors of the process must be modelled. Within the scope of this effort, mathematical models were constructed using MINITAB-17 based on experimental results. Using polynomial second-order equations, the response function for T_{tip} and R_a has been derived from observed data using the following formulas:

$$T_{tip} = 159 - 80W_1 + 4W_2 - 60P + 0.5V + 26W_1W_2 + 21.7W_1P - 0.227W_1V + 5W_2P + 0.01W_2V + 0.124PV + 36W_1^2 - 15.9W_2^2 + 4.6P^2 - 0.024V^2 \quad \textit{(3)}$$

$$R_a = 1.51 - 0.89W_1 - 0.67W_2 + 0.20P - 0.0196V - 0.083W_1W_2 + 0.046W_1P + 0.00345W_1V - 0.324W_2P + 0.0130W_2V + 0.00033PV - 0.35W_1^2 + 0.346W_2^2 - 0.020P^2 - 0.000057V^2 \quad \textit{(4)}$$

The coefficient of determination (R^2) for tooltip temperature (T_{tip}) and average surface roughness (R_a) is 81.70% and 97.48%, respectively.

Surface Plot

Examine the link between a response variable (Tooltip temperature/Surface roughness) and two predictor factors by visualizing a three-dimensional surface of the projected response using the 3D Surface Plot command.

Contour Plot

Use a contour plot to see how a response variable connects to two predictor variables. A contour plot is a two-dimensional representation in which all points with the same response are joined to form contour lines with constant responses. Contour plots can be used to investigate desired response values and operating conditions.

In this experiment, there are four control factors, two of which are always taken into account, while the other two are maintained at intermediate values in order to analyze the response behaviour.

Surface plots and contour plots are shown in Fig. 4-5, 4-6, 4-7, 4-8, 4-9, and 4-10 in terms of relationship with each variable for tooltip temperature. The contour plots show a clear image of the relation between the variables, and it is easy to be used by other unskilled machining operators.

Figure 4-5 describes the influence of Al_2O_3 concentration and TiO_2 concentration on the tooltip temperature, while the air pressure and cutting speed are kept at the middle level.

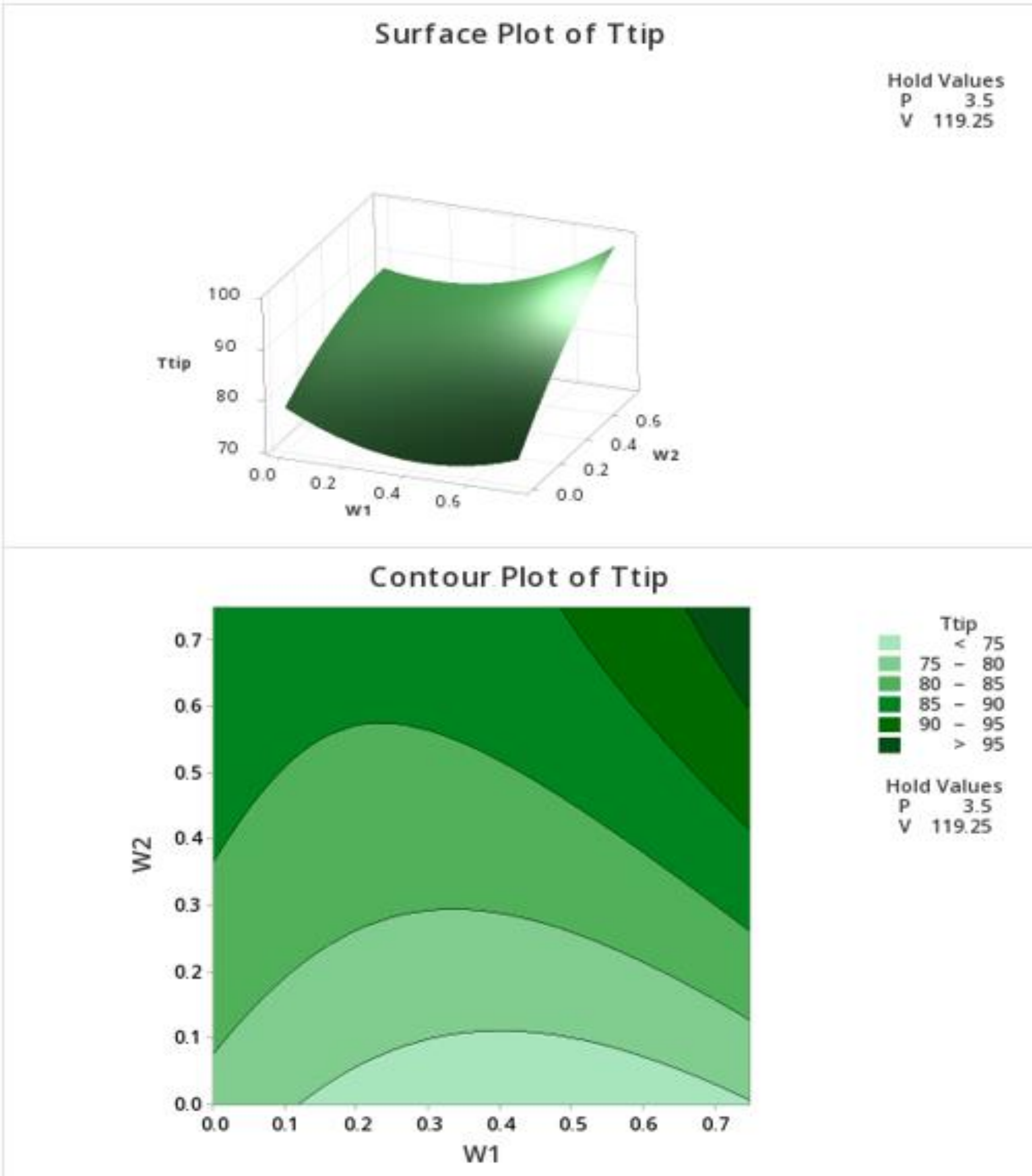

Figure 4-5: Temperature of the tooltip as a function of Al_2O_3 concentration and TiO_2 concentration

Keeping the TiO_2 concentration and cutting speed at the middle level, Figure 4-6 shows the impact of the tooltip temperature on the Al_2O_3 concentration and air pressure.

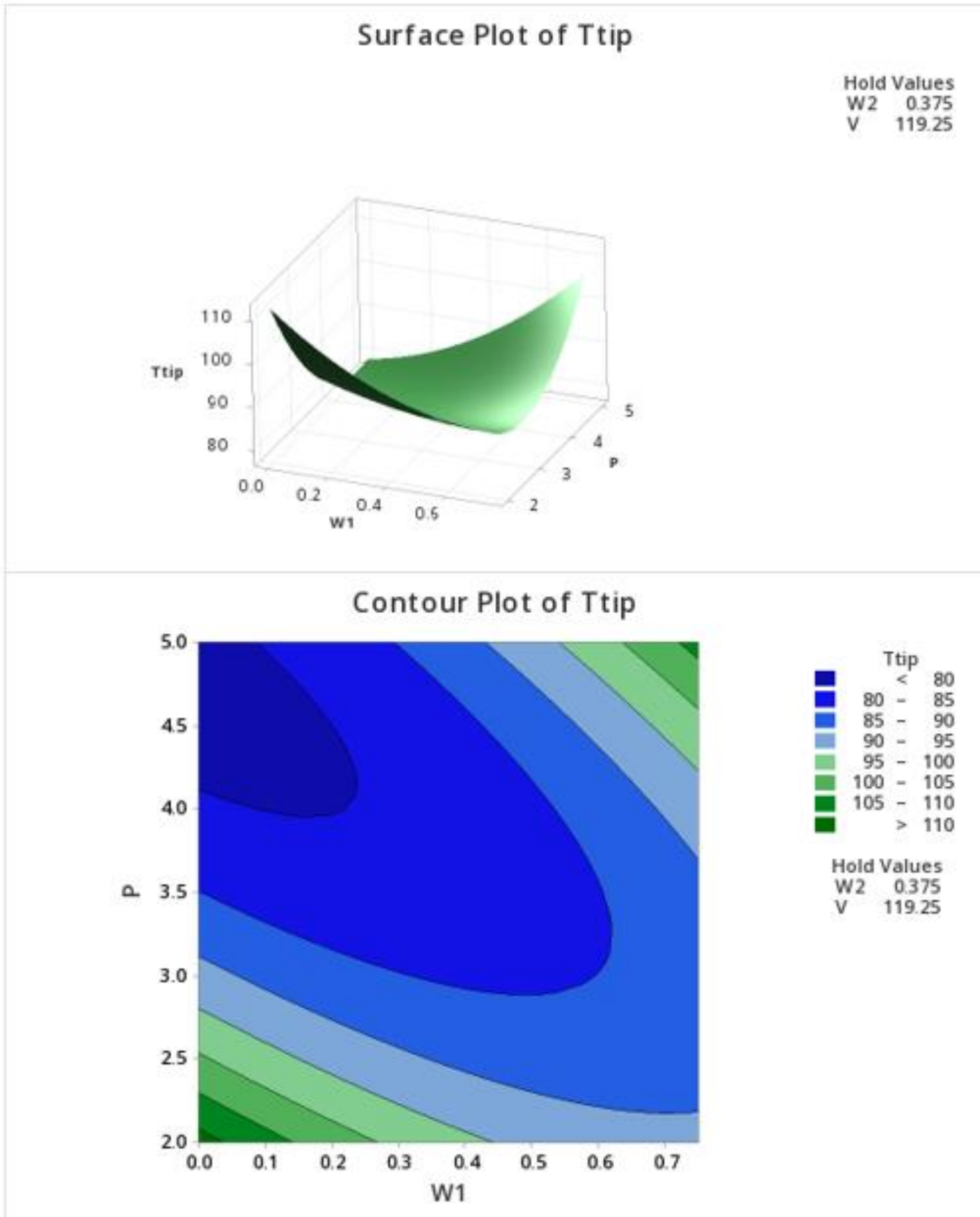

Figure 4-6: Temperature of the tooltip as a function of Al_2O_3 concentration and air pressure

Keeping the TiO_2 concentration and air pressure at the middle level, Figure 4-7 shows the impact of the tooltip temperature on the Al_2O_3 concentration and cutting speed.

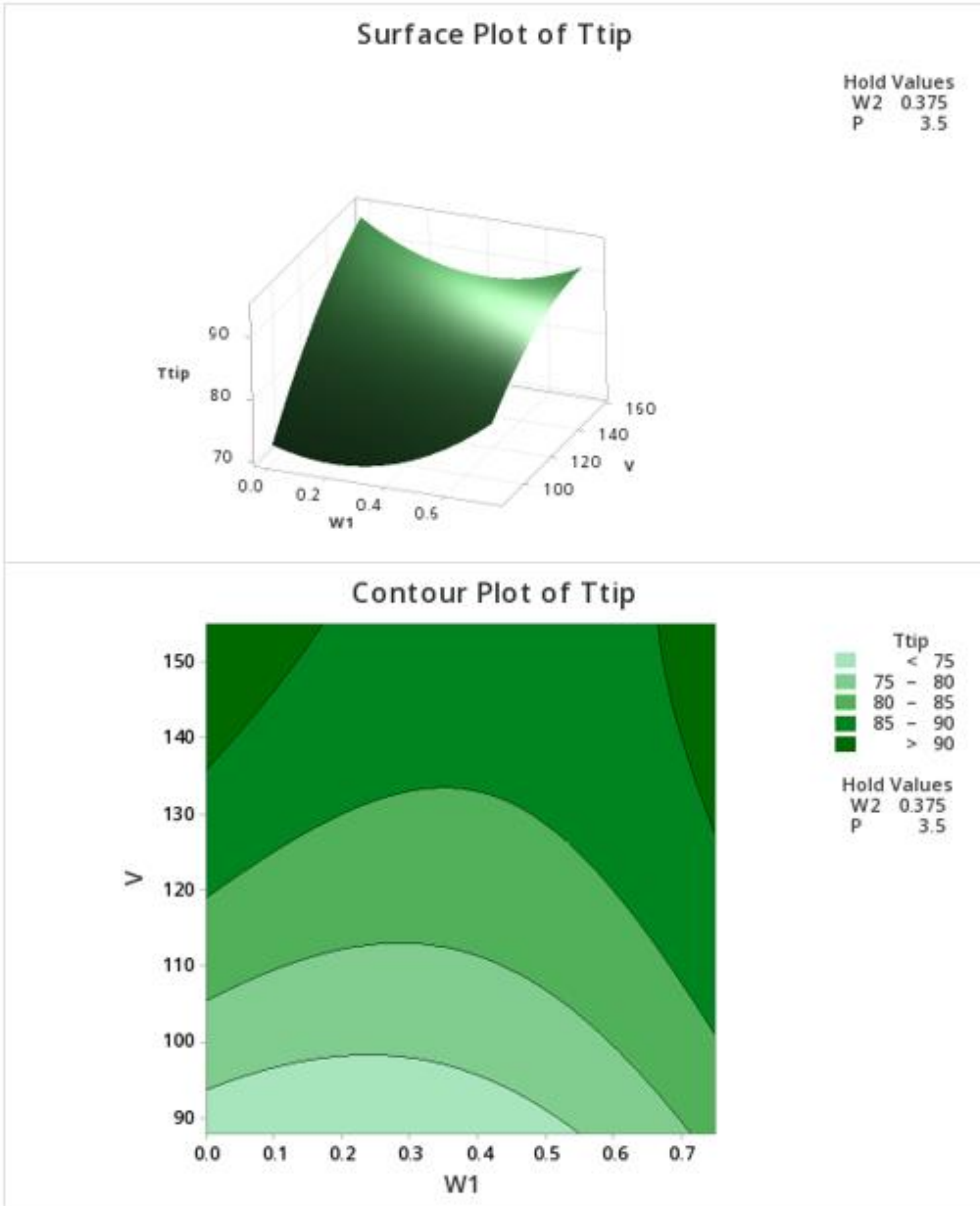

Figure 4-7: Temperature of the tooltip as a function of Al_2O_3 concentration and cutting speed

Keeping the Al_2O_3 concentration and cutting speed at the middle level, Figure 4-8 shows the impact of the tooltip temperature on the TiO_2 concentration and air pressure.

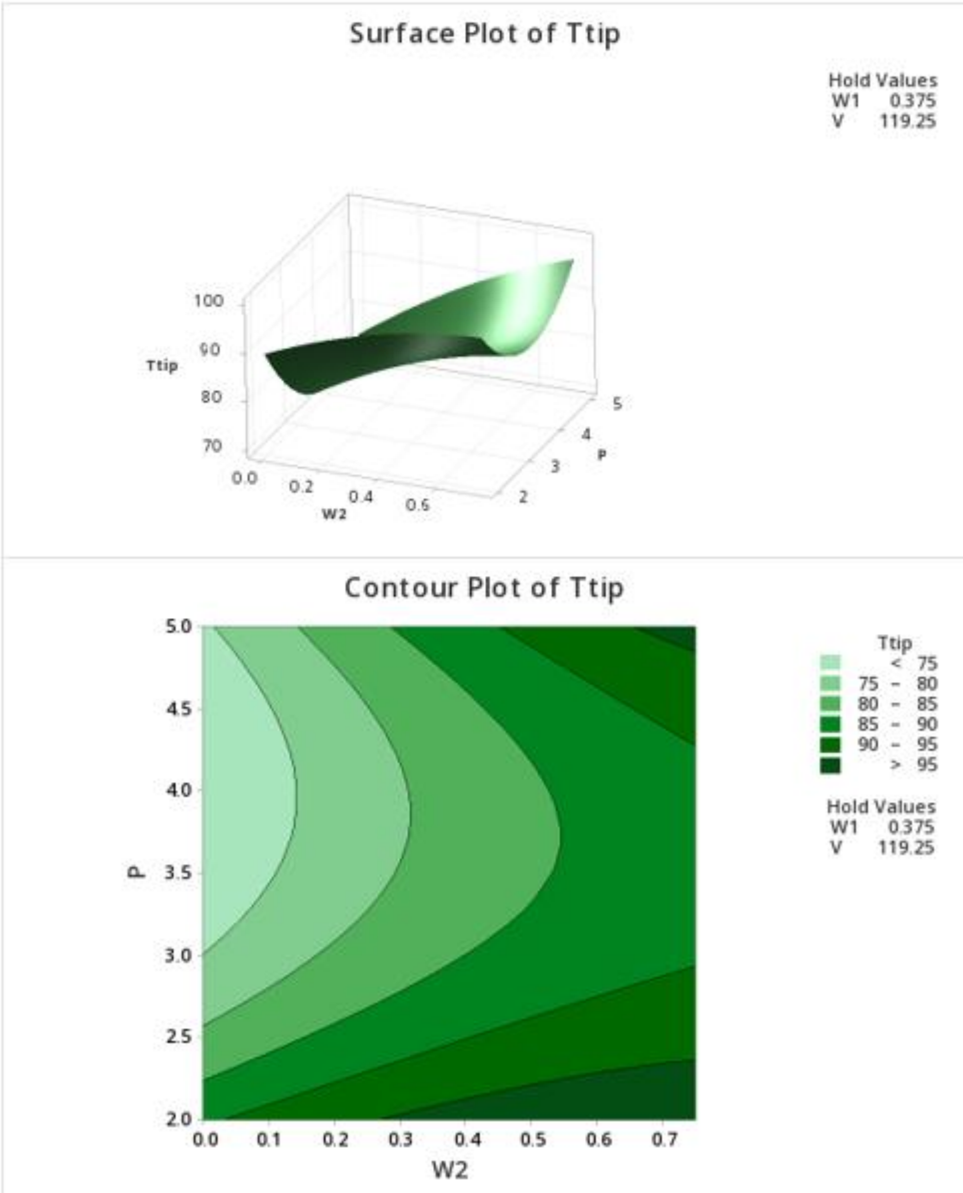

Figure 4-8: Temperature of the tooltip as a function of TiO_2 concentration and air pressure

Keeping the Al_2O_3 concentration and air pressure at the middle level, Figure 4-9 shows the impact of the tooltip temperature on the TiO_2 concentration and cutting speed.

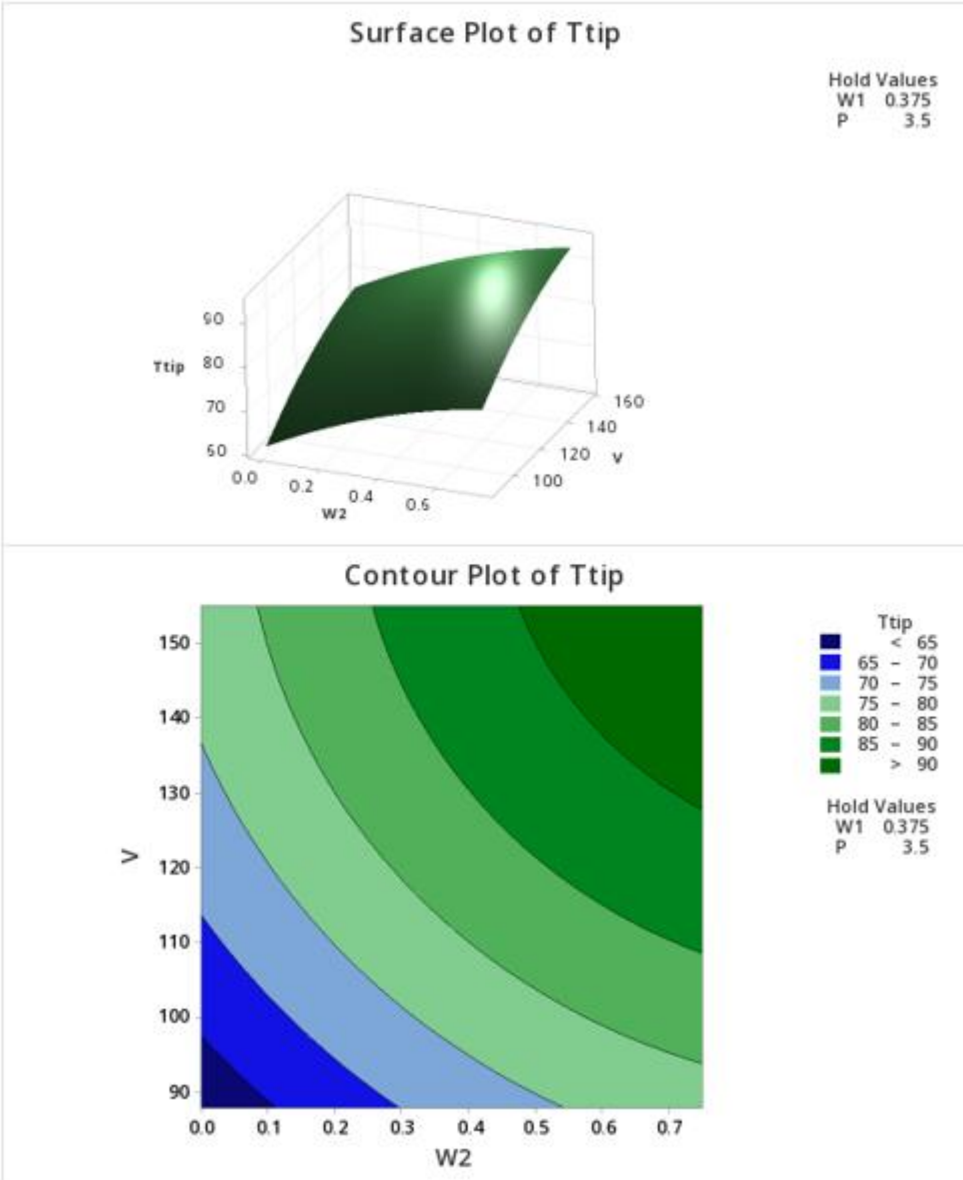

Figure 4-9: Temperature of the tooltip as a function of TiO_2 concentration and cutting speed

Keeping the TiO_2 concentration and Al_2O_3 concentration at the middle level, Figure 4-10 shows the impact of the tooltip temperature on the air pressure and cutting speed.

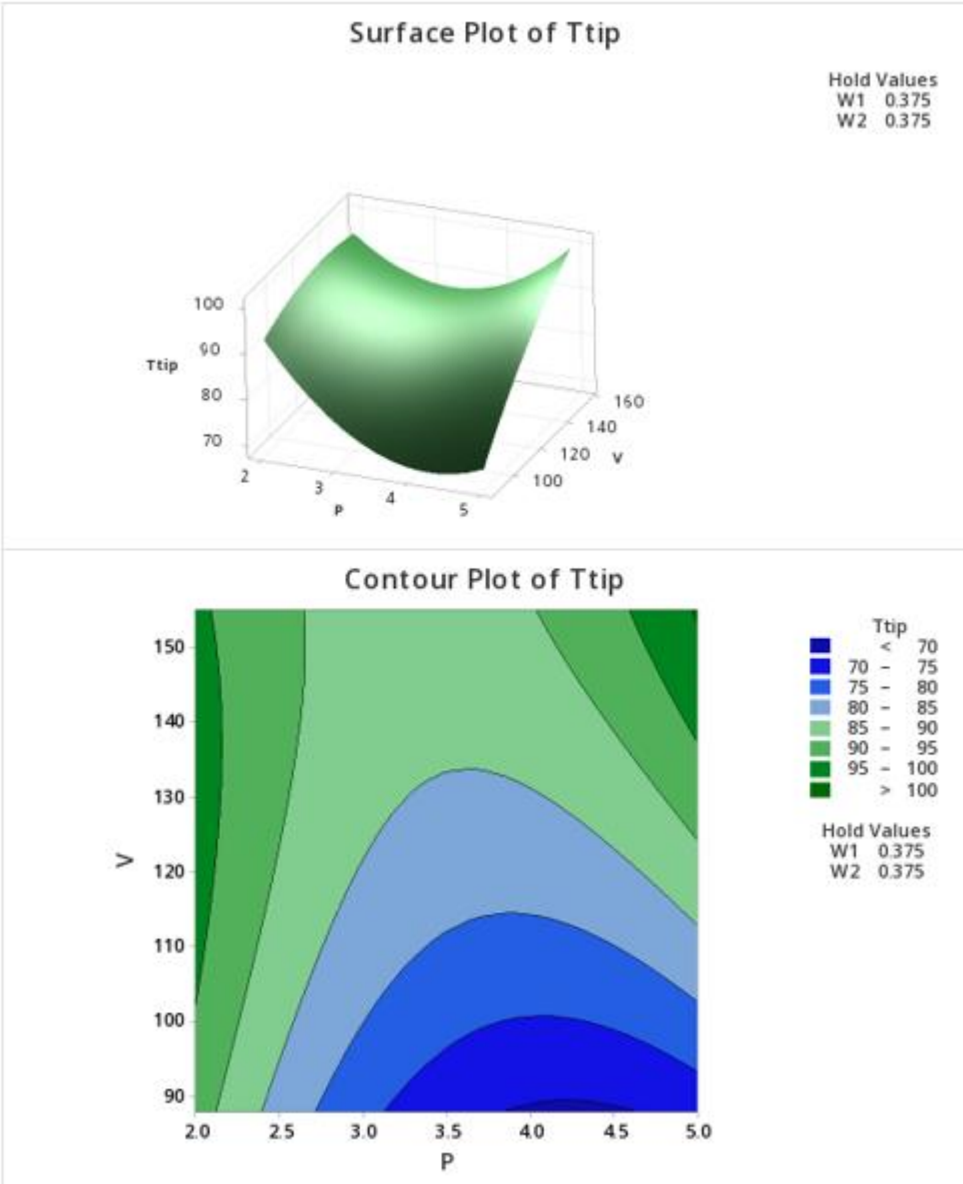

Figure 4-10: Temperature of the tooltip as a function of air pressure and cutting speed

In addition, the same scenario was conducted for the response of average surface roughness. Surface plots and contour plots are shown in figs. 4-11,4-12, 4-13, 4-14, 4-15, and 4-16 in terms of relationship with each variable for average surface roughness.

Keeping the air pressure and cutting speed at the middle level, Figure 4-11 shows the impact of average surface roughness on the Al_2O_3 concentration and TiO_2 concentration.

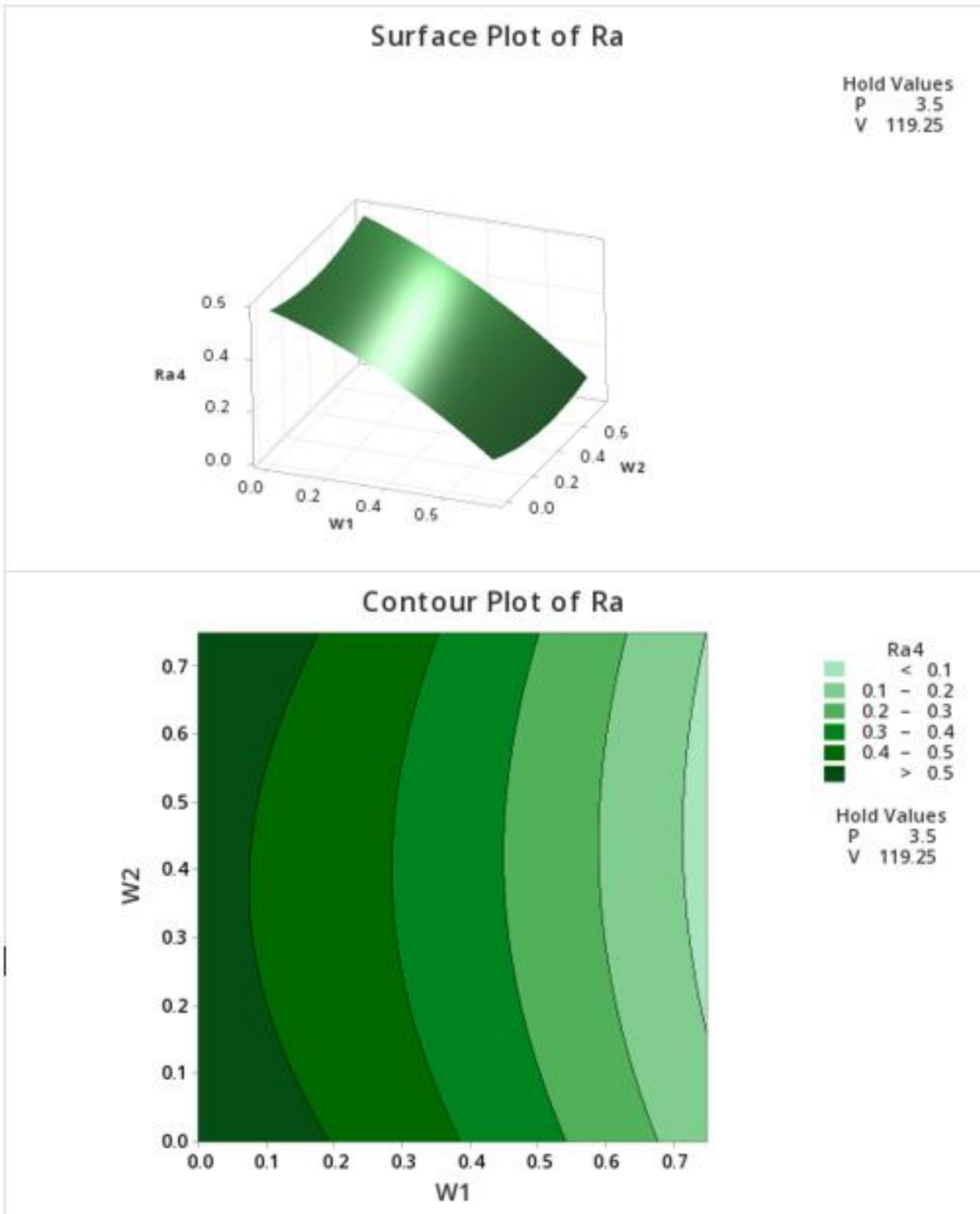

Figure 4-11: Average surface roughness as a function of Al_2O_3 concentration and TiO_2 concentration

Keeping the TiO_2 concentration and cutting speed at the middle level, Figure 4-12 shows the impact of average surface roughness on the Al_2O_3 concentration and air pressure.

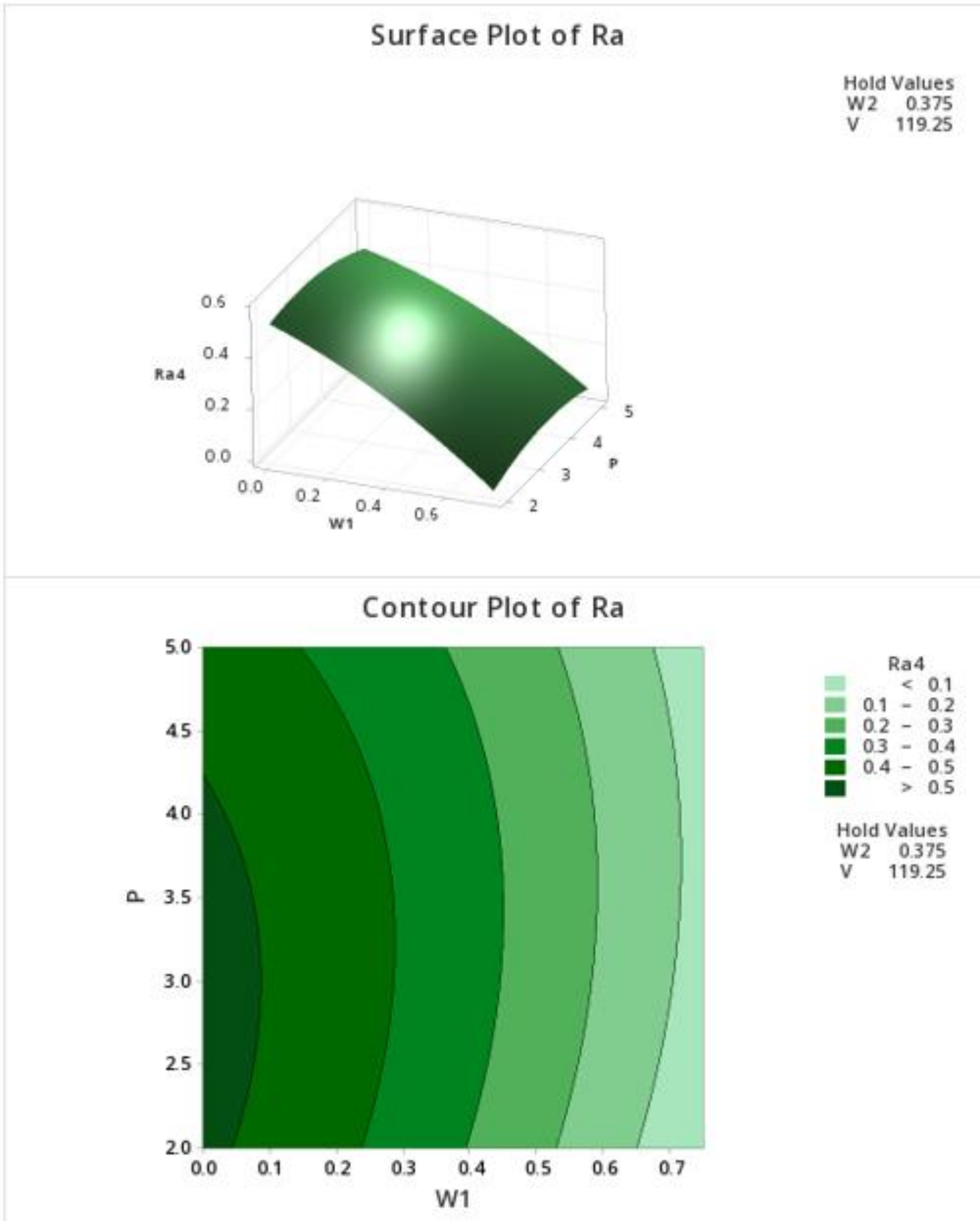

Figure 4-12: Average surface roughness as a function of Al_2O_3 concentration and air pressure

Keeping the TiO_2 concentration and air pressure at the middle level, Figure 4-13 shows the impact of average surface roughness on the Al_2O_3 concentration and cutting speed.

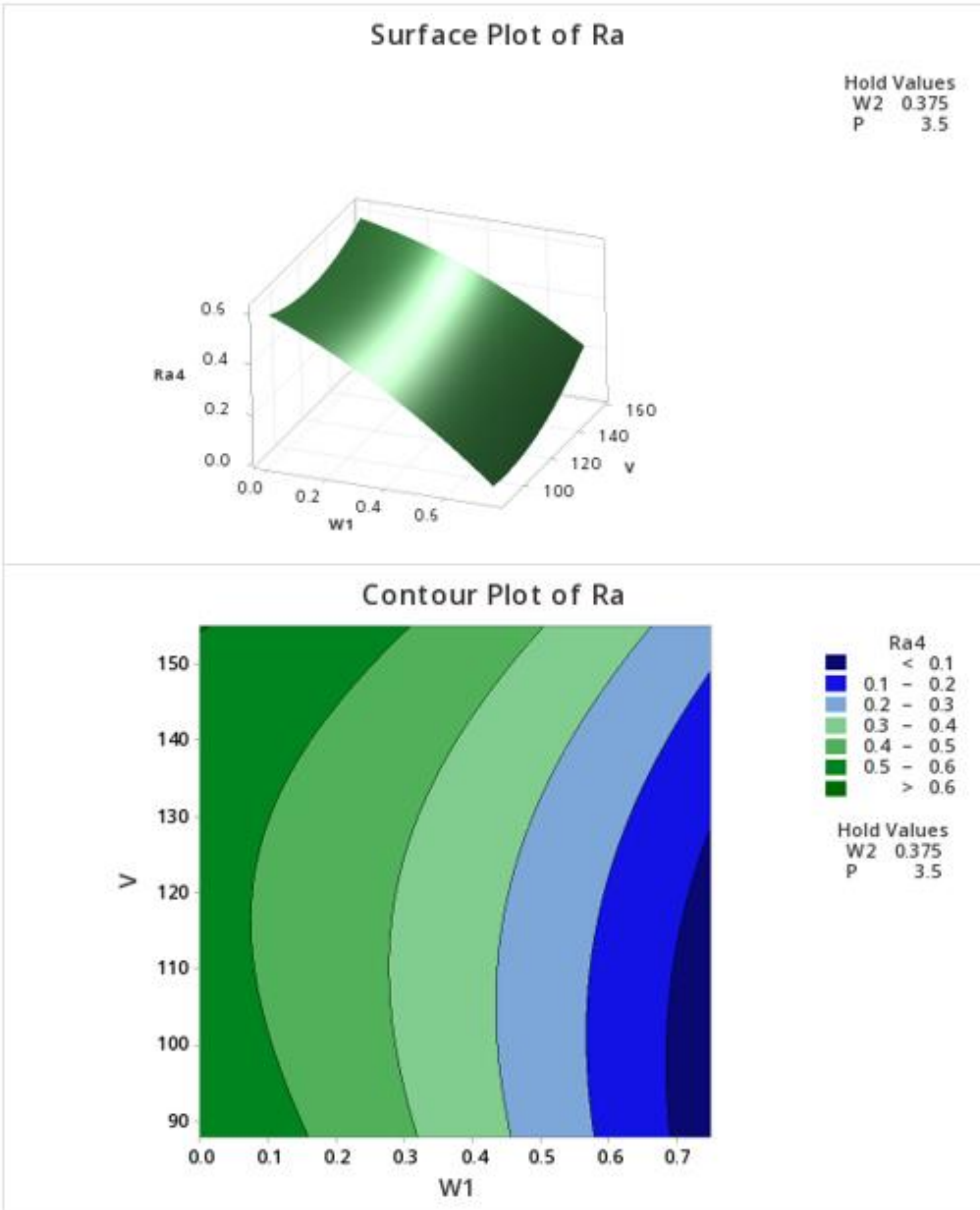

Figure 4-13: Average surface roughness as a function of Al_2O_3 concentration and cutting speed

Keeping the Al_2O_3 concentration and cutting speed at the middle level, Figure 4-14 shows the impact of average surface roughness on the TiO_2 concentration and air pressure.

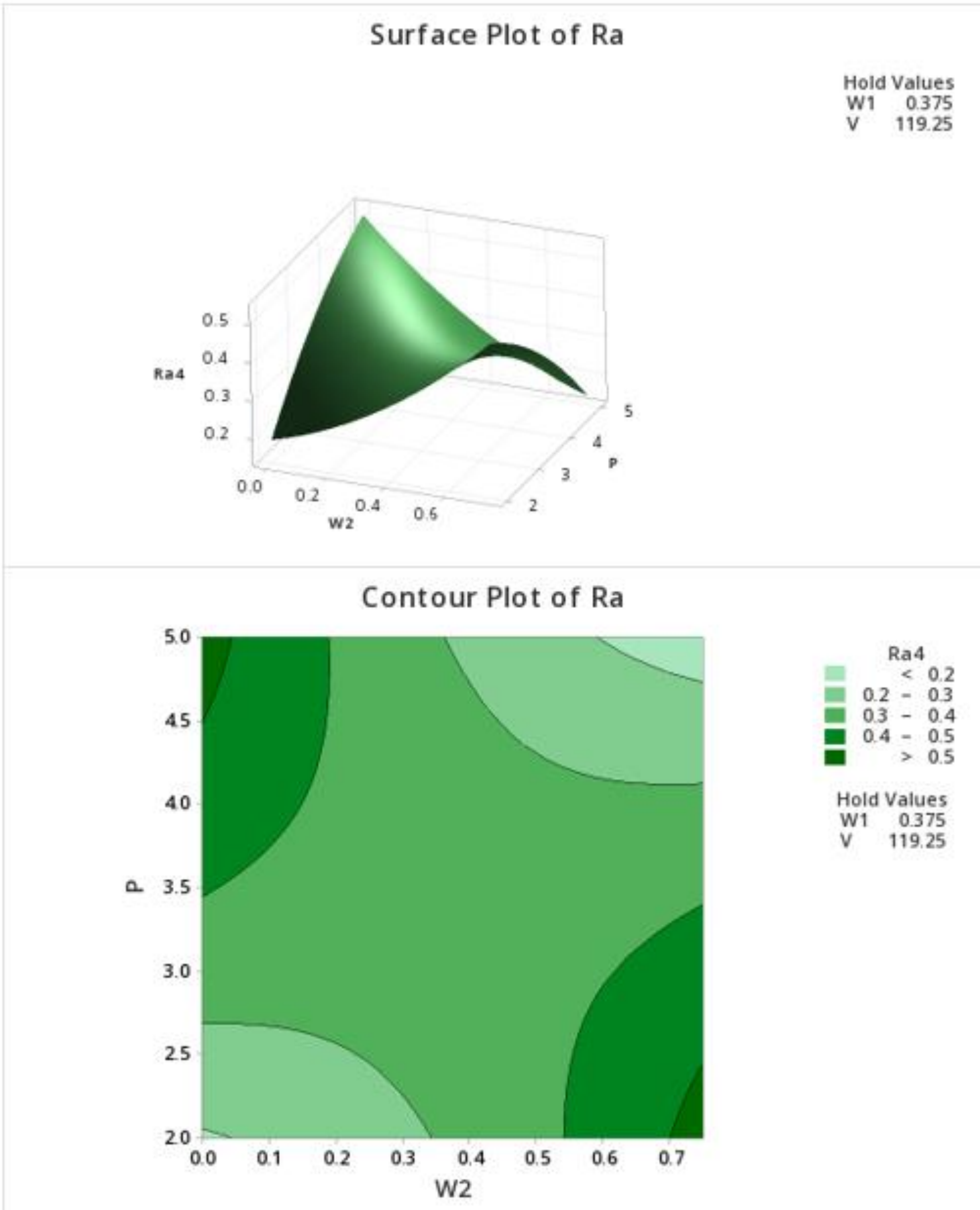

Figure 4-14: Average surface roughness as a function of TiO_2 concentration and air pressure

Keeping the Al_2O_3 concentration and air pressure at the middle level, Figure 4-15 shows the impact of average surface roughness on the TiO_2 concentration and cutting speed.

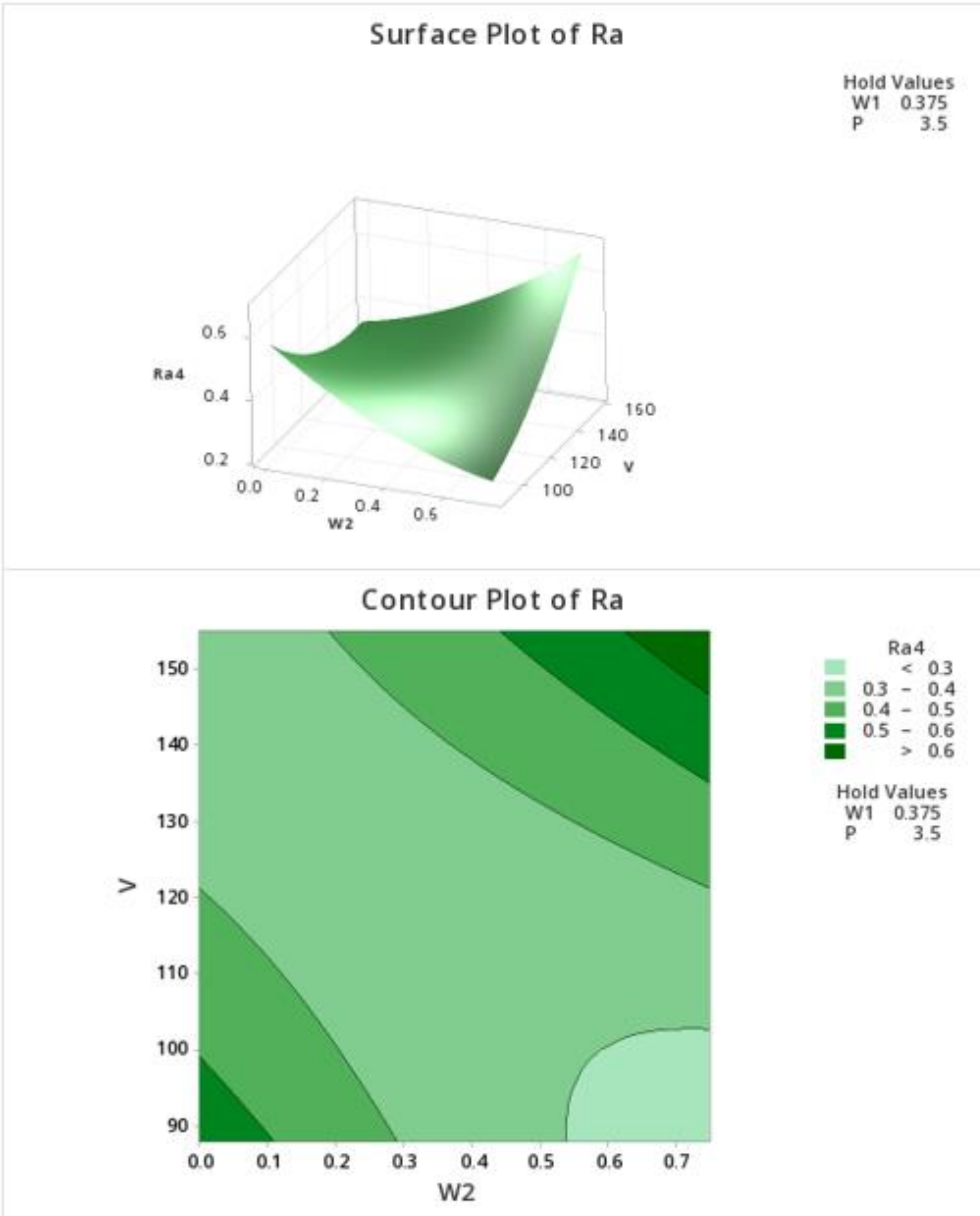

Figure 4-15: Average surface roughness as a function of TiO_2 concentration and cutting speed

Keeping the Al_2O_3 concentration and TiO_2 concentration at the middle level, Figure 4-16 shows the impact of average surface roughness on the air pressure and cutting speed.

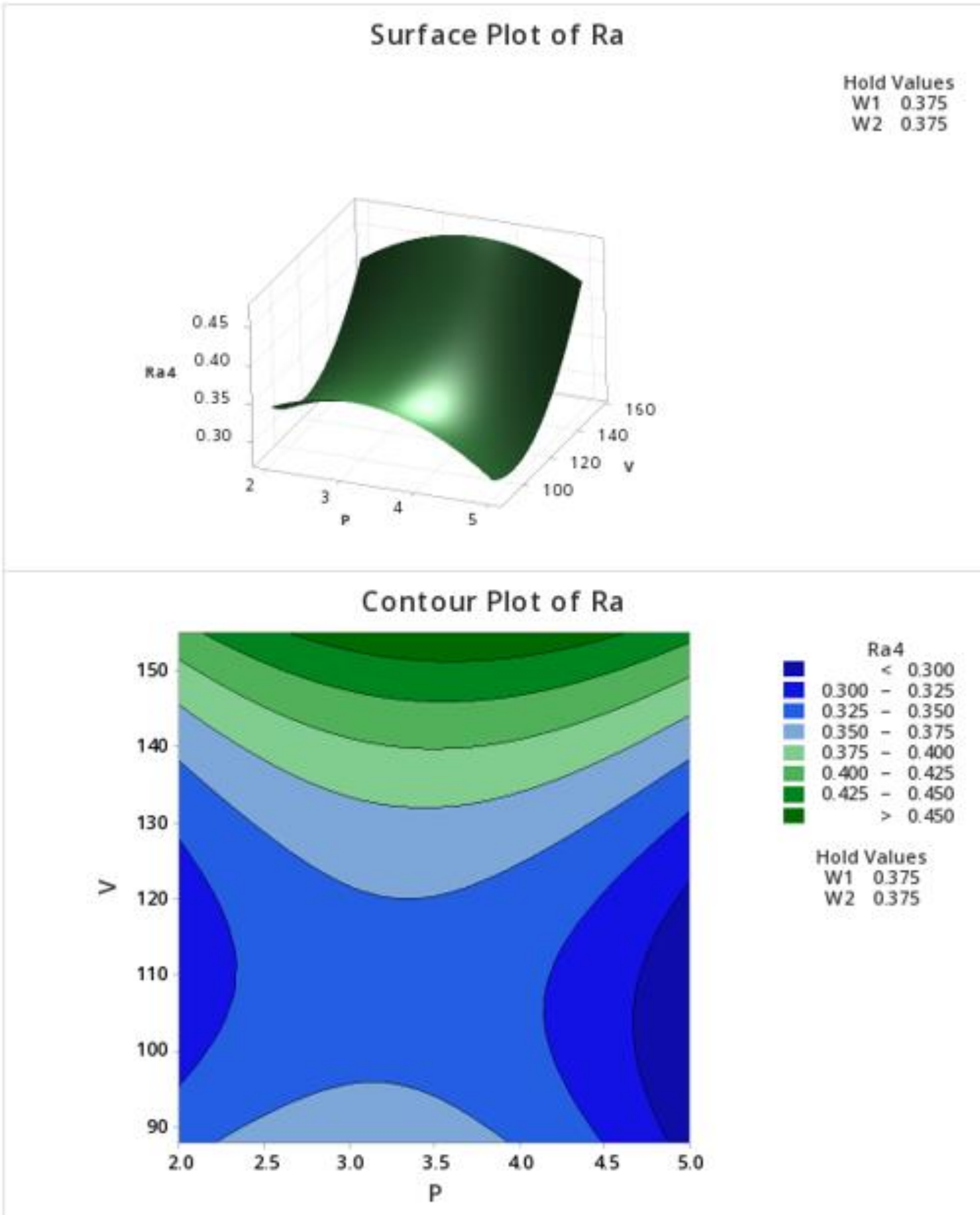

Figure 4-16: Average surface roughness as a function of air pressure and cutting speed

4.4.2 Model Validation

In order to determine whether the model is accurate, the author compared the observed values of the response variable in the experiment to the values that were predicted based on the model. For the purposes of this investigation, a standard percentage error of less than or equal to 5 was regarded. When the model's average percentage error falls within the range of 5.0, the model is considered valid and can be used to forecast the response variable in the future [158]. The error percentage was computed using Equation 5.

$$Percentage\ Error = \frac{Experimental\ value - Predicted\ value}{Experimental\ vlaue} * 100 \qquad \textbf{(5)}$$

Validation for T_{tip}

Based on the equation, the calculated results are shown in Table 4-10, and the average error percentage is -4.015 and less than ± 5, which means this model is a valid further drawn graph for "Empirical results vs Experiment model" shown in Figure 4-17.

Table 4-10: Average error percentage for T_{tip}

No	Experiment	Predicted	%Error
1	104.333	104.638	-0.292
2	75.367	87.876	-16.598
3	96.600	91.007	5.790
4	97.633	103.615	-6.127
5	82.367	85.174	-3.409
6	97.567	104.839	-7.454
7	72.167	71.558	0.844
8	74.967	81.089	-8.167
9	76.067	83.931	-10.339
10	91.567	96.960	-5.890
11	96.200	97.726	-1.586
12	87.100	84.887	2.541
13	85.633	84.742	1.041
14	74.200	79.941	-7.737
15	95.933	95.310	0.650
16	94.067	101.132	-7.511
Average	87.610	90.902	**-4.015**

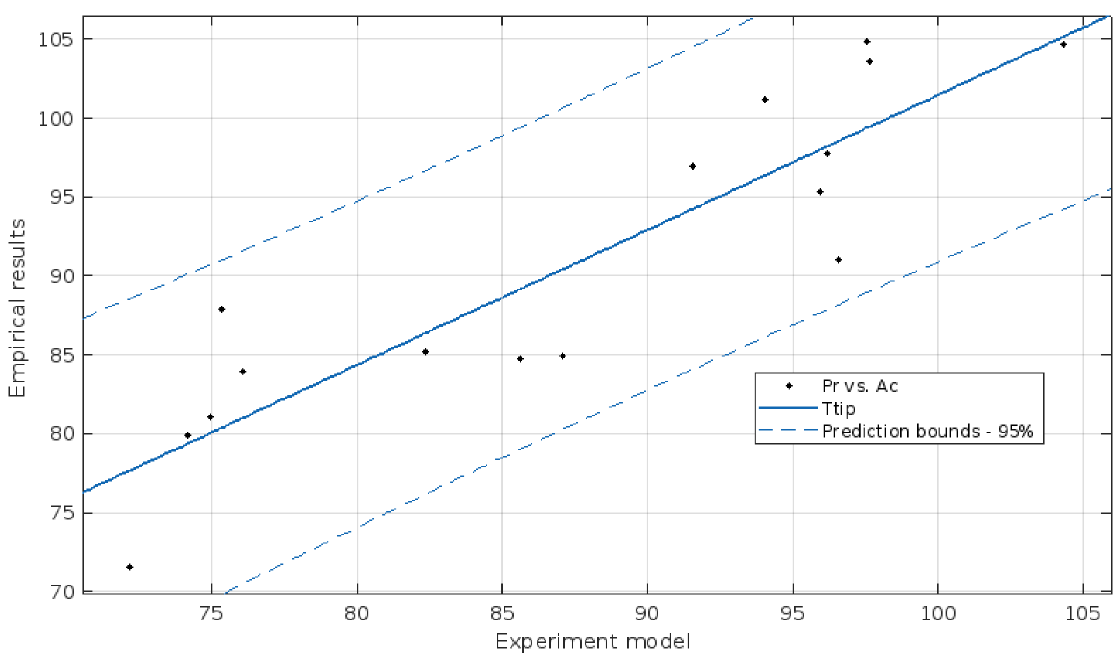

Figure 4-17: Empirical results vs Experiment model for T_{tip}

Validation for R_a

Based on equation 5, the calculated results are shown in Table 4-11, and the average error percentage is -1.279 and is less than ± 5, which means this model is a valid further drawn graph for "Empirical results vs Experiment model" is shown in Figure 4-18.

Table 4-11: Average error percentage for R_a

No	Experiment	Predicted	%Error
1	0.620	0.605	2.470
2	0.524	0.571	-9.012
3	0.580	0.535	7.753
4	0.571	0.586	-2.548
5	0.380	0.368	3.163
6	0.360	0.367	-1.868
7	0.270	0.264	2.238
8	0.280	0.303	-8.295
9	0.341	0.353	-3.490
10	0.300	0.314	-4.616
11	0.260	0.249	4.042
12	0.230	0.212	7.814
13	0.360	0.348	3.342
14	0.100	0.125	-24.656
15	0.321	0.297	7.496
16	0.310	0.324	-4.582
Average	0.363	0.364	**-1.297**

Using R^2 as a coefficient of determination, the models were also validated numerically. R^2 indicates the proportion of the data's observed variability that was accounted for by the model and then calculated using Equation 6. Where $SS_{residual}$ represents the sum of the squares for the residual and SS_{model} represents the sum of the squares for the model.

$$R^2 = 1 - \frac{SS_{residual}}{SS_{model}+SS_{residual}} \quad \textbf{\textit{(6)}}$$

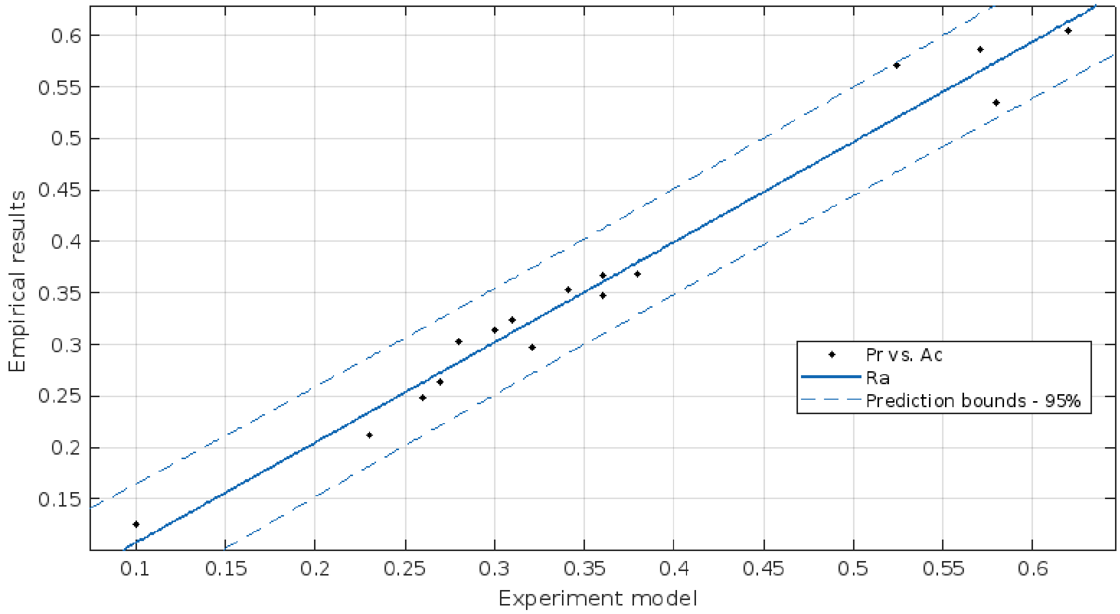

Figure 4-18: Empirical results vs Experiment model for R_a

This study produced models with R^2 values greater than 80 %, namely 81.70 % and 97.48 % for tooltip temperature and average surface roughness, respectively. Because of this circumstance, R^2 values are high and near 1, an excellent combination. Determination coefficients imply mathematical models can reliably estimate tooltip temperature and surface roughness [159].

4.4.3 Multi-Objective Optimisation

When each response is taken into account, air pressure emerges as the most important component that substantially impacts the tooltip temperature, followed by Al_2O_3 concertation, cutting speed and TiO_2 concertation. However, when evaluating the next response factor, which is average surface roughness, Al_2O_3 was the most crucial factor, followed by TiO_2. Then, cutting speed and air pressure influence the roughness values, respectively.

Desirability Function

A fundamental requirement of the machining industry is to provide a combination of conditions that create the desired outputs concurrently [160]. As a result, at the last stage of this work, multi-objective optimization (MOO) was carried out utilizing the conventional desirability approach (CDA). The desirability strategy, which Derringer and Suich first proposed, is a popular, practical, and straightforward method for reaching a destination rapidly [161].

Here, a single integer, say d, between one and zero is used to represent the average of a large number of responses. In this situation, the optimal value is one where d is either one or very close to one. It begins with sorting the responses into "larger is better," "smaller is better," and "better if the target value is reached" categories. Equation 7 is widely utilized since it allows for low temperatures and excellent surface quality to be achieved while turning [162].

$$d_i = \begin{cases} 1 \\ \left(\frac{y^{\cdot} - y_{max}}{y_{min} - y_{max}}\right)^r; \\ 0 \end{cases} \tag{7}$$

$$y_{min} \leq y^{\cdot} \leq y_{max}$$

$$y^{\cdot} \leq y_{min}$$

$$r \geq 0$$

$$y^{\cdot} \geq y_{max}$$

In Equation 6, the smaller the value, the better; y_{max} and y_{min} represent the maximum and minimum values of toleration, and r represents the target weight. In order to get the optimal combination, Using Equation 8, we first add up all of the individual desirability indices for the outputs to get the final composite desirability (D).

$$D = \sqrt[w]{d_1^{w_1} * d_2^{w_2} * d_3^{w_3} \ldots \ldots \ldots * d_i^{w_i}} \tag{8}$$

Where D represents the total desirability, d_i represents the desirability of the response individually, w_i represents the weight of response i, and w represents the sum of the weights. Based on these findings, we were able to determine that dt= 0.97770, dr= 0.99967, and D = 0.9886 represent the individual and composite desirability indices for surface roughness and temperature, respectively. Minitab 17 software was employed to derive the results, and the results are shown in Table 4-12 and graphically represented in Figure 4-19.

Table 4-12: Optimized input variables for the response parameters

Solution	W_1	W_2	P	V	Ra Fit	T_{tip} Fit	Composite Desirability
1	0.75	0	2.63	96.12	0.100171	72.8842	0.988626

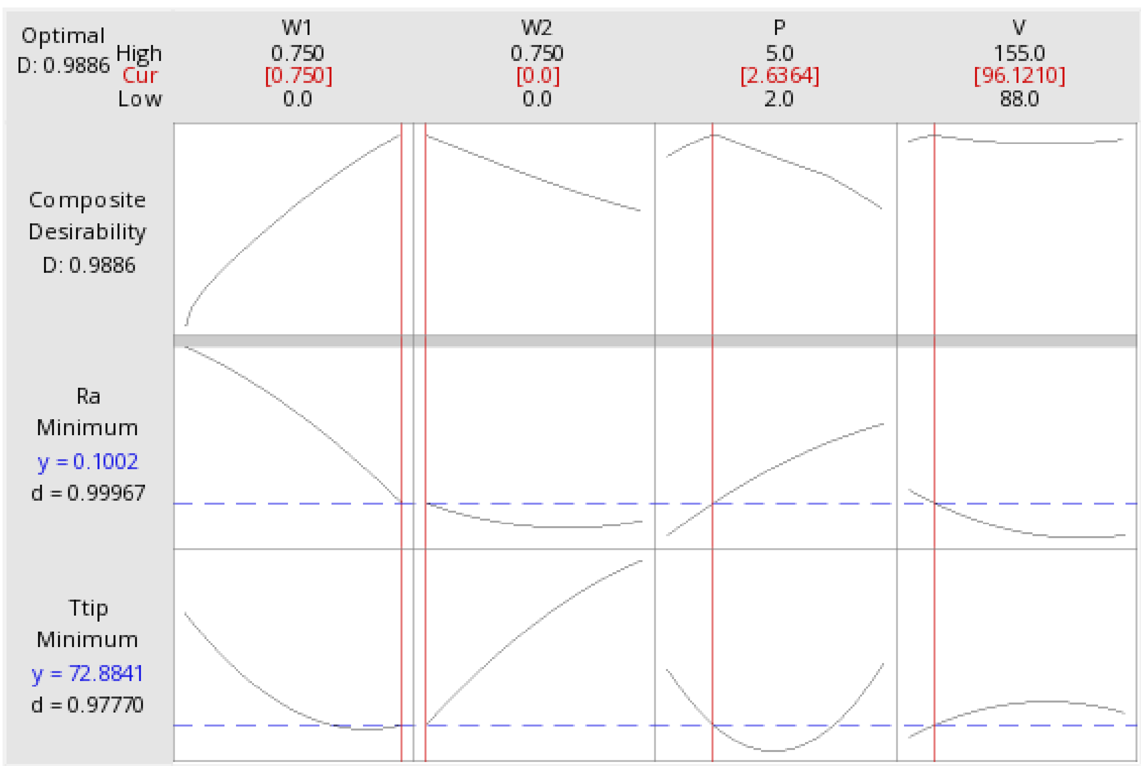

Figure 4-19: Multi-objective optimization results

As per Figure 4-19, increasing the concentration of Al_2O_3 diminishes both responses. Additionally, it boosts the overall desirability. That is because the Al_2O_3 nanoparticles' spherical shape improves lubricating capabilities by entering the tool-chip or tool-workpiece joint. By enhancing thermal conductivity, nanoparticles in base fluid improve cooling and lubrication effects for bearings [100], [163]. The best option is, therefore, the highest Al_2O_3 combination (0.75 wt%).

Comparing the two responses revealed that adding TiO_2 nanoparticles did not improve when comparing both parameters. TiO_2 has poorer thermal conductivity and specific heat compared to Al_2O_3; this is the key rationale for ignoring this particle in the studies[164]. According to the certificate analysis from the nanoparticle supplier, the particle size is also larger than Al_2O_3, which is a significant factor in this result [110].

A rise in air pressure will contribute to an increase in surface roughness. However, up to 3.5 bar, the temperature of the tool decreases. This is because air pressure significantly impacts the ability to create, transport, and maintain oil mist in the cutting zone, whereas increasing the pressure beyond that point tends to raise the tool's temperature. This incident will conclude at 2.6 bar pressure; the composite desirability will decrease. According to the literature, this is because fine atomization occurs as a result of increased particle velocity due to increased air pressure, which in turn reduces tool temperature; however, In general, larger droplets at low velocity are more cumbersome to transport to the cutting zone, whereas smaller droplets at high velocities may bounce off the cutting zone and fail to effectively penetrate it [165], [166].

According to these data, increasing cutting speed increases tool temperature and decreases surface roughness. According to the review of relevant research, cutting speed is directly proportional to tool temperature and interacts with surface roughness less frequently [167], [168]. Both responses indicate that 96 meters per minute yield the best performance.

Validation of Results

Here confirmatory experiments have been carried out to ensure the model's validity. The confirmatory experiments with optimal input parameter settings were performed to validate the tooltip temperature and average surface roughness. The error % based on equation 5 was derived by comparing the expected and experimental outcomes. Tables 4-13 and 4-14 show the average value table for the two responses, namely tooltip temperature and surface roughness. Table 4-15 displays the confirmatory experiment results and error percentage based on optimal parameter settings. The error between experimental and predicted response values is always less than ±5%[169], [170]. Hence the final results are within acceptable limits, indicating that the experimental setup and regression models were suitable for a turning operation within the parameter range selected for the Al_2O_3 and TiO_2 nanofluid hybrid base.

Table 4-13: Confirmatory experiment result for T_{tip}

Ex. No	**Test 01**	**Test 02**	**Test 03**	**Average Temp. (^0C)**
Optimal	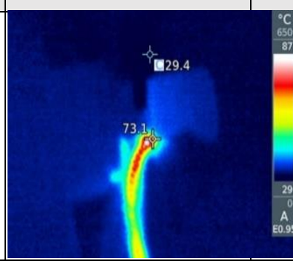	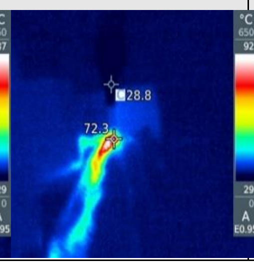	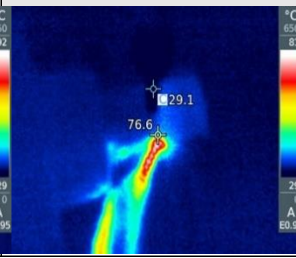	74

Table 4-14: Confirmatory experiment result for R_a

Sample No	**Test 01**	**Test 02**	**Test 03**	**Average Surface roughness (µm)**
Optimal	0.106	0.106	0.103	0.105

Table 4-15: Summary of confirmatory experiment results

Responses	**Predicated values**	**Experimental values**	**Error (%)**
T_{tip} (^0C)	72.88	74	0.78
R_a (µm)	0.100	0.105	4.76

The author also compared these optimal values with dry cutting and novel coconut oil-based MQL technology. It concluded that nanofluid-based MQL provides the best responses for the T_{tip} and R_a under given conditions. The results for the T_{tip} and R_a at the optimum machining parameters are shown in Tables 4-16 and 4-17, respectively.

Table 4-16: Dry and MQL+ CC machining for optimum T_{tip}

Method	**Test 01**	**Test 02**	**Test 03**	**Average Temp. (^{0}C)**
Dry	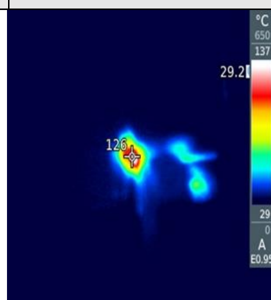	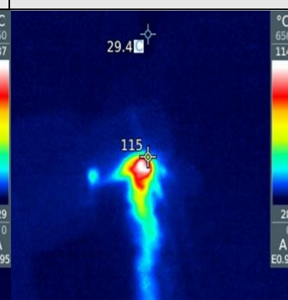	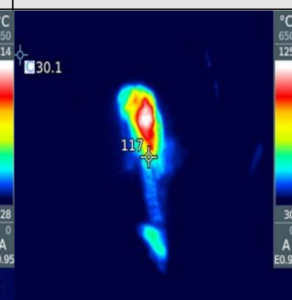	119.3
Novel CC+ MQL	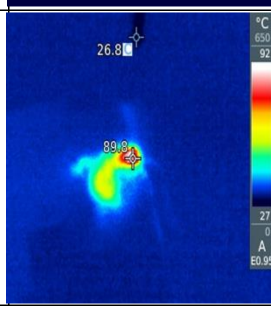	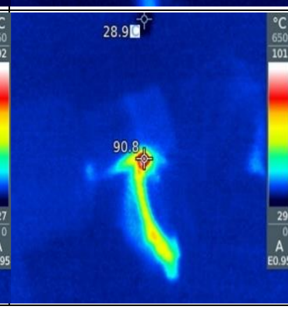	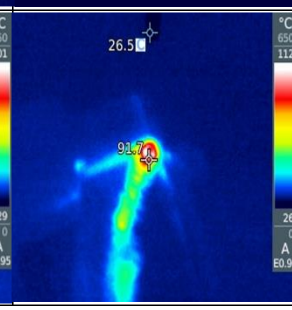	90.76

Table 4-17: Dry and MQL+ CC machining for optimum R_a

Method	**Test 01**	**Test 02**	**Test 03**	**Average Surface roughness (μm)**
Dry	2.022	2.034	2.066	2.04
Novel CC + MQL	1.436	1.309	1.304	1.349

Figure 4-20 represents a combo chart for responses based on the applied cooling techniques, and Figure 4-21 shows the percentage-wise increment in response with the developed MWFs with other cooling techniques.

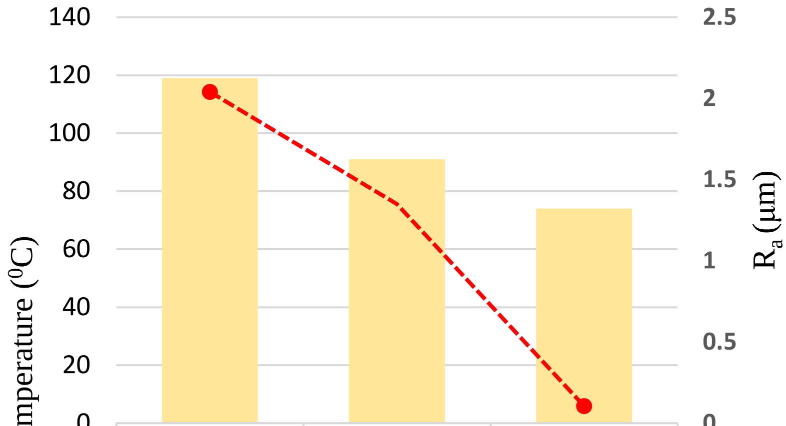

	Dry	MQL + CC	MQL + CC + Nano
Average Temperature	119	91	74
Average Surface Roughness	2.04	1.349	0.105

Figure 4-20: Cooling condition comparisons

Based on Fig 4-20, it is clear that developed MWFs provide the best output than the other cooling techniques.

The developed new coolant shows better performance than the dry and coconut oil+ MQL cooling techniques. Optimal parameter setting was utilized for the experiments, and it finally revealed that compared to dry conditions, 37.8 % and 94.9 % increment in developed MWF for tool tip temperature and average surface roughness, respectively. When comparing it with coconut oil+ MQL condition, 18.7 % and 92.2 % increments are shown for the tool tip temperature and average surface roughness.

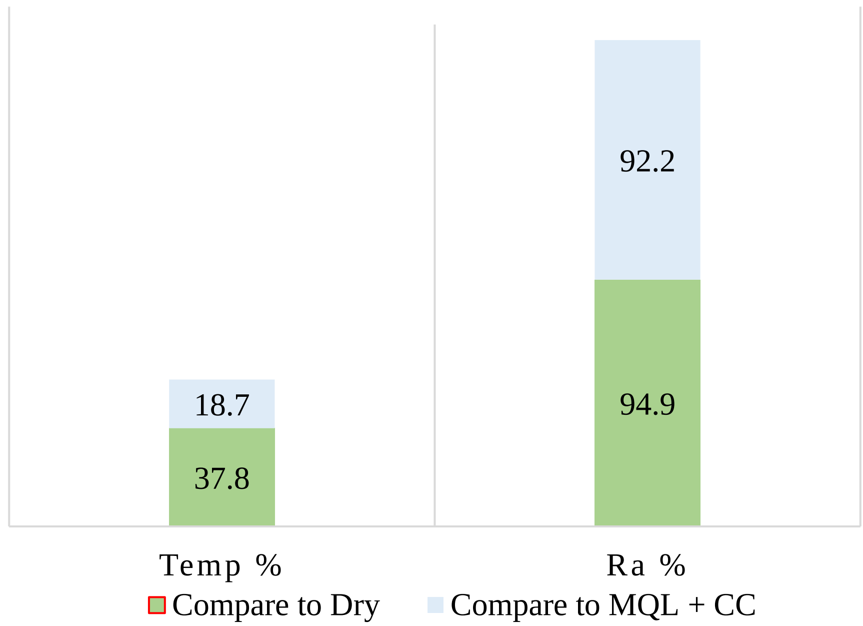

Figure 4-21: Performance comparison (%)

The generated results demonstrate that the author met his study objectives in order to accomplish the research objective.

5 CHAPTER: CONCLUSION

This study examined the influence of four variables (Al_2O_3 wt%, TiO_2 wt%, cutting speed, and air pressure) on T_{tip} and R_a during the turning of AISI 1045 medium carbon steel using coconut oil and MQL technology. As part of this research, an orthogonal design was utilised in order to carry out the experiment, and Minitab 17 was used for model fitting and optimisation.

The analysis results indicate that air pressure plays the most significant effect (40.29 %) on the tooltip temperature (T_{tip}). Al_2O_3 concentration, cutting speed, and TiO_2 concentration also influenced the tooltip temperature. Air pressure of 4 bar, Al_2O_3; 0.25 wt %, cutting speed of 101 m/min, and TiO_2; 0.25 wt% can produce the lowest tooltip temperature in the planned machining conditions.

The results further indicate that the concertation of Al_2O_3 plays the most significant effect (79.62 %) on the average surface roughness (R_a). TiO_2 concentration, cutting speed, and air pressure also contribute to surface roughness. 0.75 wt%; Al_2O_3 concertation, 0.25 wt%; TiO_2 concertation, 88 m/min cutting speed, and 4 bar of air pressure observed the minimum average surface roughness in the planned machining conditions.

Regression equations exist in the average error range and can predict the tooltip temperature and surface roughness under the conditions and parameters of the experiment. A combination of Al_2O_3 and air pressure has the greatest impact on tooltip temperature (8.31 %), and for the R_a; both nanoparticle concentrations (Al_2O_3 and TiO_2) show a substantial effect (2.07 %).

Considering the machining of AISI 1045, the optimal cutting parameters to maximise machinability are 0.75 weight percent Al_2O_3 concentration, 2.5 bar air pressure, and 91 m/min cutting speed. The nanoparticle TiO_2 contribution was zero. TiO_2 had the least impact on tooltip temperature and the second-most impact on surface roughness of the four factors considered. Therefore, it is concluded that achieving both responses simultaneously has no significant effect under the given conditions.

The individual composite values for the average surface roughness and tooltip temperature are 0.99967 and 0.97770, respectively. Furthermore, the composite desirability (0.9886) is close to 1, indicating that the settings produce favourable results for the entirety of the responses.

The developed MWFs perform much better than the other two approaches, dry cutting and coconut oil-based MQL. When compared to dry cutting conditions, the percentages reveal a 23.92% and 37.97% drop in tooltip temperature for MQL+ CC and Nano+ MQL+CC conditions, respectively. In addition, the average surface roughness for MQL+ CC and Nano+ MQL+ CC conditions was reduced by 33.87% and 94.85%, respectively, compared to dry cutting conditions.

Limitations:

The selection of nanoparticles for the experiments is conducted based on the frequency of popularity. Based on that, the author selected the top five nanoparticles. Then the cost of nanoparticles is considered due to available financial support and selected as the lowest-cost material for the experiments. Although the author limited the nanoparticle selection to the above two methods, there are many other factors in selecting the suitable nanoparticle, such as low friction-ability, chemical stability, spreadability (low viscosity), wettability, lubricity, thermal conductivity, particle size, shape, and acidity (pH) value as per the literature [110], [171].

Additionally, the MQL system with the nozzle was evaluated and developed by FOE and UOR, and this equipment was utilized for all studies. The nozzle angle, feed rate, and DOC are maintained based on prior research.

Future work:

The derived results eliminated the TiO_2 from the experiment and provided better responses with Al_2O_3. As per the literature, the hybrid concept will provide a better output for the response/s. Rather than the selection of cost factor, if we can select any other thermophysical or tribological parameters and select the suitable nanoparticles, we can further improve the responses. Further, the biodegradability of developed MWFs and any health hazards are needed to be investigated before introducing the CSCL workshop.

Funding:

This research was partially financed by the Staff Research Funds, Faculty of Engineering at the University of Ruhuna, while the author gave the remaining funds. In addition, testing materials were provided by Ceylon Steel Corporation.

Author Contributions:

Conceptualization, Literature Review, Methodology, Analysis, and Discussion, Writing- W.V.N. Abeweera

Supervision- Dr. G.I.P Perera, Dr. H.K.G. Punchihewa, Mr. R.K.P.S. Ranaweera

REFERENCES

[1] D. Y. Pimenov *et al.*, “Resource saving by optimization and machining environments for sustainable manufacturing: A review and future prospects,” *Renew. Sustain. Energy Rev.*, vol. 166, p. 112660, Sep. 2022.

[2] A. M. Khorasani, M. R. S. Yazdi, and M. S. Safizadeh, “Analysis of machining parameters effects on surface roughness: a review,” *Int. J. Comput. Mater. Sci. Surf. Eng.*, vol. 5, no. 1, p. 68, 2012.

[3] S. Şap, Ü. A. Usca, M. Uzun, M. Kuntoğlu, E. Salur, and D. Y. Pimenov, “Investigation of the Effects of Cooling and Lubricating Strategies on Tribological Characteristics in Machining of Hybrid Composites,” *Lubricants*, vol. 10, no. 4, Apr. 2022.

[4] R. K. Singh, A. K. Sharma, A. R. Dixit, A. K. Tiwari, A. Pramanik, and A. Mandal, “Performance Evaluation of Alumina-graphene Hybrid Nano-cutting Fluid in Hard Turning,” *J. Clean. Prod.*, 2017.

[5] G. Hao and Z. Liu, “The heat partition into cutting tool at tool-chip contact interface during cutting process: a review,” *Int. J. Adv. Manuf. Technol. 2020 1081*, vol. 108, no. 1, pp. 393–411, May 2020.

[6] J. Singh, S. S. Gill, M. Dogra, and R. Singh, “A review on cutting fluids used in machining processes,” *Eng. Res. Express*, vol. 3, no. 1, p. 12002, Mar. 2021.

[7] P. Pranav, E. Sneha, and S. Rani, “Vegetable oil-based cutting fluids and its behavioral characteristics in machining processes: a review,” *Ind. Lubr. Tribol.*, vol. 73, no. 9, pp. 1159–1175, 2021.

[8] V. S. Sharma, G. Singh, and K. Sorby, “A Review on Minimum Quantity Lubrication for Machining Processes,” *http://dx.doi.org/10.1080/10426914.2014.994759*, vol. 30, no. 8, pp. 935–953, Aug. 2015.

[9] Y. Shokoohi, E. Khosrojerdi, and B. H. Rassolian Shiadhi, “Machining and ecological effects of a new developed cutting fluid in combination with different cooling techniques on turning operation,” *J. Clean. Prod.*, vol. 94, pp. 330–339, 2015.

[10] A. K. Sharma, A. K. Tiwari, and A. R. Dixit, “Effects of Minimum Quantity Lubrication (MQL) in machining processes using conventional and nanofluid based cutting fluids: A comprehensive review,” *J. Clean. Prod.*, vol. 127, pp. 1–18, Jul. 2016.

[11] V. Vasu and G. P. K. Reddy, “Effect of minimum quantity lubrication with Al 2 O 3 nanoparticles on surface roughness , tool wear and temperature dissipation in machining Inconel 600 alloy,” vol. 225, pp. 3–15, 2011.

[12] R. Padmini, P. V. Krishna, and G. K. Mohana, “Author ’ s Accepted Manuscript,” *Tribiology Int.*, 2015.

[13] M. M. A. Khan, M. A. H. Mithu, and N. R. Dhar, “Effects of minimum quantity lubrication on turning AISI 9310 alloy steel using vegetable oil-based cutting fluid,” *J. Mater. Process. Technol.*, vol. 209, no. 15–16, pp. 5573–5583, 2009.

[14] C. H. R. V. Kumar and B. Ramamoorthy, “Performance of coated tools during hard turning under minimum fluid application,” vol. 185, pp. 210–216, 2007.

[15] M. C. Kang, K. H. Kim, S. H. Shin, S. H. Jang, J. H. Park, and C. Kim, “Surface & Coatings Technology Effect of the minimum quantity lubrication in high-speed end-milling of AISI D2 cold-worked die steel (62 HRC) by coated carbide tools,” vol. 202, pp. 5621–5624, 2008.

[16] N. R. Dhar, M. Kamruzzaman, and M. Ahmed, “Effect of minimum quantity lubrication (MQL) on tool wear and surface roughness in turning AISI-4340 steel,” vol. 172, pp. 299–304, 2006.

[17] S. Chinchanikar, H. M. Bawangaonwala, and S. Bokade, “Investigations on the

Machining Performance using Solid Lubricant Mixed with Varying Proportions in Vegetable Oil during Hard Turning Investigations on the Machining Performance using Solid Lubricant Mixed with Varying Proportions in Vegetable Oil during ,” 2020.

[18] P. Taylor, S. K. Das, S. U. S. Choi, and H. E. Patel, “Heat Transfer in Nanofluids — A Review Heat Transfer in Nanofluids —,” no. July 2012, pp. 37–41, 2007.

[19] R. J. Aitken, M. Q. Chaudhry, A. B. A. Boxall, and M. Hull, “Manufacture and use of nanomaterials : current status in the UK and global trends,” pp. 300–306, 2015.

[20] I. Khan, K. Saeed, and I. Khan, “Nanoparticles: Properties, Applications and Toxicities,” *Arab. J. Chem.*, no. May, 2017.

[21] P. B. Patole, V. V. Kulkarni, and S. G. Bhatwadekar, “MQL Machining with nano fluid: a review,” *Manuf. Rev.*, vol. 8, p. 13, 2021.

[22] K. A. Hamid, W. H. Azmi, M. F. Nabil, R. Mamat, and K. V Sharma, “International Journal of Heat and Mass Transfer Experimental investigation of thermal conductivity and dynamic viscosity on nanoparticle mixture ratios of TiO 2 -SiO 2 nanofluids Society of Automotive Engineers,” *Int. J. Heat Mass Transf.*, vol. 116, pp. 1143–1152, 2018.

[23] H. Nanofluids, F. Amini, S. Z. Miry, A. Karimi, and M. Ashjaee, “Experimental Investigation of Thermal Conductivity and Viscosity of SiO 2 / Multiwalled Carbon Nanotube,” pp. 3398–3407, 2019.

[24] Z. A. Wahaizad Safiei1,*, Md Mustafizur Rahman2, Ratnakar Kulkarni3, Md Noor Ariffin4 and A. Malek2, “Thermal Conductivity and Dynamic Viscosity of Nanofluids : A Review,” vol. 2, no. 2, pp. 66–84, 2020.

[25] R. Sankaranarayanan, R. Jesudoss, N. Hynes, S. K. J, and G. M. Krolczyk, “A comprehensive review on research developments of vegetable-oil based cutting fluids for sustainable machining challenges,” *J. Manuf. Process.*, vol. 67, no.

November 2020, pp. 286–313, 2021.

[26] S. Debnath, M. M. Reddy, and Q. S. Yi, “Environmental friendly cutting fluids and cooling techniques in machining: a review,” *J. Clean. Prod.*, vol. 83, pp. 33–47, Nov. 2014.

[27] R. Katna, K. Singh, N. Agrawal, and S. Jain, “Green Manufacturing – Performance of a Biodegradable Cutting Fluid,” vol. 6914, no. May, 2017.

[28] T. Norrby and T. Norrby, “Feature Environmentally adapted lubricants – where are the opportunities ?,” 2015.

[29] A. K. Singh and A. K. Gupta, “Metalworking fluids from vegetable oils,” no. September, pp. 167–176, 2006.

[30] T. P. Jeevan and S. R. Jayaram, “Tribological Properties and Machining Performance of Vegetable Oil Based Metal Working Fluids — A Review,” pp. 42–65, 2018.

[31] G. I. P. Perera, H. M. C. M. Herath, I. M. S. J. Perera, and M. G. H. M. M. P. Medagoda, “Investigation on white coconut oil to use as a metal working fluid during turning:,” *http://dx.doi.org/10.1177/0954405414525610*, vol. 229, no. 1, pp. 38–44, Apr. 2014.

[32] D. A. and S. M. A. A. N. Perera G. I., “Investigation on white coconut oil to use as a metal working fluid during turning,” vol. 229, no. 1, pp. 38–44, 2015.

[33] K. C. Wickramasinghe, H. M. C. M. Herath, and G. I. P. Perera, “Empirical investigation of surface quality and temperature during turning AISI 304 steel with vegetable oil based metalworking fluids,” no. October, pp. 1–4, 2016.

[34] K. C. Wickramasinghe, G. I. P. Perera, and H. M. C. M. Herath, “Formulation and performance evaluation of a novel coconut oil–based metalworking fluid,” *http://dx.doi.org/10.1080/10426914.2016.1257858*, vol. 32, no. 9, pp. 1026–1033, Jul. 2017.

[35] K. C. Wickramasinghe, G. I. P. Perera, S. W. M. A. I. Senevirathne, H. K. Punchihewa, and H. Sasahara, “Surface quality evaluation of 0.2 % C and AISI 304 steels in turning with sustainable lubricating condition,” *J. Mech. Sci. Technol.*, vol. 33, no. 12, pp. 5753–5759, Dec. 2019.

[36] W. L. R. Fernando, N. Sarmilan, K. C. Wickramasinghe, H. M. C. M. Herath, and G. I. P. Perera, “Experimental investigation of Minimum Quantity Lubrication (MQL) of coconut oil based Metal Working Fluid,” *Mater. Today Proc.*, vol. 23, pp. 23–26, Jan. 2020.

[37] H. Babar, “Towards hybrid nanofluids : Preparation , thermophysical properties , applications , and challenges Towards hybrid nano fl uids : Preparation , thermophysical properties , applications , and challenges,” *J. Mol. Liq.*, vol. 281, no. March, pp. 598–633, 2019.

[38] V. S. Sharma, M. Dogra, and N. M. Suri, “Cooling techniques for improved productivity in turning,” *Int. J. Mach. Tools Manuf.*, vol. 49, no. 6, pp. 435–453, May 2009.

[39] K. K. Gajrani, P. S. Suvin, S. V. Kailas, and M. R. Sankar, “Hard machining performance of indigenously developed green cutting fluid using flood cooling and minimum quantity cutting fluid,” *J. Clean. Prod.*, vol. 206, pp. 108–123, 2019.

[40] S. Debnath, M. M. Reddy, and Q. S. Yi, “AC SC,” *J. Clean. Prod.*, 2014.

[41] “A Critical review on Minimum Quantity Lubrication (MQL) Coolant System for Machining Operations System for Machining Operations,” no. November, 2016.

[42] E. O. Ezugwu and A. Force, *Overview of the Machining of Titanium Alloys*, vol. 2. Elsevier, 2017.

[43] S. Chinchanikar, S. S. Kore, and P. Hujare, “A review on nanofluids in minimum quantity lubrication machining,” vol. 68, no. May, pp. 56–70, 2021.

[44] H. H. Al-kayiem, S. C. Lin, and A. Lukmon, “Review on Nanomaterials for

Thermal Energy Storage Technologies Review on Nanomaterials for Thermal Energy Storage Technologies," no. September, 2013.

[45] P. V. Krishna, R. R. Srikant, and D. N. Rao, "International Journal of Machine Tools & Manufacture Experimental investigation on the performance of nanoboric acid suspensions in SAE-40 and coconut oil during turning of AISI 1040 steel," *Int. J. Mach. Tools Manuf.*, vol. 50, no. 10, pp. 911–916, 2010.

[46] M. M. S. Prasad and R. R. Srikant, "PERFORMANCE EVALUATION OF NANO GRAPHITE INCLUSIONS IN CUTTING FLUIDS WITH MQL TECHNIQUE IN TURNING OF AISI 1040," pp. 381–393, 2013.

[47] N. Saravanakumar, L. Prabu, M. Karthik, and A. Rajamanickam, "Experimental analysis on cutting fluid dispersed with silver nano particles," *J. Mech. Sci. Technol.*, vol. 28, no. 2, pp. 645–651, 2014.

[48] R. Padmini, P. V. Krishna, and G. K. M. Rao, "Proceedings of the Institution of Mechanical Engineers , Part B : Journal of Engineering Manufacture," 2014.

[49] A. Kumar, R. Kumar, A. Rai, and A. Kumar, "ScienceDirect Characterization and experimental investigation of Al 2 O 3 nanoparticle based cutting fluid in turning of AISI 1040 steel under minimum quantity lubrication (MQL)," *Mater. Today Proc.*, vol. 3, no. 6, pp. 1899–1906, 2016.

[50] A. Kumar, A. Kumar, R. Kumar, and A. Rai, "ScienceDirect Tribological Investigation of TiO 2 Nanoparticle based Cutting Fluid in Machining under Minimum Quantity Lubrication (MQL)," *Mater. Today Proc.*, vol. 3, no. 6, pp. 2155–2162, 2016.

[51] M. K. Gupta, P. K. Sood, and V. S. Sharma, "SC," *J. Clean. Prod.*, 2016.

[52] B. C. Behera, S. Ghosh, and P. V Rao, "Tribology International Application of nano fl uids during minimum quantity lubrication : A case study in turning process," vol. 101, pp. 234–246, 2016.

[53] R. A. Raju, A. Andhare, and N. K. Sahu, "Performance of multi-walled carbon nanotube-based nanofluid in turning operation," *http://dx.doi.org/10.1080/10426914.2017.1279291*, vol. 32, no. 13, pp. 1490–1496, Oct. 2017.

[54] B. C. Behera, D. Setti, S. Ghosh, and P. V. Rao, "Spreadability studies of metal working fluids on tool surface and its impact on minimum amount cooling and lubrication turning," *J. Mater. Process. Tech.*, 2017.

[55] M. Ukamanal, P. Chandra, and A. Kumar, "ScienceDirect Temperature distribution during AISI 316 steel turning under TiO 2 -water based nanofluid spray environments," *Mater. Today Proc.*, vol. 5, no. 9, pp. 20741–20749, 2018.

[56] K. Kishore and R. K. Behera, "Effect of minimum quantity lubrication with Al 2 O 3 Nanofluid on Surface Roughness and its prediction using hybrid fuzzy controller in turning operation of Inconel 600," *Mater. Today Proc.*, vol. 5, no. 9, pp. 20660–20668, 2018.

[57] M. Nouby, "ScienceDirect ScienceDirect ScienceDirect Application of Taguchi-Response surface analysis to optimize the Application of Taguchi-Response surface X-750 analysis to optimize the cutting parameters on turning of Inconel using Nanofluids Engineering on cutt," *Procedia Manuf.*, vol. 30, pp. 90–97, 2019.

[58] Ç. V. Yıldırım, M. Sarıkaya, T. Kıvak, and Ş. Şirin, "The effect of addition of hBN nanoparticles to nanofluid-MQL on tool wear patterns, tool life, roughness and temperature in turning of Ni-based Inconel 625," *Tribol. Int.*, 2019.

[59] K. Venkatesan, S. Devendiran, N. M. Ghazaly, R. Rahul, and T. Mughilan, "Optimization of Cutting Parameters on turning of Incoloy 800H Optimization of Cutting Parameters on turning of Incoloy 800H using Al Nanofluid in Coconut using Al Nanofluid in Coconut oil Costing models for capaci," *Procedia Manuf.*, vol. 30, pp. 268–275, 2019.

[60] Ç. V. Yıldırım, "Experimental comparison of the performance of nanofluids, cryogenic and hybrid cooling in turning of Inconel 625," *Tribol. Int.*, 2019.

[61] R. Kumar, A. K. Sahoo, P. C. Mishra, and R. K. Das, "Influence of Al2O3 and TiO2 nanofluid on hard turning performance," 2019.

[62] M. Khajehzadeh, J. Moradpour, and M. R. Razfar, "Influence of nanolubricant particles ' size on flank wear in hard turning," *Mater. Manuf. Process.*, vol. 0, no. 0, pp. 1–8, 2019.

[63] T. Eli, "Tuning nanofluids for improved lubrication performance in turning biomedical grade titanium alloy," *J. Clean. Prod.*, 2018.

[64] A. Das, S. K. Patel, and S. R. Das, "Performance comparison of vegetable oil based nano fl uids towards machinability improvement in hard turning of HSLA steel using minimum quantity lubrication," vol. 506, 2019.

[65] M. K. Gupta *et al.*, "Performance Evaluation of Vegetable Oil-Based Nano-Cutting Fluids in Environmentally Friendly Machining of Inconel-800 Alloy," 2019.

[66] K. Park and B. Ewald, "Effect of Nano-Enhanced Lubricant in Minimum Quantity Lubrication Balling Milling," vol. 133, no. July, pp. 1–8, 2011.

[67] M. S. Najiha and M. M. Rahman, "Experimental investigation of flank wear in end milling of aluminum alloy with water-based TiO 2 nanofluid lubricant in minimum quantity lubrication technique," 2016.

[68] M. S. Najiha, M. M. Rahman, and K. Kadirgama, *Performance of water-based TiO2 nanofluid during the minimum quantity lubrication machining of aluminium alloy, AA6061-T6*. Elsevier Ltd, 2016.

[69] A. Uysal, F. Demiren, and E. Altan, "Applying Minimum Quantity Lubrication (MQL) Method on Milling of Martensitic Stainless Steel by Using Nano Mos 2 Reinforced Vegetable Cutting Fluid," *Procedia - Soc. Behav. Sci.*, vol. 195, pp. 2742–2747, 2015.

[70] Ş. Şirin and T. Kıvak, "Performances of different eco-friendly nanofluid lubricants in the milling of Inconel X-750 superalloy," *Tribol. Int.*, 2019.

[71] B. Sen, M. Mia, U. K. Mandal, and S. P. Mondal, "Synergistic effect of silica and pure palm oil on the machining performances of Inconel 690: A study for promoting minimum quantity nano doped-green lubricants," *J. Clean. Prod.*, p. 120755, 2020.

[72] W. Huang, D. Wu, and J. Chen, "Robust design of using nanofluid / MQL in micro-drilling," pp. 1–7, 2015.

[73] S. Singh, A. Pal, and T. Singh, "Performance evaluation of aluminium 6063 drilling under the in fl uence of nano fl uid minimum quantity lubrication," vol. 137, pp. 537–545, 2016.

[74] A. Garg, S. Sarma, B. N. Panda, J. Zhang, and L. Gao, "Study of effect of nano fl uid concentration on response characteristics of machining process for cleaner production," *J. Clean. Prod.*, vol. 135, pp. 476–489, 2016.

[75] H. Salimi-yasar, S. Z. Heris, M. Shanbedi, A. Amiri, and A. Kameli, "SC," *Powder Technol.*, 2016.

[76] H. Salimi-yasar, S. Zeinali, and M. Shanbedi, "Tribology International In fl uence of soluble oil-based TiO 2 nano fl uid on heat transfer performance of cutting fl uid," no. December 2016, 2017.

[77] S. Muthuvel, M. N. Babu, and N. Muthukrishnan, "Copper nanofluids under minimum quantity lubrication during drilling of AISI 4140 steel," *Aust. J. Mech. Eng.*, vol. 0, no. 0, pp. 1–14, 2018.

[78] V. Shalimba and B. Sopko, "Nanofluids Application in the Drilling Process Introdution Samples Preparation and Characterizations," *Manuf. Technol.*, vol. 18, no. 3, pp. 493–498, 2018.

[79] A. M. Centre, F. K. Pembuatan, U. Teknikal, H. T. Jaya, and G. District,

"Experimental Investigation of Drilling Process using Nanofluid as Coolant Journal of Advanced Manufacturing Technology (JAMT)," pp. 11–22, 2018.

[80] J. Nam and S. W. Lee, "Machinability of Titanium Alloy (Ti-6Al-4V) in Environmentally-Friendly Micro-Drilling Process with Nanofluid Minimum Quantity Lubrication Using Nanodiamond Particles," vol. 5, no. 1, pp. 29–35, 2018.

[81] J. Soo, P. Lee, and S. Won, "International Journal of Machine Tools & Manufacture Experimental characterization of micro-drilling process using nanofluid minimum quantity lubrication," *Int. J. Mach. Tools Manuf.*, vol. 51, no. 7–8, pp. 649–652, 2011.

[82] W. T. Huang, D. H. Wu, and J. T. Chen, "Robust design of using nanofluid/MQL in micro-drilling," *Int. J. Adv. Manuf. Technol.*, vol. 85, no. 9–12, pp. 2155–2161, 2016.

[83] H. Salimi-Yasar, S. Zeinali Heris, M. Shanbedi, A. Amiri, and A. Kameli, "Experimental investigation of thermal properties of cutting fluid using soluble oil-based TiO2 nanofluid," *Powder Technol.*, vol. 310, pp. 213–220, Apr. 2017.

[84] K. H. Park, B. Ewald, and P. Y. Kwon, "Effect of nano-enhanced lubricant in minimum quantity lubrication balling milling," *J. Tribol.*, vol. 133, no. 3, Jul. 2011.

[85] M. Amrita and S. A. Shariq, "Experimental investigation on application of emulsifier oil based nano cutting fluids in metal cutting process," *Procedia Eng.*, vol. 97, pp. 115–124, 2014.

[86] R. Padmini, P. Vamsi Krishna, and G. Krishna Mohana Rao, "Effectiveness of vegetable oil based nanofluids as potential cutting fluids in turning AISI 1040 steel," *Tribol. Int.*, vol. 94, pp. 490–501, Feb. 2016.

[87] M. K. Gupta, P. K. Sood, and V. S. Sharma, "Optimization of machining parameters and cutting fluids during nano-fluid based minimum quantity lubrication turning of titanium alloy by using evolutionary techniques," *J. Clean.*

Prod., vol. 135, pp. 1276–1288, Nov. 2016.

[88] A. K. Sharma, A. K. Tiwari, A. R. Dixit, and R. K. Singh, “Investigation into Performance of SiO2 Nanoparticle Based Cutting Fluid in Machining Process,” *Mater. Today Proc.*, vol. 4, no. 2, pp. 133–141, 2017.

[89] Chetan, B. C. Behera, S. Ghosh, and P. V. Rao, “Application of nanofluids during minimum quantity lubrication: A case study in turning process,” *Tribol. Int.*, vol. 101, pp. 234–246, Sep. 2016.

[90] Ç. V. Yıldırım, “Experimental comparison of the performance of nanofluids, cryogenic and hybrid cooling in turning of Inconel 625,” *Tribol. Int.*, vol. 137, pp. 366–378, Sep. 2019.

[91] K. Venkatesan, S. Devendiran, N. M. Ghazaly, and Nishanth, “Application of Taguchi-Response surface analysis to optimize the cutting parameters on turning of Inconel X-750 using Nanofluids suspended Al2O3 in coconut oil,” *Procedia Manuf.*, vol. 30, pp. 90–97, Jan. 2019.

[92] J. W. Kim *et al.*, “Parametric analysis and optimization of nanofluid minimum quantity Parametric analysis and optimization of nanofluid minimum quantity lubrication micro-drilling process for titanium Conference alloy lubrication mi,” *Procedia Manuf.*, vol. 26, pp. 403–414, 2018.

[93] S. S. Rahman, M. Z. I. Ashraf, A. N. Amin, M. S. Bashar, M. F. K. Ashik, and M. Kamruzzaman, “Tuning nanofluids for improved lubrication performance in turning biomedical grade titanium alloy,” *J. Clean. Prod.*, vol. 206, pp. 180–196, Jan. 2019.

[94] H. A. Kishawy, H. Hegab, and I. Deiab, “Sustainability Assessment during Machining Ti-6Al-4V with Nano-Additives-Based Minimum Quantity Lubrication,” 2019.

[95] M. K. Gupta *et al.*, “Performance Evaluation of Vegetable Oil-Based Nano-Cutting

Fluids in Environmentally Friendly Machining of Inconel-800 Alloy," 2019.

[96] V. Vasu and G. P. K. Reddy, "Effect of minimum quantity lubrication with Al2O3 nanoparticles on surface roughness, tool wear and temperature dissipation in machining Inconel 600 alloy," *http://dx.doi.org/10.1177/1740349911427520*, vol. 225, no. 1, pp. 3–15, Nov. 2011.

[97] H. Hegab, H. A. Kishawy, M. H. Gadallah, U. Umer, and I. Deiab, "On machining of Ti-6Al-4V using multi-walled carbon nanotubes-based nano-fluid under minimum quantity lubrication," 2018.

[98] T. Jadam, M. Rakesh, S. Datta, and N. Mql, "Machinability of Ti – 6Al – 4V Superalloy : Performance of Dry Cutting and Nanofluid MQL (MWCNT-Added Rice Bran Oil)," *Arab. J. Sci. Eng.*, 2020.

[99] S. Sarkar and S. Datta, "Machining Performance of Inconel 718 Under Dry , MQL , and Nanofluid MQL Conditions : Application of Coconut Oil (Base Fluid) and Multi-walled Carbon Nanotubes as Additives," *Arab. J. Sci. Eng.*, vol. 718, 2020.

[100] S. Kumar *et al.*, "An Investigation Of Multi Walled Carbon Nanotubes Based Nano Cutting Fluids In Turning Of Martensitic Stainless Steel By Using Taguchi And Anova Analysis," pp. 08–15.

[101] H. Hegab, U. Umer, M. Soliman, and H. A. Kishawy, "Effects of nano-cutting fluids on tool performance and chip morphology during machining Inconel 718," *Int. J. Adv. Manuf. Technol.*, vol. 96, no. 9–12, pp. 3449–3458, 2018.

[102] M. A. Makhesana and K. M. Patel, "Performance assessment of vegetable oil-based nanofluid in Minimum Quantity Lubrication (MQL) during machining of Inconel 718," *Adv. Mater. Process. Technol.*, vol. 0, no. 0, pp. 1–17, 2021.

[103] P. Rapeti, V. K. Pasam, K. M. Rao Gurram, and R. S. Revuru, "Performance evaluation of vegetable oil based nano cutting fluids in machining using grey relational analysis-A step towards sustainable manufacturing," *J. Clean. Prod.*, vol.

172, pp. 2862–2875, 2016.

[104] Y. Wang *et al.*, “Processing Characteristics of Vegetable Oil-based Nanofluid MQL for Grinding Different Workpiece Materials,” *Int. J. Precis. Eng. Manuf. - Green Technol.*, vol. 5, no. 2, pp. 327–339, 2018.

[105] T. M. Duc, T. T. Long, and T. Q. Chien, “Performance evaluation of MQL parameters using Al2O3 and MoS2 nanofluids in hard turning 90CrSi steel,” *Lubricants*, vol. 7, no. 5, 2019.

[106] K. R. Wattoo, “A Novel Study on The Effects of Minimum Quantity Lubrication and Machining Parameters in Turning of Ti-6Al-4V Alloy By Applying Al2O3-Graphene Hybrid Nanoparticle Enriched Cutting Fluid,” pp. 1–15, 2021.

[107] M. Jamil *et al.*, “Effects of hybrid Al2O3-CNT nanofluids and cryogenic cooling on machining of Ti–6Al–4V,” *Int. J. Adv. Manuf. Technol.*, vol. 102, no. 9–12, pp. 3895–3909, 2019.

[108] M. Sandeep Kumar and V. Murali Krishna, “An Investigation on Turning AISI 1018 Steel with Hybrid Biodegradeable Nanofluid/MQL Incorporated with Combinations of CuO-Al2O3 Nanoparticles,” *Mater. Today Proc.*, vol. 24, pp. 1577–1584, 2020.

[109] S. Gugulothu and V. K. Pasam, “Experimental investigation to study the performance of CNT/MoS2 hybrid nanofluid in turning of AISI 1040 stee,” *Aust. J. Mech. Eng.*, vol. 0, no. 0, pp. 1–11, 2020.

[110] S. Chinchanikar, S. S. Kore, and P. Hujare, “A review on nanofluids in minimum quantity lubrication machining,” *J. Manuf. Process.*, vol. 68, no. PA, pp. 56–70, 2021.

[111] K. A. Sharma, A. K. Tiwari, and A. R. Dixit, “Mechanism of Nanoparticles Functioning and Effects in Machining Processes: A Review,” *Mater. Today Proc.*, vol. 2, no. 4–5, pp. 3539–3544, Jan. 2015.

[112] A. K. Sharma, A. K. Tiwari, and A. R. Dixit, "Progress of Nanofluid Application in Machining: A Review," *https://doi.org/10.1080/10426914.2014.973583*, vol. 30, no. 7, pp. 813–828, Jul. 2015.

[113] A. Kotia, P. Rajkhowa, G. S. Rao, and S. K. Ghosh, "Thermophysical and tribological properties of nanolubricants: A review," *Heat Mass Transf. und Stoffuebertragung*, vol. 54, no. 11, pp. 3493–3508, 2018.

[114] I. O. P. C. Series and M. Science, "Effect of TiO 2 and Al 2 O 3 -ethylene glycol-based nanofluids on cutting temperature and surface roughness during turning process of AISI 1018 Effect of TiO 2 and Al 2 O 3 -ethylene glycol-based nanofluids on cutting temperature and surface roughness dur," 2020.

[115] I. O. P. C. Series and M. Science, "An overview on performance of metal working fluids with enrichment of nanoparticles for machining process An overview on performance of metal working fluids with enrichment of nanoparticles for machining process," 2018.

[116] R. Kumar, S. Amit, R. Dixit, A. Mandal, and A. Kumar, "Emerging application of nanoparticle - enriched cutting fluid in metal removal processes : a review," 2017.

[117] M. Saravana Kumar and K. L. Senthil Kumar, "An Investigation Of Multi Walled Carbon Nanotubes Based Nano Cutting Fluids In Turning Of Martensitic Stainless Steel By Using Taguchi And Anova Analysis," *IOSR J. Mech. Civ. Eng.*, vol. 15, no. 7, pp. 8–15, 2014.

[118] A. Raihan, I. Ali, and B. Salam, "A review on nanofluid : preparation , stability , thermophysical properties , heat transfer characteristics and application," no. August, 2020.

[119] A. M. Khorasani, M. R. S. Yazdi, and M. S. Safizadeh, "Analysis of machining parameters effects on surface roughness: A review," *Int. J. Comput. Mater. Sci. Surf. Eng.*, vol. 5, no. 1, pp. 68–84, 2012.

[120] M. Santhanakrishnan, P. S. Sivasakthivel, and R. Sudhakaran, “Modeling of geometrical and machining parameters on temperature rise while machining Al 6351 using response surface methodology and genetic algorithm,” *J. Brazilian Soc. Mech. Sci. Eng. 2015 392*, vol. 39, no. 2, pp. 487–496, Jun. 2015.

[121] P. S. Sivasakthivel and R. Sudhakaran, “Optimization of machining parameters on temperature rise in end milling of Al 6063 using response surface methodology and genetic algorithm,” *Int. J. Adv. Manuf. Technol.*, vol. 67, no. 9–12, pp. 2313–2323, Aug. 2013.

[122] S. Debnath, M. M. Reddy, and Q. S. Yi, “Influence of cutting fluid conditions and cutting parameters on surface roughness and tool wear in turning process using Taguchi method,” *Measurement*, vol. 78, pp. 111–119, Jan. 2016.

[123] V. Vasu and G. P. K. Reddy, “Effect of minimum quantity lubrication with Al 2O 3 nanoparticles on surface roughness, tool wear and temperature dissipation in machining Inconel 600 alloy,” *Proc. Inst. Mech. Eng. Part N J. Nanoeng. Nanosyst.*, vol. 225, no. 1, pp. 3–15, Mar. 2012.

[124] A. C. S, A. M. H, A. C. K, A. P. M, and R. Rajan, “Measurement of Cutting Temperature during Machining,” *IOSR J. Mech. Civ. Eng. e-ISSN*, vol. 13, no. 2, pp. 102–116.

[125] K. A. Risbood, U. S. Dixit, and A. D. Sahasrabudhe, “Prediction of surface roughness and dimensional deviation by measuring cutting forces and vibrations in turning process,” *J. Mater. Process. Technol.*, vol. 132, no. 1–3, pp. 203–214, Jan. 2003.

[126] M. Brezocnik, M. Kovacic, and M. Ficko, “Prediction of surface roughness with genetic programming,” *J. Mater. Process. Technol.*, vol. 157–158, no. SPEC. ISS., pp. 28–36, Dec. 2004.

[127] A. M. Zain, H. Haron, and S. Sharif, “Application of GA to observe the optimal

effect of the radial rake angle for minimising surface roughness in end milling," *Int. J. Mach. Mach. Mater.*, vol. 8, no. 3/4, p. 283, 2010.

[128] H. M. C. M. H. K. C. Wickramasinghe, G. I. P. Perera, "Formulation and Performance Evaluation of a Novel Coconut Oil-based Metalworking Fluid," pp. 1–27, 2017.

[129] W. L. R. Fernando, N. Sarmilan, K. C. Wickramasinghe, H. M. C. M. Herath, and G. I. P. Perera, "Materials Today : Proceedings Experimental investigation of Minimum Quantity Lubrication (MQL) of coconut oil based Metal Working Fluid," *Mater. Today Proc.*, no. xxxx, 2019.

[130] Alibaba.com, "Nano Comparision." [Online]. Available: https://www.alibaba.com/detail/compareProducts.html?ids=1600336932381,1600486328033,1600191865971,1600397702495,1600278768231,62012739070&compareId=890fa549b2be48709597c384214d4944&pids=. [Accessed: 18-May-2022].

[131] H. M. Ali, H. Babar, T. R. Shah, M. U. Sajid, M. A. Qasim, and S. Javed, "Preparation Techniques of TiO2 Nanofluids and Challenges: A Review," *Appl. Sci. 2018, Vol. 8, Page 587*, vol. 8, no. 4, p. 587, Apr. 2018.

[132] L. S. Sundar, K. V. Sharma, M. K. Singh, and A. C. M. Sousa, "Hybrid nanofluids preparation, thermal properties, heat transfer and friction factor – A review," *Renew. Sustain. Energy Rev.*, vol. 68, no. March 2016, pp. 185–198, 2017.

[133] A. A. Junankar *et al.*, "Materials Today : Proceedings A Review : Enhancement of turning process performance by effective utilization of hybrid nanofluid and MQL," *Mater. Today Proc.*, no. xxxx, 2020.

[134] W. Tasnim, M. M. Rahman, K. Kadirgama, D. Ramasamy, and M. A. Maleque, "Materials Today : Proceedings An overview on synthesis , stability , opportunities and challenges of nanofluids," *Materials Today: Proceedings*, 2021. .

[135] M. Y. Noordin, V. C. Venkatesh, S. Sharif, S. Elting, and A. Abdullah, "Application of response surface methodology in describing the performance of coated carbide tools when turning AISI 1045 steel," *J. Mater. Process. Technol.*, vol. 145, no. 1, pp. 46–58, Jan. 2004.

[136] S. A. S. Amiril, E. A. Rahim, and A. Z. Hishamudin, "Effect of nozzle distance and cutting parameters on MQL machining of AISI 1045," *J. Phys. Conf. Ser.*, vol. 1150, no. 1, 2019.

[137] A. Yassin and C. Y. Teo, "Effect of Pressure and Nozzle Angle of Minimal Quantity Lubrication on Cutting Temperature and Tool Wear in Turning," *Appl. Mech. Mater.*, vol. 695, pp. 676–679, 2014.

[138] R. Kumar, S. Amit, R. Dixit, A. Mandal, and A. Kumar, "Emerging application of nanoparticle - enriched cutting fluid in metal removal processes : a review," *J. Brazilian Soc. Mech. Sci. Eng.*, 2017.

[139] B. Rahmati, A. A. D. Sarhan, and M. Sayuti, "Investigating the optimum molybdenum disulfide (MoS 2) nanolubrication parameters in CNC milling of AL6061-T6 alloy," pp. 1143–1155, 2014.

[140] Y. H. Chai, S. Yusup, V. S. Chok, M. T. Arpin, and S. Irawan, "Investigation of Thermal Conductivity of Multi Walled Carbon Nanotube Dispersed in Hydrogenated Oil Based Drilling Fluids," *Appl. Therm. Eng.*, 2016.

[141] P. Kalita, A. P. Malshe, and K. P. Rajurkar, "CIRP Annals - Manufacturing Technology Study of tribo-chemical lubricant film formation during application of nanolubricants in minimum quantity lubrication (MQL) grinding," *CIRP Ann. - Manuf. Technol.*, vol. 61, no. 1, pp. 327–330, 2012.

[142] C. Mao, H. Zou, and X. Huang, "The influence of spraying parameters on grinding performance for nanofluid minimum quantity lubrication," pp. 1791–1799, 2013.

[143] M. Sayuti, A. A. D. Sarhan, and M. Hamdi, "An investigation of optimum SiO 2

nanolubrication parameters in end milling of aerospace Al6061-T6 alloy," pp. 833–849, 2013.

[144] S. Sharif, I. O. Sadiq, and M. A. Suhaimi, "Overview of Nanofluid Application through Minimum Quantity Lubrication (MQL) in Metal Cutting Process," vol. 20199, 2017.

[145] A. Mishra, "Application of Taguchi method in optimization of toolflank wear width in turning operation of AISI 1045 steel."

[146] A. Qasim, S. Nisar, A. Shah, M. Saeed, and M. A. Sheikh, "Simulation Modelling Practice and Theory Optimization of process parameters for machining of AISI-1045 steel using Taguchi design and ANOVA," *Stimul. Model. Pract. THEORY*, vol. 59, pp. 36–51, 2015.

[147] E. Kilickap, M. Huseyinoglu, and A. Yardimeden, "Optimization of drilling parameters on surface roughness in drilling of AISI 1045 using response surface methodology and genetic algorithm," pp. 79–88, 2011.

[148] Z. Xiao, X. Liao, Z. Long, and M. Li, "Effect of cutting parameters on surface roughness using orthogonal array in hard turning of AISI 1045 steel with YT5 tool," *Int. J. Adv. Manuf. Technol.*, 2016.

[149] A. Bhattacharya, Æ. S. Das, and P. M. Æ. A. Batish, "Estimating the effect of cutting parameters on surface finish and power consumption during high speed machining of AISI 1045 steel using Taguchi design and ANOVA," pp. 31–40, 2009.

[150] N. S. T. T. S. Gobikannan, "Application of Response Surface Methodology and Firefly Algorithm for Optimizing Multiple Responses in Turning AISI 1045 Steel," pp. 8015–8030, 2014.

[151] METALWORKING SOLUTIONS COMPANY, "Effects of Cutting Conditions for Turning | MITSUBISHI MATERIALS CORPORATION," *MITSUBISHI*

MATERIALS, 2021. [Online]. Available: http://www.mitsubishicarbide.com/en/technical_information/tec_turning_tools/tec_hsk-t/tec_hsk-t_technical/tec_turning_effects. [Accessed: 13-May-2022].

[152] S. A. Lawal, I. A. Choudhury, and Y. Nukman, “A critical assessment of lubrication techniques in machining processes: A case for minimum quantity lubrication using vegetable oil-based lubricant,” *J. Clean. Prod.*, vol. 41, pp. 210–221, 2013.

[153] S. Ekinović, E. Begović, and A. Lušija, “MQL Machining – Oil on Water Droplet System,” *4th Int. Symp. Sustain. Dev.*, no. September, pp. 15–25, 2013.

[154] A. Çiçek, T. Kivak, and G. Samtas, “Application of taguchi method for surface roughness and roundness error in drilling of AISI 316 stainless steel,” *Stroj. Vestnik/Journal Mech. Eng.*, vol. 58, no. 3, pp. 165–174, 2012.

[155] K. N. Bharath, G. B. Manjunatha, and K. Santhosh, *Failure analysis and the optimal toughness design of sheep-wool reinforced epoxy composites*. Elsevier Ltd, 2018.

[156] J. Laxman and K. G. Raj, “Mathematical modeling and analysis of EDM process parameters based on Taguchi design of experiments,” *J. Phys. Conf. Ser.*, vol. 662, no. 1, 2015.

[157] M. Nouioua, M. A. Yallese, R. Khettabi, S. Belhadi, M. L. Bouhalais, and F. Girardin, “Investigation of the performance of the MQL, dry, and wet turning by response surface methodology (RSM) and artificial neural network (ANN),” *Int. J. Adv. Manuf. Technol.*, vol. 93, no. 5–8, pp. 2485–2504, 2017.

[158] A. Rathi, A. Mahor, R. Ranjan, A. Gajbhiye, A. Rehman, and C. M. Krishna, “Prediction of Chip Morphology for Aluminum Metal Matrix Composites in End Milling Machining,” *Univers. J. Mech. Eng.*, vol. 2, no. 7, pp. 240–247, 2014.

[159] M. Sarikaya and A. Güllü, “Multi-response optimization of minimum quantity lubrication parameters using Taguchi-based grey relational analysis in turning of

difficult-to-cut alloy Haynes 25," *J. Clean. Prod.*, vol. 91, pp. 347–357, 2015.

[160] O. Öndin, T. Kıvak, M. Sarıkaya, and Ç. V. Yıldırım, "Investigation of the influence of MWCNTs mixed nanofluid on the machinability characteristics of PH 13-8 Mo stainless steel," *Tribol. Int.*, vol. 148, p. 106323, Aug. 2020.

[161] R. Amdoun *et al.*, "The Desirability Optimization Methodology; a Tool to Predict Two Antagonist Responses in Biotechnological Systems: Case of Biomass Growth and Hyoscyamine Content in Elicited Datura starmonium Hairy Roots," *Iran. J. Biotechnol.*, vol. 16, no. 1, pp. 11–19, Feb. 2018.

[162] G. Derringer and R. Suich, "Simultaneous Optimization of Several Response Variables," *J. Qual. Technol.*, vol. 12, no. 4, pp. 214–219, Oct. 1980.

[163] M. Huo *et al.*, "Understanding the role of water-based nanolubricants in micro flexible rolling of aluminium," *Tribol. Int.*, vol. 151, p. 106378, Nov. 2020.

[164] Z. Said *et al.*, "Enhancing the performance of automotive radiators using nanofluids," *Renew. Sustain. Energy Rev.*, vol. 112, pp. 183–194, Sep. 2019.

[165] P. A. Jadhav and R. Deivanathan, "Numerical analysis of the effect of air pressure and oil flow rate on droplet size and tool temperature in MQL machining," *Mater. Today Proc.*, vol. 38, pp. 2499–2505, Jan. 2021.

[166] T. M. Duc, T. T. Long, and N. M. Tuan, "Performance investigation of mql parameters using nano cutting fluids in hard milling," *Fluids*, vol. 6, no. 7, 2021.

[167] H. Saglam, S. Yaldiz, and F. Unsacar, "The effect of tool geometry and cutting speed on main cutting force and tool tip temperature," *Mater. Des.*, vol. 28, no. 1, pp. 101–111, Jan. 2007.

[168] N. Lungu and M. Borzan, "EFFECT OF CUTTING SPEED AND FEED RATE ON TOOL GEOMETRY, TEMPERATURE AND CUTTING FORCES IN MACHINING AISI 1045 CARBON STEEL USING FEM SIMULATION," *Proc. Manuf. Syst.*, vol. 7, no. 4, 2012.

[169] A. K. Sharma, J. K. Katiyar, S. Bhaumik, and S. Roy, “Influence of alumina / MWCNT hybrid nanoparticle additives on tribological properties of lubricants in turning operations,” vol. 7, no. 2, pp. 153–168, 2019.

[170] A. Thakur, A. Manna, and S. Samir, “Experimental investigation of nanofluids in minimum quantity lubrication during turning of EN-24 steel,” *Proc. Inst. Mech. Eng. Part J J. Eng. Tribol.*, vol. 234, no. 5, pp. 712–729, 2020.

[171] H. Babar and H. M. Ali, “Towards hybrid nanofluids: Preparation, thermophysical properties, applications, and challenges,” *J. Mol. Liq.*, vol. 281, pp. 598–633, May 2019.

LIST OF APPENDICES

Appendix - A ANOVA calculation for Tooltip Temperature

1	2	3	4	5	6	7	8	9	10	11	12	13	14	15	16
104	60.6	88.8	89.2	77.3	82.7	59.5	61.7	58.2	80.9	80.6	73.7	75.7	69.9	84.8	85.6
104	88.2	95	98.7	81	106	74.8	76.3	81.3	88.8	103	82.6	81.7	75.6	102	98.2
105	77.3	106	105	88.8	104	82.2	86.9	88.7	105	105	105	99.5	77.1	101	98.4
104.333	**75.367**	**96.600**	**97.633**	**82.367**	**97.567**	**72.167**	**74.967**	**76.067**	**91.567**	**96.200**	**87.100**	**85.633**	**74.200**	**95.933**	**94.067**

1	2	3	4	5	6	7	8	9	10	11	12	13	14	15	16
104.333	75.367	96.600	97.633	82.367	97.567	72.167	74.967	76.067	91.567	96.200	87.100	85.633	74.200	95.933	94.067

	ontrol factors & experiment level				Control factors & experiment levels				Temperature (°C)
Exp. No	**W_1**	**W_2**	**P**	**V**	**W_1**	**W_2**	**P**	**V**	
1	1	1	1	1	0.00	0.00	2	88	104
2	1	2	2	2	0.00	0.25	3	101	75
3	1	3	3	3	0.00	0.50	4	133	97
4	1	4	4	4	0.00	0.75	5	155	98
5	2	1	2	3	0.25	0.00	3	133	82
6	2	2	1	4	0.25	0.25	2	155	98
7	2	3	4	1	0.25	0.50	5	88	72
8	2	4	3	2	0.25	0.75	4	101	75
9	3	1	3	4	0.50	0.00	4	155	76
10	3	2	4	3	0.50	0.25	5	133	92
11	3	3	1	2	0.50	0.50	2	101	96
12	3	4	2	1	0.50	0.75	3	88	87
13	4	1	4	2	0.75	0.00	5	101	86
14	4	2	3	1	0.75	0.25	4	88	74
15	4	3	2	4	0.75	0.50	3	155	96
16	4	4	1	3	0.75	0.75	2	133	94

	Level 01				Level 02				Level 03				Level 04			
Exp. No	**W_1**	**W_2**	**P**	**V**	**W_1**	**W_2**	**P**	**V**	**W_1**	**W_2**	**P**	**V**	**W_1**	**W_2**	**P**	**V**
1	104.33	104.33	104.33	104.33	0.00	0.00	0.00	0.00	0.00	0.00	0.00	0.00	0.00	0.00	0.00	0.00
2	75.37	0.00	0.00	0.00	0.00	75.37	75.37	75.37	0.00	0.00	0.00	0.00	0.00	0.00	0.00	0.00
3	96.60	0.00	0.00	0.00	0.00	0.00	0.00	0.00	0.00	96.60	96.60	96.60	0.00	0.00	0.00	0.00
4	97.63	0.00	0.00	0.00	0.00	0.00	0.00	0.00	0.00	0.00	0.00	0.00	0.00	97.63	97.63	97.63
5	0.00	82.37	0.00	0.00	82.37	0.00	82.37	0.00	0.00	0.00	0.00	82.37	0.00	0.00	0.00	0.00
6	0.00	0.00	97.57	0.00	97.57	97.57	0.00	0.00	0.00	0.00	0.00	0.00	0.00	0.00	0.00	97.57
7	0.00	0.00	0.00	72.17	72.17	0.00	0.00	0.00	0.00	72.17	0.00	0.00	0.00	0.00	72.17	0.00
8	0.00	0.00	0.00	0.00	74.97	0.00	0.00	74.97	0.00	0.00	74.97	0.00	0.00	74.97	0.00	0.00
9	0.00	76.07	0.00	0.00	0.00	0.00	0.00	0.00	76.07	0.00	76.07	0.00	0.00	0.00	0.00	76.07
10	0.00	0.00	0.00	0.00	0.00	91.57	0.00	0.00	91.57	0.00	0.00	91.57	0.00	0.00	91.57	0.00
11	0.00	0.00	96.20	0.00	0.00	0.00	0.00	96.20	96.20	96.20	0.00	0.00	0.00	0.00	0.00	0.00
12	0.00	0.00	0.00	87.10	0.00	0.00	87.10	0.00	87.10	0.00	0.00	0.00	0.00	87.10	0.00	0.00
13	0.00	85.63	0.00	0.00	0.00	0.00	0.00	85.63	0.00	0.00	0.00	0.00	85.63	0.00	85.63	0.00
14	0.00	0.00	0.00	74.20	0.00	74.20	0.00	0.00	0.00	0.00	74.20	0.00	74.20	0.00	0.00	0.00
15	0.00	0.00	0.00	0.00	0.00	0.00	95.93	0.00	0.00	95.93	0.00	0.00	95.93	0.00	0.00	95.93
16	0.00	0.00	94.07	0.00	0.00	0.00	0.00	0.00	0.00	0.00	0.00	94.07	94.07	94.07	0.00	0.00

Total 1401.767

T	1401.767
n	16
T^2/n	122809.362
SS_T	1653.488
SS_A	274.715
SS_B	65.617
SS_C	666.216
SS_D	243.772

ANOVA SUMMARY (unpooled)

Factor	DoF	SS	Mean Sq	F-Ratio	% of Contribution
W1	3	274.715	91.572	0.681	16.614
W2	3	65.617	21.872	0.163	3.968
P	3	666.216	222.072	1.652	40.292
V	3	243.772	81.257	0.605	14.743
Error	3	403.169	134.390		24.383
Total	15	1653.488	110.23		100.000

Appendix - B ANOVA calculation for Average Surface Roughness

1	2	3	4	5	6	7	8	9	10	11	12	13	14	15	16
0.641	0.531	0.591	0.575	0.376	0.364	0.301	0.271	0.349	0.301	0.249	0.233	0.355	0.104	0.341	0.337
0.612	0.511	0.576	0.572	0.391	0.366	0.267	0.293	0.345	0.306	0.264	0.241	0.381	0.101	0.323	0.301
0.607	0.530	0.573	0.566	0.373	0.350	0.242	0.276	0.329	0.293	0.267	0.216	0.344	0.095	0.299	0.292
0.620	**0.524**	**0.580**	**0.571**	**0.380**	**0.360**	**0.270**	**0.280**	**0.341**	**0.300**	**0.260**	**0.230**	**0.360**	**0.100**	**0.321**	**0.310**

1	2	3	4	5	6	7	8	9	10	11	12	13	14	15	16
0.620	0.524	0.580	0.571	0.380	0.360	0.270	0.280	0.341	0.300	0.260	0.230	0.360	0.100	0.321	0.310

	Control factors & experiment levels				Control factors & experiment levels				Ra (μm)
Exp. No	W_1	W_2	P	V	W_1	W_2	P	V	
1	1	1	1	1	0.00	0.00	2	88	0.620
2	1	2	2	2	0.00	**0.25**	**3**	**101**	0.524
3	1	3	3	3	0.00	**0.50**	**4**	**133**	0.580
4	1	4	4	4	0.00	**0.75**	**5**	**155**	0.571
5	2	1	2	3	0.25	0.00	3	133	0.380
6	2	2	1	4	0.25	0.25	2	155	0.360
7	2	3	4	1	0.25	0.50	5	88	0.270
8	2	4	3	2	0.25	0.75	4	101	0.280
9	3	1	3	4	0.50	0.00	4	155	0.341
10	3	2	4	3	0.50	0.25	5	133	0.300
11	3	3	1	2	0.50	0.50	2	101	0.260
12	3	4	2	1	0.50	0.75	3	88	0.230
13	4	1	4	2	0.75	0.00	5	101	0.360
14	4	2	3	1	0.75	0.25	4	88	0.100
15	4	3	2	4	0.75	0.50	3	155	0.321
16	4	4	1	3	0.75	0.75	2	133	0.310
								Total	5.807

	Level 01				Level 02				Level 03				Level 04			
Exp. No	W_1	W_2	P	V	W_1	W_2	P	V	W_1	W_2	P	V	W_1	W_2	P	V
1	0.62	0.62	0.62	0.62	0.00	0.00	0.00	0.00	0.00	0.00	0.00	0.00	0.00	0.00	0.00	0.00
2	0.52	0.00	0.00	0.00	0.00	0.52	0.52	0.52	0.00	0.00	0.00	0.00	0.00	0.00	0.00	0.00
3	0.58	0.00	0.00	0.00	0.00	0.00	0.00	0.00	0.00	0.58	0.58	0.58	0.00	0.00	0.00	0.00
4	0.57	0.00	0.00	0.00	0.00	0.00	0.00	0.00	0.00	0.00	0.00	0.00	0.00	0.57	0.57	0.57
5	0.00	0.38	0.00	0.00	0.38	0.00	0.38	0.00	0.00	0.00	0.00	0.38	0.00	0.00	0.00	0.00
6	0.00	0.00	0.36	0.00	0.36	0.36	0.00	0.00	0.00	0.00	0.00	0.00	0.00	0.00	0.00	0.36
7	0.00	0.00	0.00	0.27	0.27	0.00	0.00	0.00	0.00	0.27	0.00	0.00	0.00	0.00	0.27	0.00
8	0.00	0.00	0.00	0.00	0.28	0.00	0.00	0.28	0.00	0.00	0.28	0.00	0.00	0.28	0.00	0.00
9	0.00	0.34	0.00	0.00	0.00	0.00	0.00	0.00	0.34	0.00	0.34	0.00	0.00	0.00	0.00	0.34
10	0.00	0.00	0.00	0.00	0.00	0.30	0.00	0.00	0.30	0.00	0.00	0.30	0.00	0.00	0.30	0.00
11	0.00	0.00	0.26	0.00	0.00	0.00	0.00	0.26	0.26	0.26	0.00	0.00	0.00	0.00	0.00	0.00
12	0.00	0.00	0.00	0.23	0.00	0.00	0.23	0.00	0.23	0.00	0.00	0.00	0.00	0.23	0.00	0.00
13	0.00	0.36	0.00	0.00	0.00	0.00	0.00	0.36	0.00	0.00	0.00	0.00	0.36	0.00	0.36	0.00
14	0.00	0.00	0.00	0.10	0.00	0.10	0.00	0.00	0.00	0.00	0.10	0.00	0.10	0.00	0.00	0.00
15	0.00	0.00	0.00	0.00	0.00	0.00	0.32	0.00	0.00	0.32	0.00	0.00	0.32	0.00	0.00	0.32
16	0.00	0.00	0.31	0.00	0.00	0.00	0.00	0.00	0.00	0.00	0.00	0.31	0.31	0.31	0.00	0.00

T	5.807
n	16
T^2/n	2.108
SS_T	0.305
SS_A	0.243
SS_B	0.024
SS_C	0.009
SS_D	0.022

ANOVA SUMMARY (unpooled)

Factor	DoF	SS	Mean Sq	F-Ratio	% of Contribution
W1	3	0.243	0.081	31.528	79.618
W2	3	0.024	0.008	3.067	7.745
P	3	0.009	0.003	1.131	2.857
V	3	0.022	0.007	2.873	7.255
Error	3	0.008	0.003		2.525
Total	15	0.305	0.0203		100.000

Appendix - C Model fitting for Tooltip Temperature

Tooltip Report

Send to Minitab Connect®

Regression Equation

Temperature = 159 - 80 W1 + 4 W2 - 60 P + 0.5 V + 36 W1*W1 - 15.9 W2*W2 + 4.6 P*P - 0.0024 V*V + 26 W1*W2 + 21.7 W1*P - 0.227 W1*V + 5 W2*P + 0.01 W2*V + 0.124 P*V

Coefficients

Term	Coef	SE Coef	T-Value	P-Value	VIF
Constant	159	349	0.46	0.727	
W1	-80	458	-0.18	0.889	867.41
W2	4	503	0.01	0.995	1044.69
P	-60	212	-0.28	0.824	2973.2
V	0.5	10.2	0.05	0.971	3783.72
W1*W1	36	680	0.05	0.966	1168.47
W2*W2	-15.9	75.7	-0.21	0.869	14.5
P*P	4.6	21.9	0.21	0.868	1577.63
V*V	-0.0024	0.0338	-0.07	0.956	2482.83
W1*W2	26	154	0.17	0.895	35.42
W1*P	21.7	32.2	0.67	0.623	67.44
W1*V	-0.227	0.947	-0.24	0.85	59.84
W2*P	5	112	0.05	0.969	815.93
W2*V	0.01	6.91	0	0.999	3192.87
P*V	0.124	0.212	0.59	0.663	64.63

Model Summary

S	R-sq	R-sq(adj)	R-sq(pred)
17.3939	81.70%	0.00%	0.00%

Analysis of Variance

Source	DF	Adj SS	Adj MS	F-Value	P-Value	
Regression	14	1350.89	96.492	0.32	0.902	
W1	1	9.3	9.303	0.03	0.889	0.56
W2	1	0.02	0.019	0	0.995	0.00
P	1	24.44	24.436	0.08	0.824	1.48
V	1	0.62	0.623	0	0.971	0.04
W1*W1	1	0.84	0.84	0	0.966	0.05
W2*W2	1	13.28	13.276	0.04	0.869	0.80

P*P	1	13.46	13.465	0.04	0.868	0.81
V*V	1	1.48	1.478	0	0.956	0.09
W1*W2	1	8.41	8.412	0.03	0.895	0.51
W1*P	1	137.33	137.326	0.45	0.623	8.31
W1*V	1	17.47	17.466	0.06	0.85	1.06
W2*P	1	0.7	0.696	0	0.969	0.04
W2*V	1	0	0.001	0	0.999	0.00
P*V	1	103.8	103.796	0.34	0.663	6.28
Error	1	302.55	302.548			18.30
Total	15	1653.44				100.00

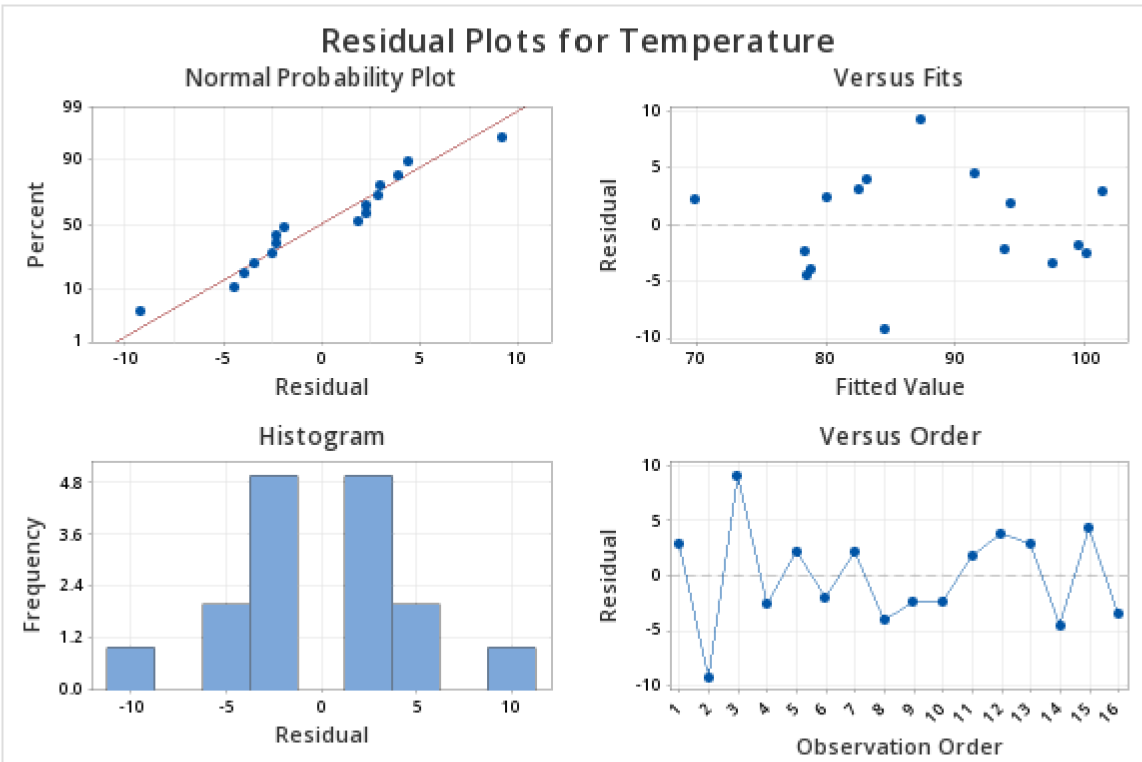

Regression Analysis: Ra versus W1, W2, P, V

Regression Equation

Ra = 1.51 - 0.89 W1 - 0.67 W2 + 0.20 P - 0.0196 V - 0.35 W1*W1 + 0.346 W2*W2 - 0.020 P*P + 0.000057 V*V - 0.083 W1*W2 + 0.046 W1*P + 0.00345 W1*V - 0.324 W2*P + 0.0130 W2*V + 0.00033 P*V

Coefficients

Term	Coef	SE Coef	T-Value	P-Value	VIF
Constant	1.51	1.76	0.86	0.548	
W1	-0.89	2.31	-0.39	0.765	867.41
W2	-0.67	2.53	-0.27	0.835	1044.69
P	0.2	1.07	0.18	0.884	2973.2
V	-0.0196	0.0511	-0.38	0.767	3783.72
W1*W1	-0.35	3.42	-0.1	0.936	1168.47
W2*W2	0.346	0.381	0.91	0.531	14.5
P*P	-0.02	0.11	-0.18	0.886	1577.63
V*V	0.000057	0.00017	0.33	0.794	2482.83
W1*W2	-0.083	0.778	-0.11	0.933	35.42
W1*P	0.046	0.162	0.28	0.824	67.44
W1*V	0.00345	0.00477	0.72	0.601	59.84
W2*P	-0.324	0.564	-0.58	0.668	815.93
W2*V	0.013	0.0348	0.37	0.772	3192.87
P*V	0.00033	0.00107	0.31	0.807	64.63

Model Summary

S	R-sq	R-sq(adj)	R-sq(pred)
0.0875812	97.48%	62.23%	0.00%

Analysis of Variance

Source	DF	Adj SS	Adj MS	F-Value	P-Value
Regression	14	0.29699	0.021214	2.77	0.443
W1	1	0.001144	0.001144	0.15	0.765
W2	1	0.000539	0.000539	0.07	0.835
P	1	0.000262	0.000262	0.03	0.884
V	1	0.001124	0.001124	0.15	0.767
W1*W1	1	0.000079	0.000079	0.01	0.936
W2*W2	1	0.006314	0.006314	0.82	0.531
P*P	1	0.00025	0.00025	0.03	0.886

V*V	1	0.000859	0.000859	0.11	0.794
W1*W2	1	0.000087	0.000087	0.01	0.933
W1*P	1	0.000618	0.000618	0.08	0.824
W1*V	1	0.004016	0.004016	0.52	0.601
W2*P	1	0.00254	0.00254	0.33	0.668
W2*V	1	0.001073	0.001073	0.14	0.772
P*V	1	0.000749	0.000749	0.1	0.807
Error	1	0.00767	0.00767		
Total	15	0.304661